

# Measurement of Hyperfine Splitting of Positronium

Akira Ishida

The University of Tokyo

T2K Seminar @ J-PARC      14/07/2010

# Outline

## Positronium Hyperfine Splitting (Ps-HFS)

A. Ishida

### 1. Indirect Measurement

- Our new experiment
- Prototype run and its results
- Prospects & Current status

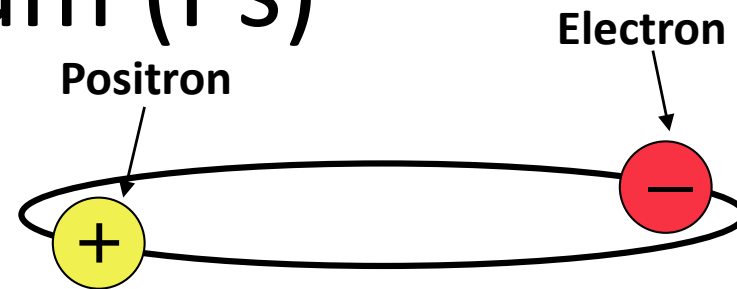
T. Yamazaki

### 2. Direct Measurement

- Experimental Concept: First Direct Measurement of Ps-HFS
- Experimental setup
- Expected performance

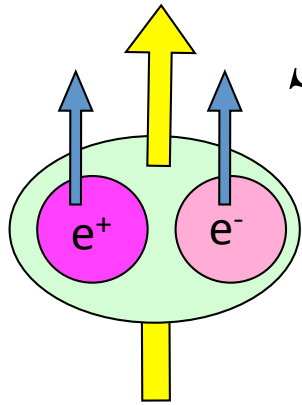


# Positronium (Ps)



- Bound state of an electron ( $e^-$ ) and a positron ( $e^+$ )
  - Purely leptonic system (free from hadronic uncertainties)
  - The lightest hydrogen-like “atom”
  - Bound state of particle and antiparticle → Sensitive to new physics beyond the Standard Model.
- Described by bound-state QED.

# Two Spin Eigenstates of Positronium

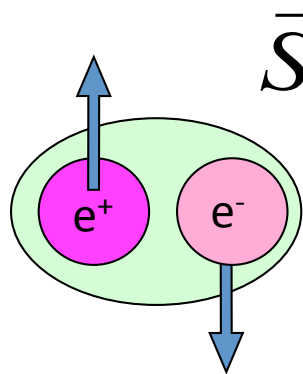


$\vec{S} = 1$  (Triplet)

Ortho-positronium (o-Ps)

Spin=1 The same quantum number as photon

$\text{o-Ps} \rightarrow 3\gamma$  (,  $5\gamma$ , ...)



$\vec{S} = 0$  (Singlet)

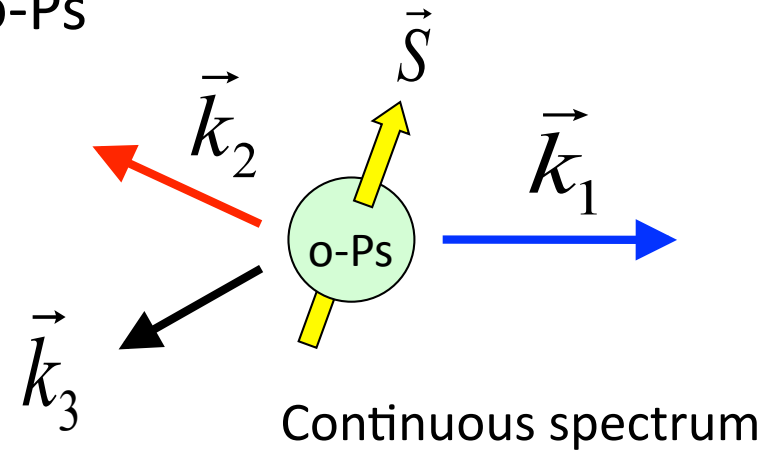
Para-positronium (p-Ps)

Spin=0 Scalar particle

$\text{p-Ps} \rightarrow 2\gamma$  (,  $4\gamma$ , ...)

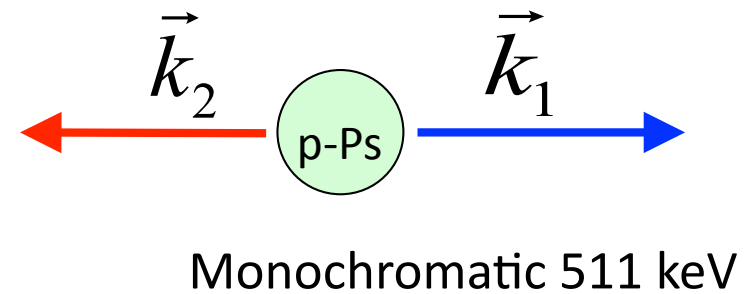
o-Ps

Lifetime 142 ns



p-Ps

Lifetime 125 ps



# Positronium Hyperfine Splitting (Ps-HFS)

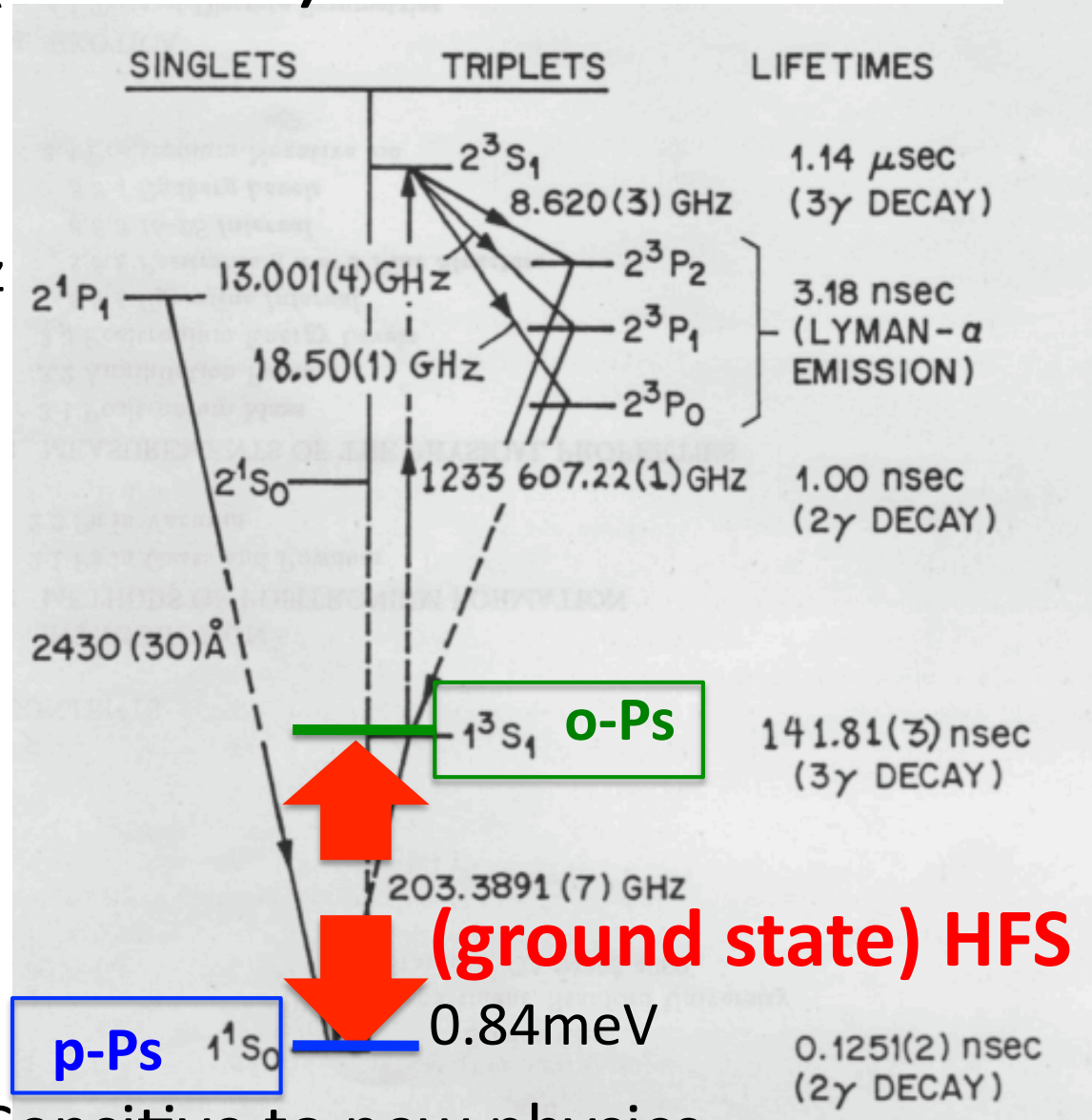
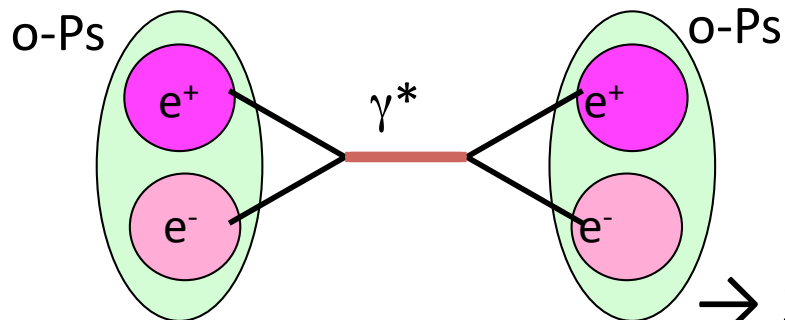
Energy difference between two spin eigenstates of the ground state Ps  $\rightarrow$  Ps-HFS

Large value of Ps-HFS 203 GHz (cf. Hydrogen HFS 1.4 GHz)

1. Large spin-spin interaction

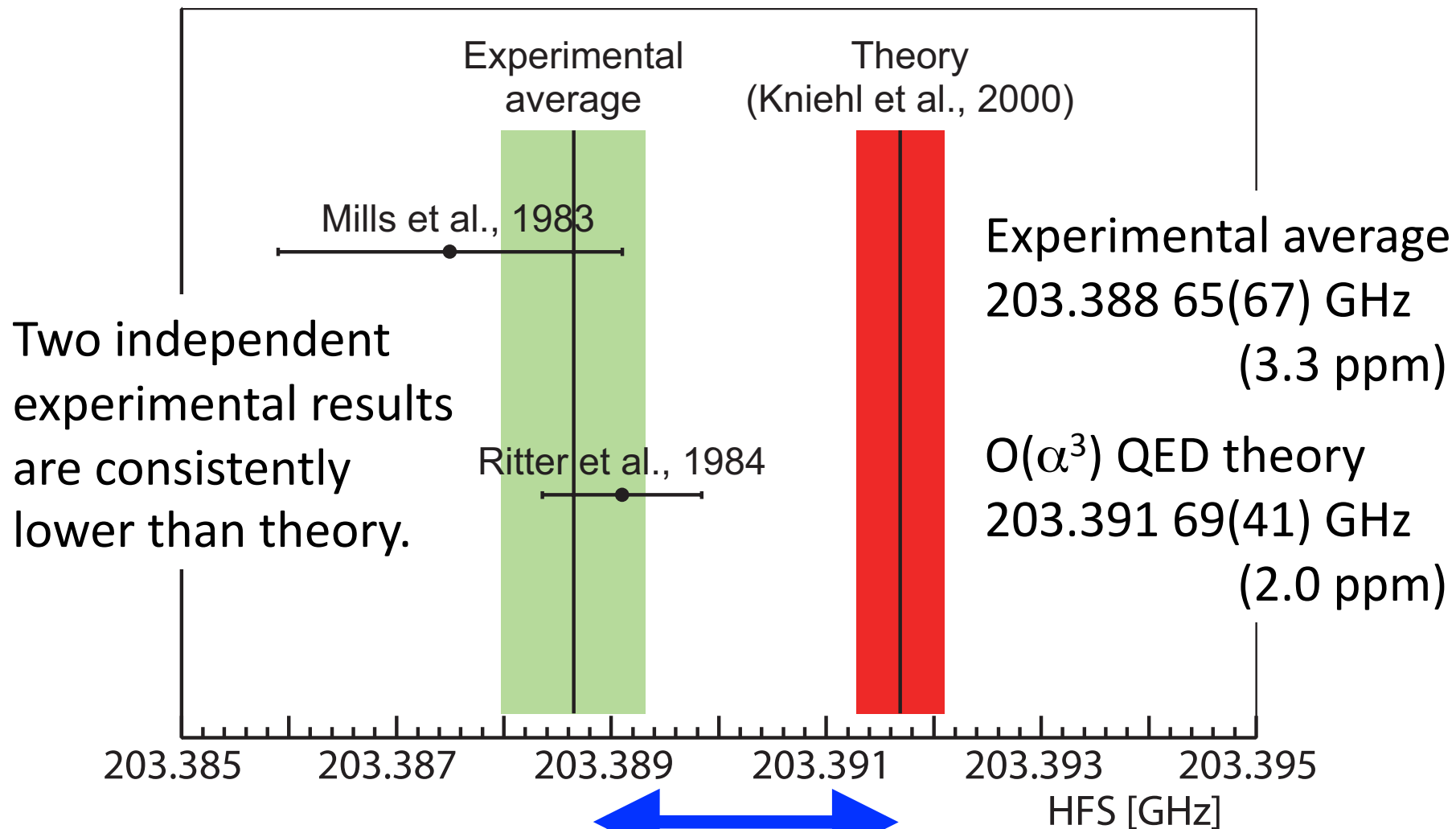
$$\vec{\mu} = \frac{e}{2m} \vec{\sigma} \quad (\text{small mass})$$

2. Contribution of Quantum oscillation in higher order correction



$\rightarrow$  Sensitive to new physics

# Discrepancy Between Experiments and Theory

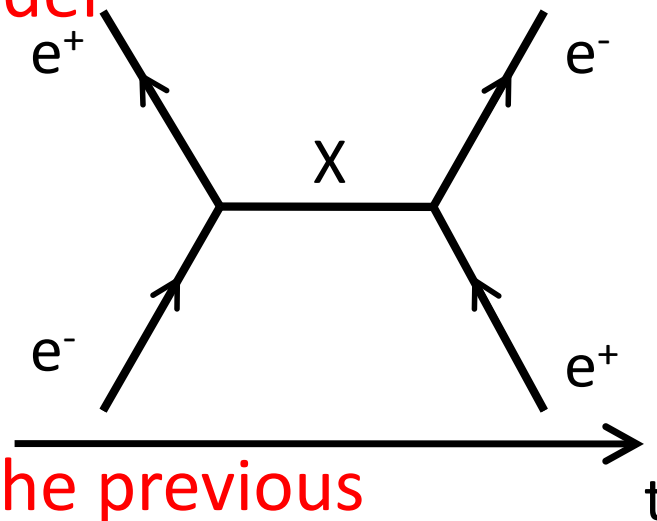


15 ppm ( $3.9 \sigma$ ) discrepancy

# Possible reasons for the discrepancy

- **New physics beyond the Standard Model**

- Weak interacting unknown particle
- Sensitive to light particle (s-channel)  
(ex.  $O(\text{MeV})$ ,  $\alpha \sim 10^{-8}$  pseudo scalar)
- o-Ps is sensitive to extra dimensions



- **Common systematic uncertainties in the previous experiments**

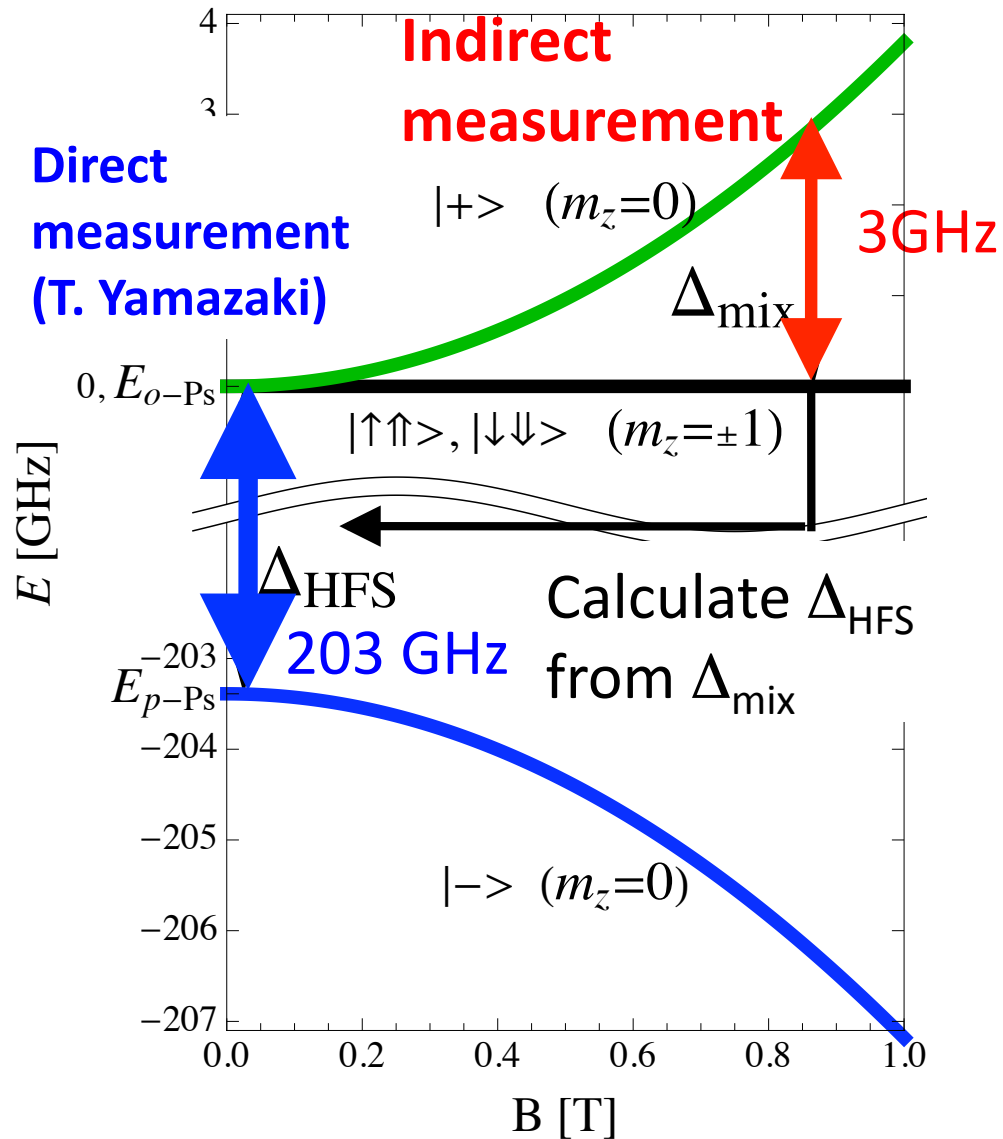
- Underestimation of material effects. Unthermalized o-Ps can have a significant effect especially at low material density. *cf. o-Ps lifetime puzzle (1990's)*
- Non-uniformity of the magnetic field. It is quite difficult to get ppm level uniform field in a large Ps formation volume.

- **Mistakes in the theoretical calculations**

# 1. Indirect Measurement

# Experimental Technique

## Indirect Measurement using Zeeman Effect



In a static magnetic field, the **p-Ps** state mixes with the  **$m_z=0$  state of o-Ps** (Annihilate into 2  $\gamma$ -rays).

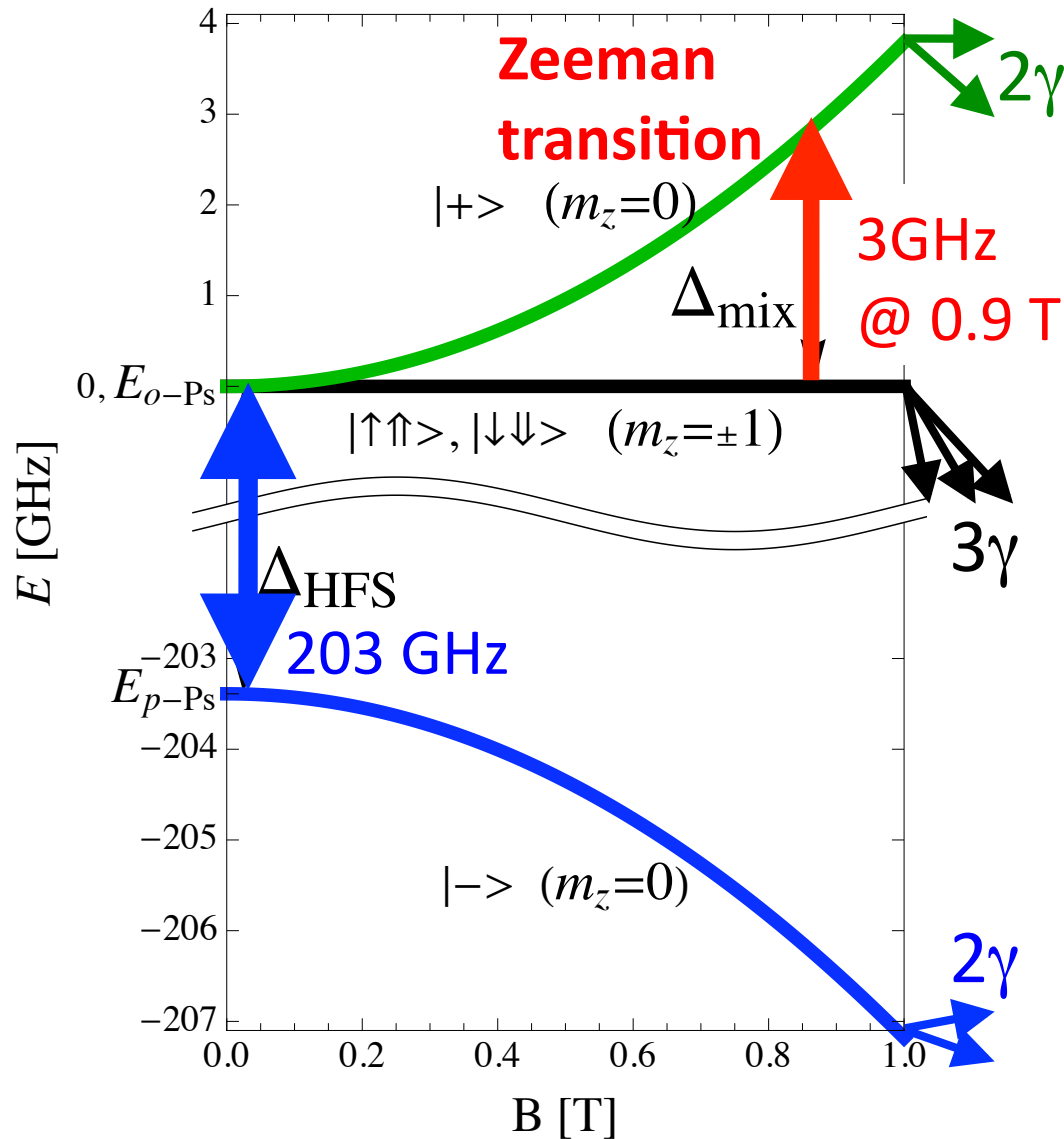
Precisely measure the  $\Delta_{mix}$  and calculate  $\Delta_{HFS}$  by the equation,

$$\Delta_{mix} = \frac{1}{2} \Delta_{HFS} \left( \sqrt{1 + 4x^2} - 1 \right),$$

$$x = \frac{g' \mu_B B}{\Delta_{HFS}}.$$

# Experimental Technique

## Indirect Measurement using Zeeman Effect



When a microwave field with a frequency of  $\Delta_{mix}$  is applied, transitions between the  $m_z=0$  and  $m_z=\pm 1$  states of o-Ps are induced.

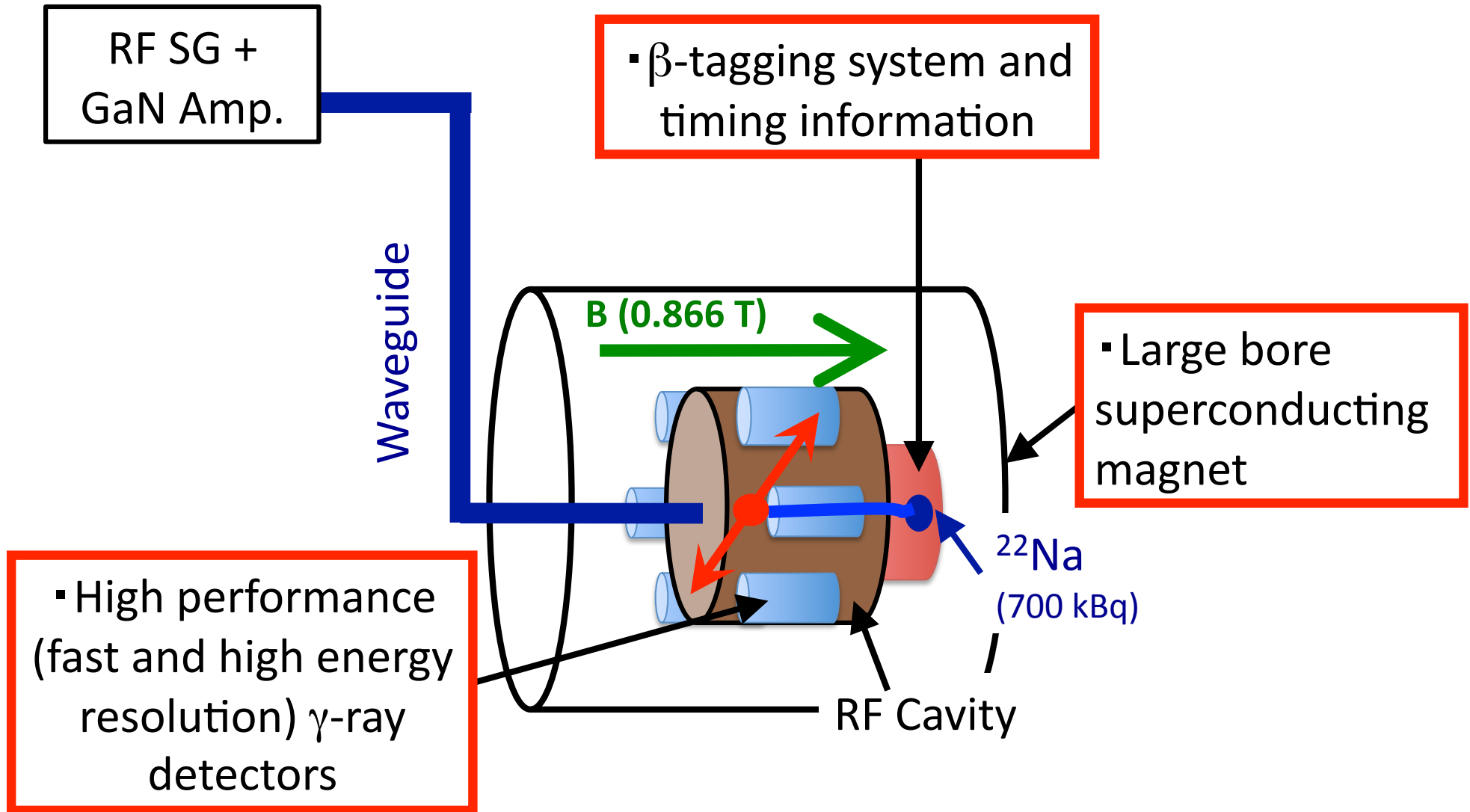
→ 2 $\gamma$ -ray annihilation (**511 keV monochromatic signal**) rate increases.

This increase is our experimental signal.

→ This is the same approach as previous experiments.



# Our New Experiment

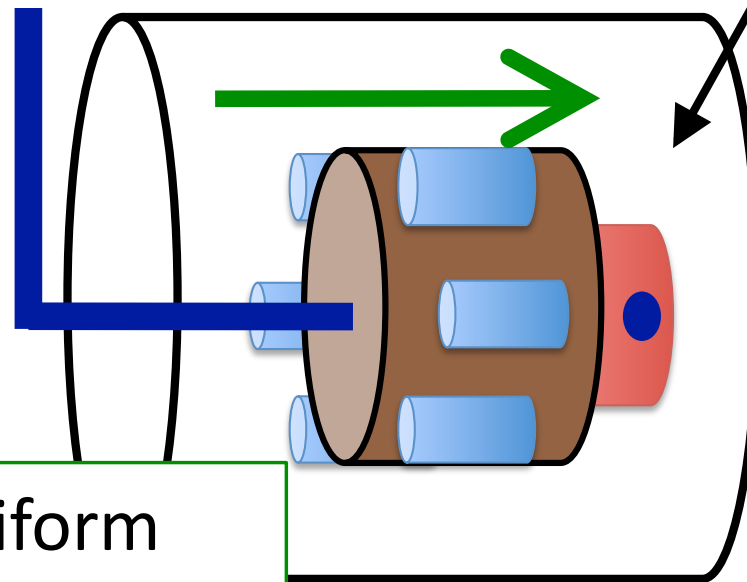


# Our New Experiment

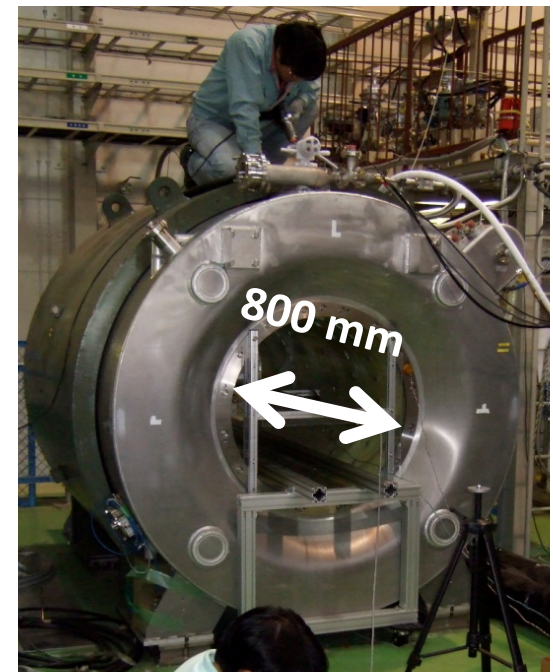
RF SG +  
GaN Amp.

Static magnetic field  
 $B$  (0.866 T)

▪ Large bore  
superconducting  
magnet



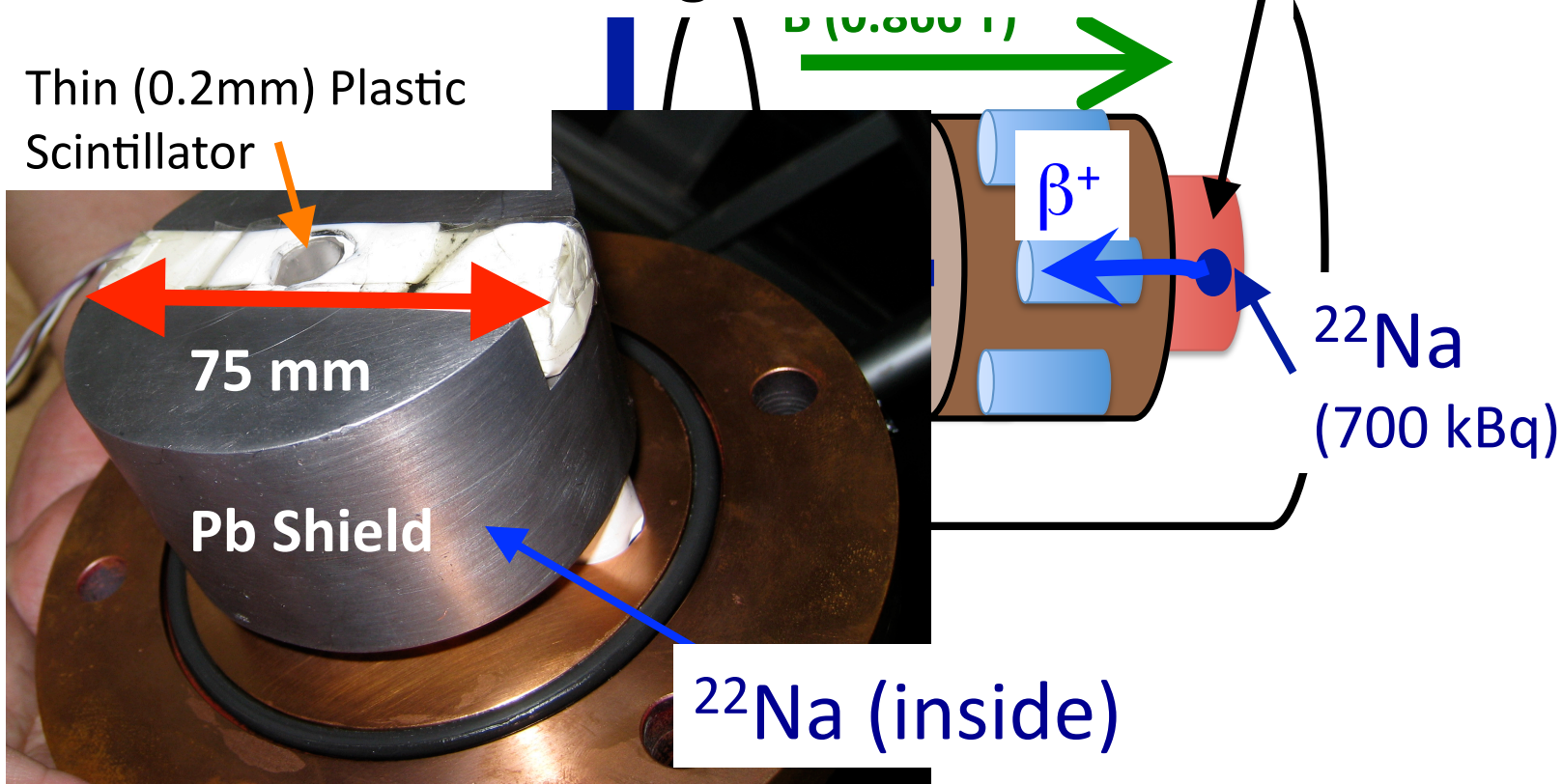
Large size → Uniform  
Persistent Current mode  
→ Stable



# Our New Experiment

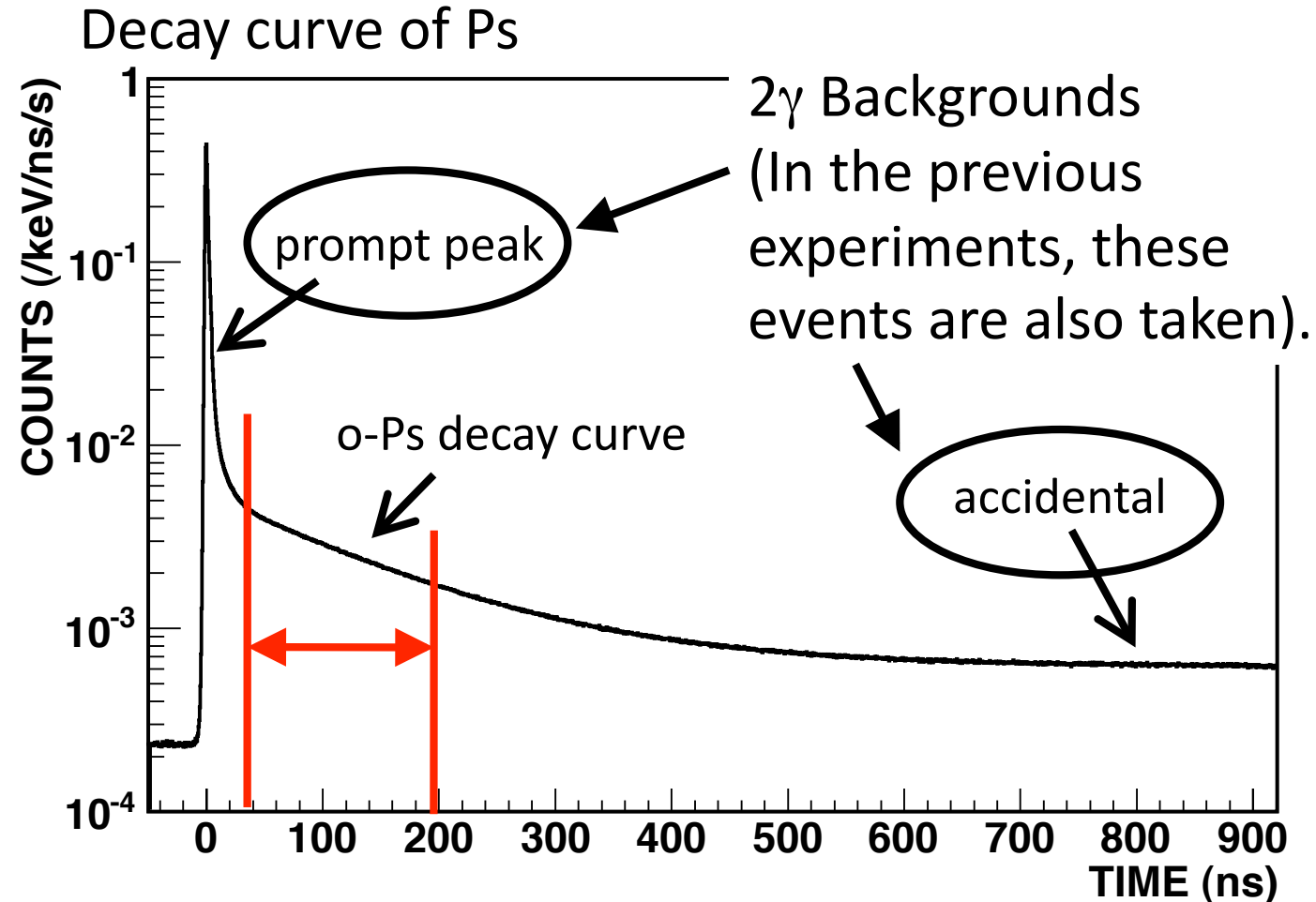
## ▪ $\beta$ -tagging system and timing information

- (1) Prompt suppression ( $\rightarrow$  Next page)
- (2) Necessary for material effect estimation including Ps thermalization



# Prompt Suppression

High S/N



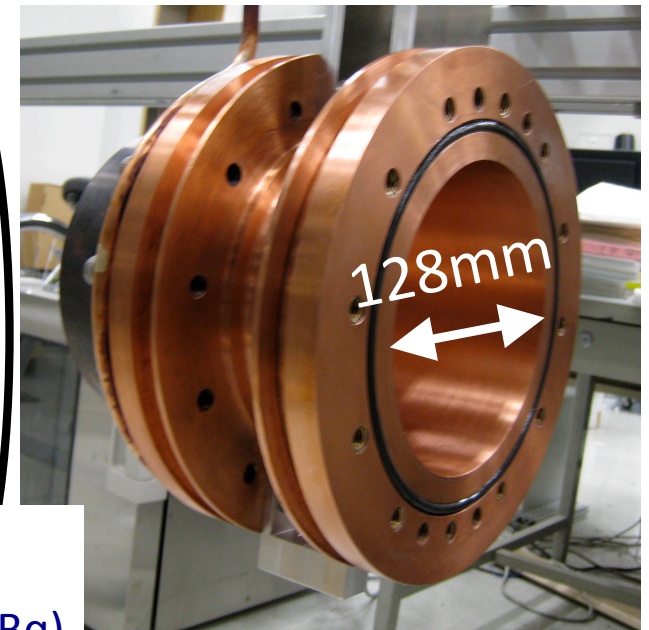
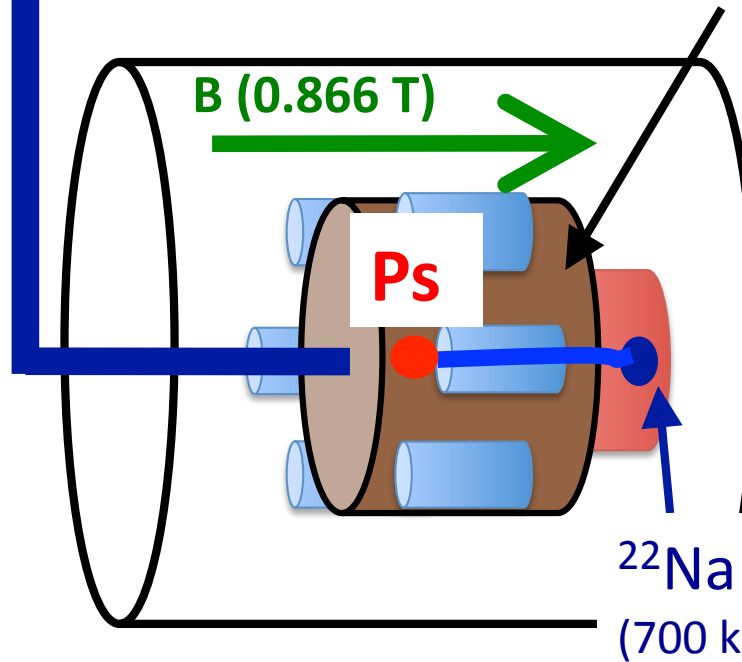
Select the o-Ps events (and Zeeman transition events) with  
Timing window  $\rightarrow$  About 20 times higher S/N

# Our New Experiment

RF SG +  
GaN Amp.  
2.9 GHz  
500 W CW

Waveguide

RF Cavity  
TM<sub>110</sub> mode, Q<sub>L</sub>=10,300  
Filled with gas  
(iso-C<sub>4</sub>H<sub>10</sub> 100%)

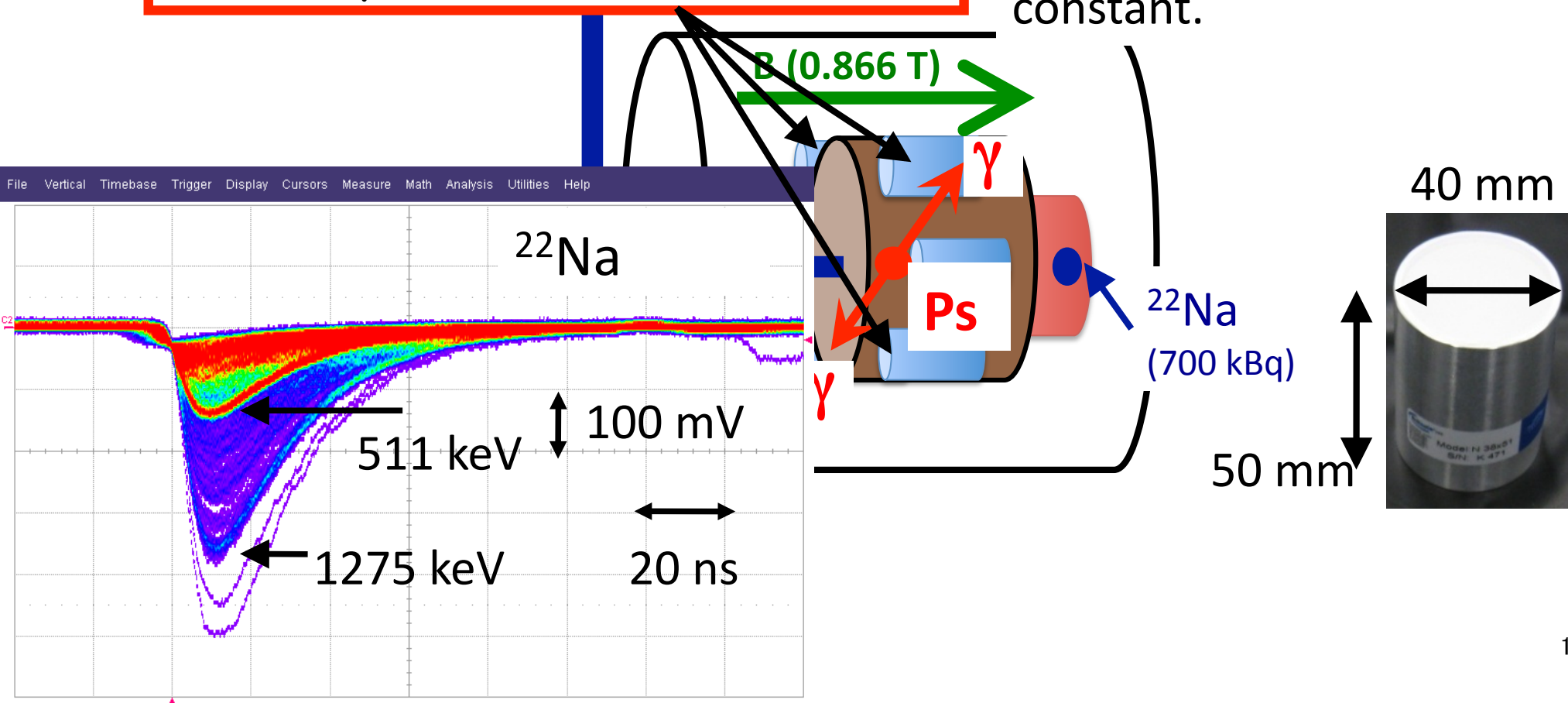




# Our New Experiment

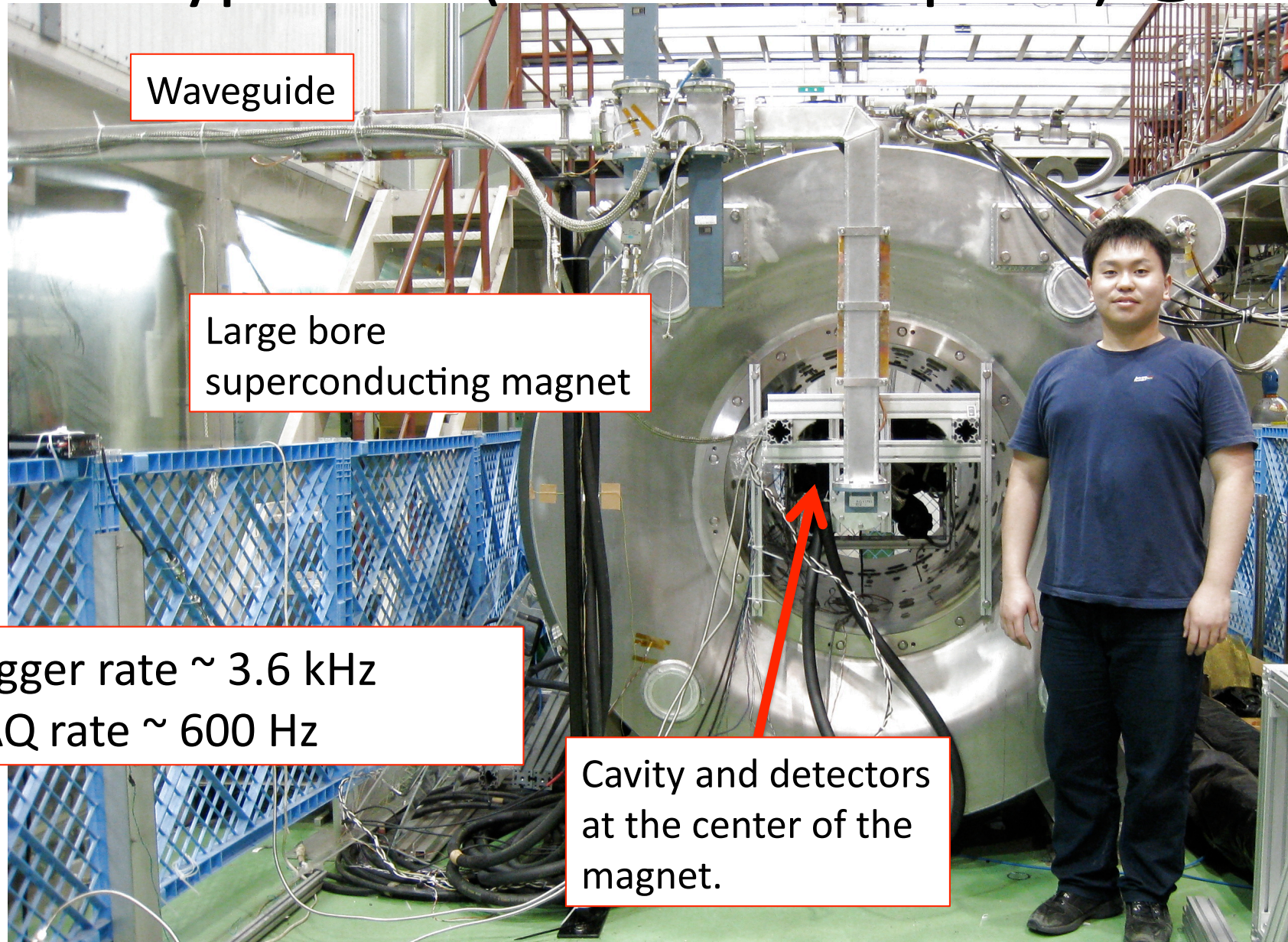
▪ High performance (fast and high energy resolution)  $\gamma$ -ray detectors

-LaBr<sub>3</sub>(Ce) scintillators x 6  
-High energy (4%) and timing (200 ps) resolutions, short (16 ns) decay constant.



# Our Experimental Setup

## Prototype Run (2 Jul – 24 Sep '09) @KEK



Waveguide

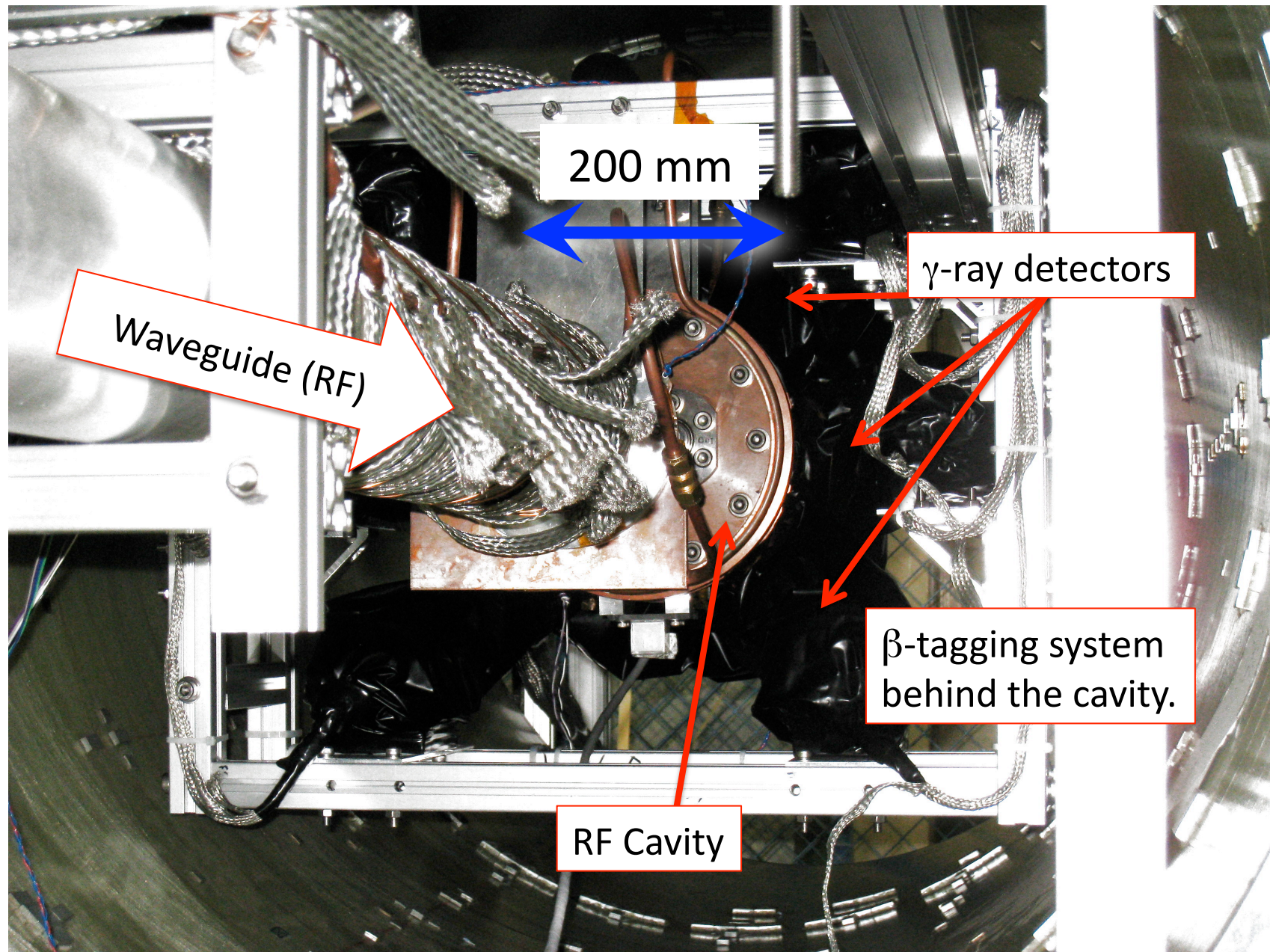
Large bore  
superconducting magnet

Trigger rate  $\sim 3.6$  kHz  
DAQ rate  $\sim 600$  Hz

Cavity and detectors  
at the center of the  
magnet.

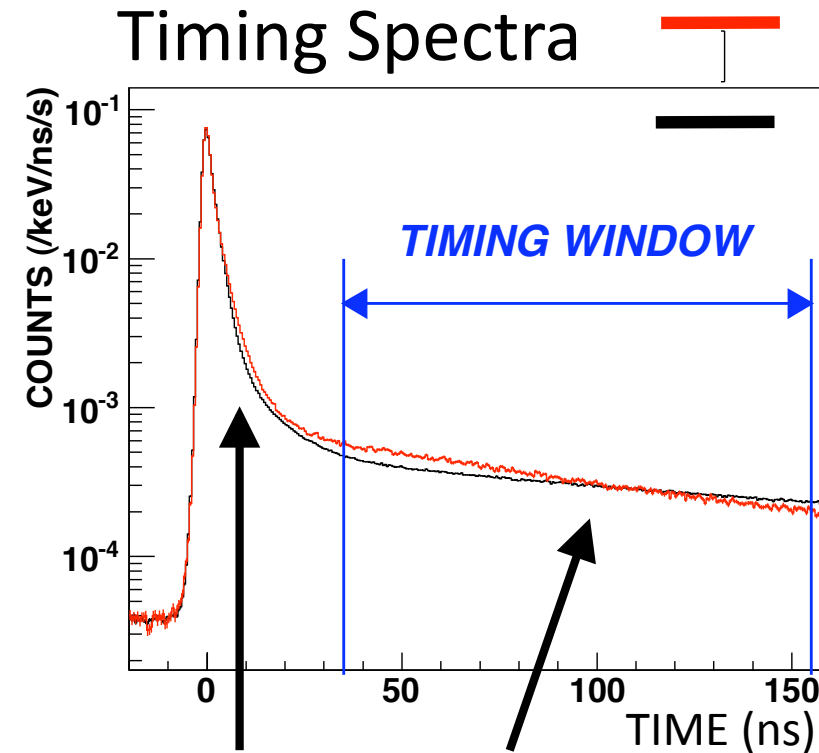


# Center of the Magnet





# Analysis



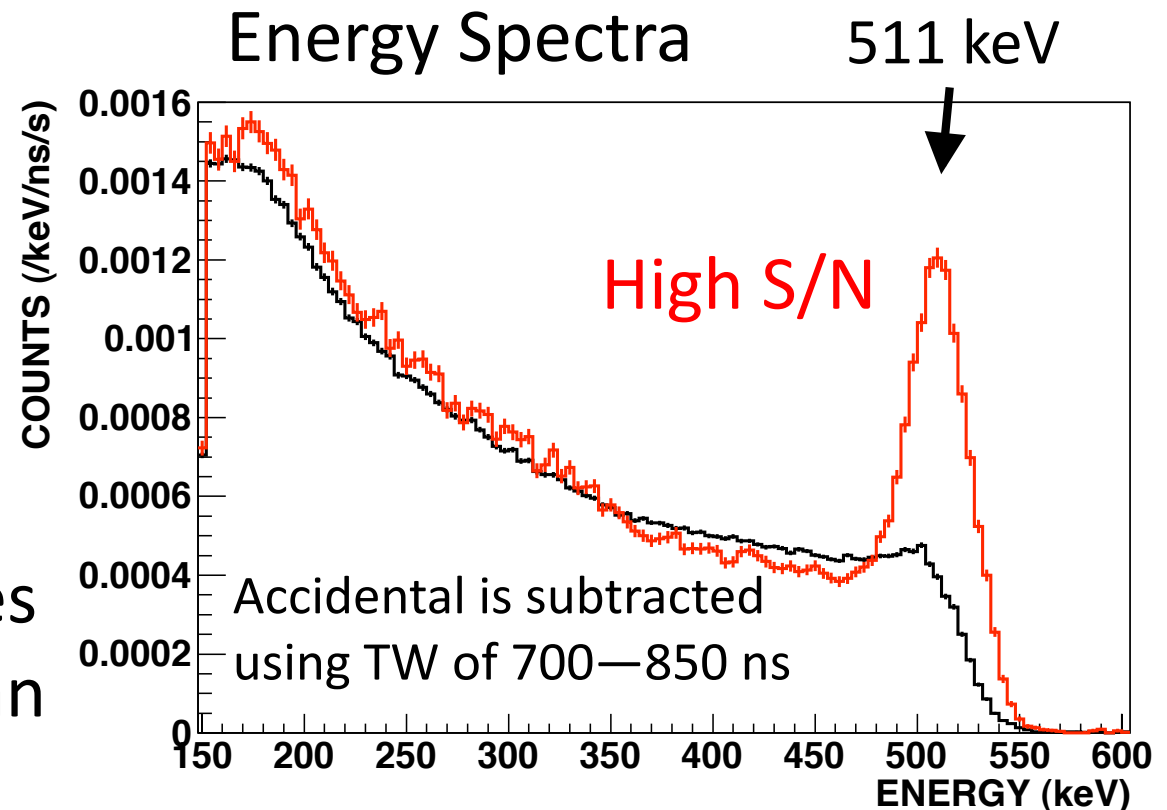
— ON Resonance RF ON

— ON Resonance RF OFF

Suppress Prompt and Accidental backgrounds with a Timing window of 35 ns – 155 ns

Short Component ( $m_z = 0$ )      Long Component ( $m_z = \pm 1$ )

$2\gamma$  decay rate increases because of the Zeeman transition.

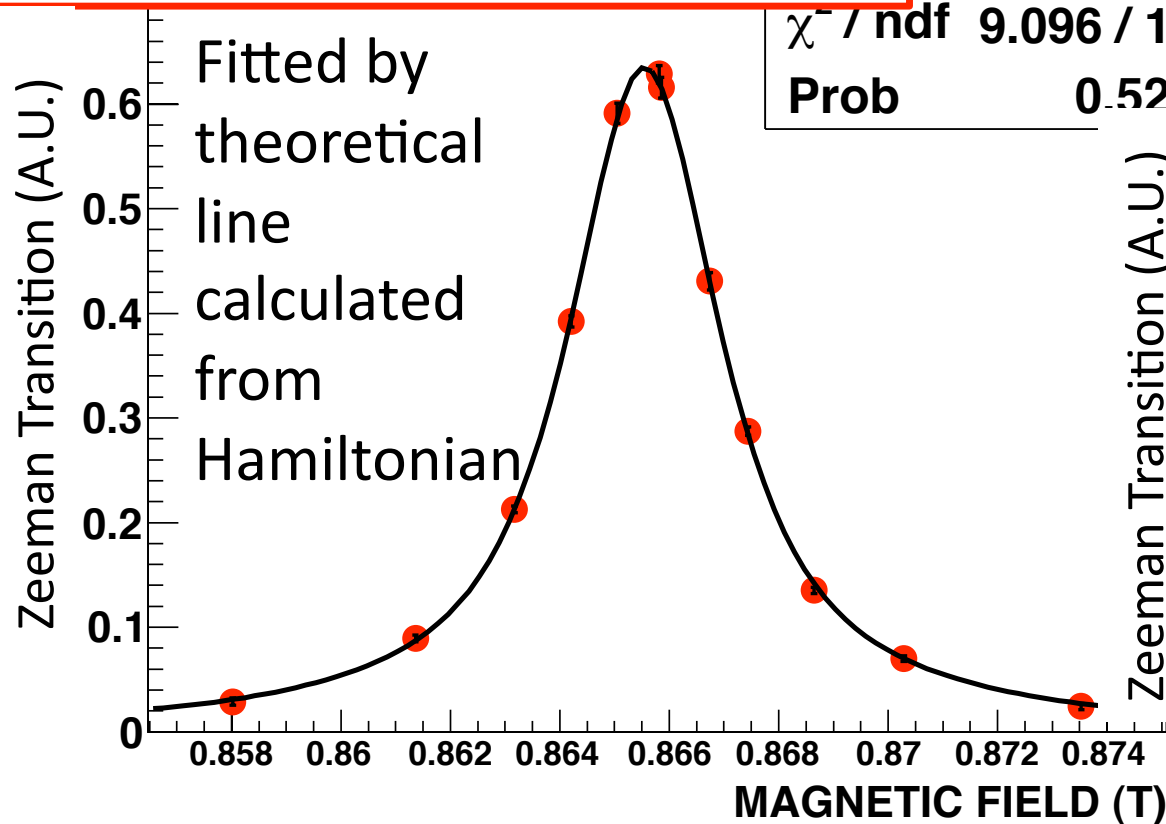


# Resonance Lines

Scan by Magnetic Field with the fixed RF frequency and power.

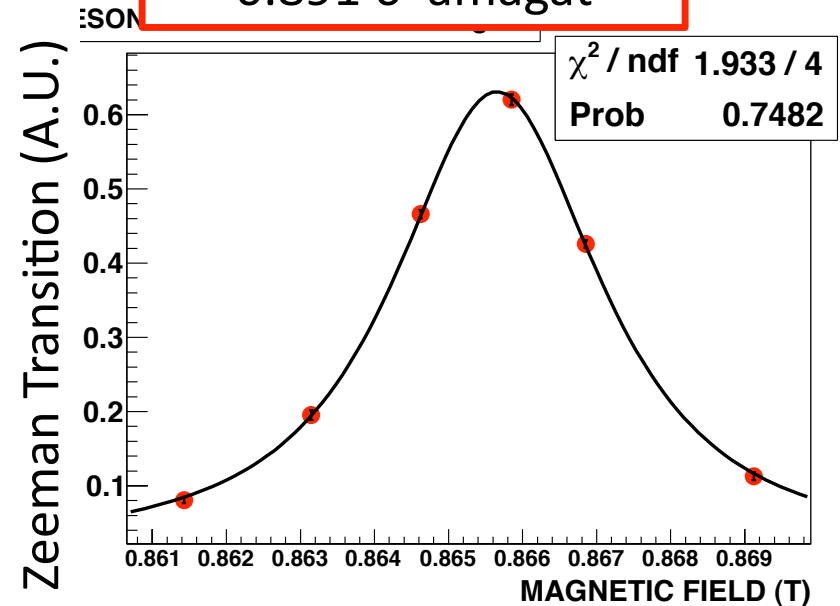
$2\gamma/3\gamma$  decay ratio is taken to be a Zeeman transition amount.

Resonance Line at 1.350 1 amagat



$$\Delta_{\text{HFS}} = 203.368\,3(55) \text{ GHz (27 ppm)}$$

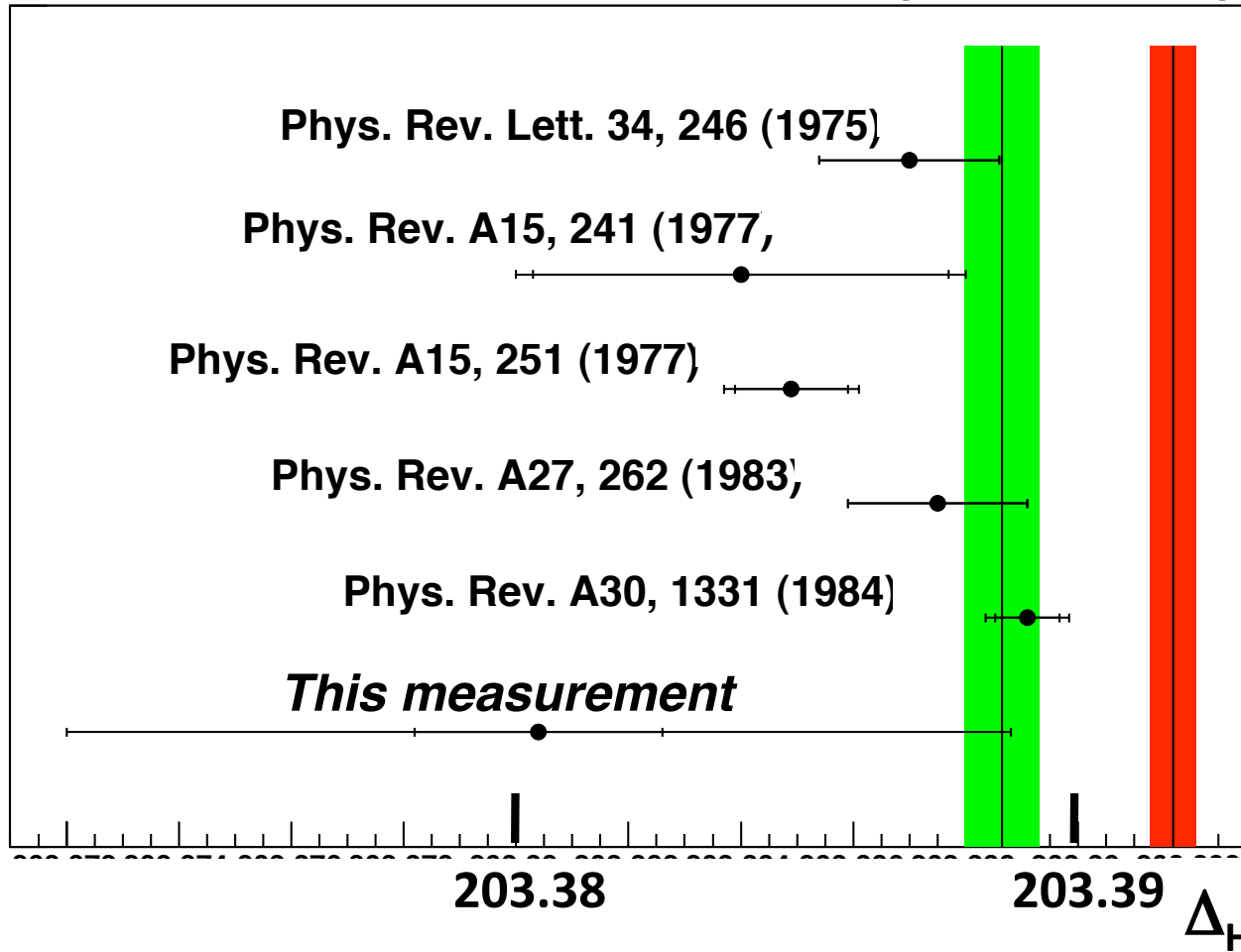
Resonance Line at 0.891 6 amagat



$$\Delta_{\text{HFS}} = 203.379\,3(70) \text{ GHz (34 ppm)}$$

→ Obtain the  $\Delta_{\text{HFS}}$  in vacuum with density correction.

# Result of the prototype run



- Our system has worked well.
- The result of the prototype run is consistent with the previous experiments and the theory.

Ps-HFS obtained from the Prototype Run:

$$\Delta_{\text{HFS}} = 203.3804 \pm 0.0022 \text{ (stat., 11 ppm)} \\ \pm 0.0081 \text{ (sys., 40 ppm) GHz}$$

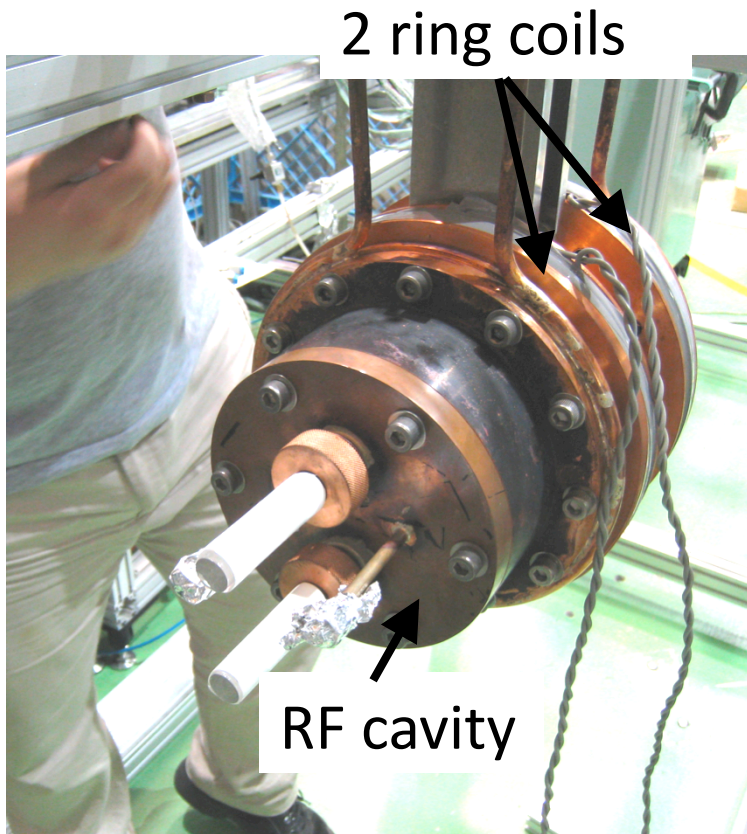
# Systematic Errors

|                                 | Source                             | ppm in $\Delta_{\text{HFS}}$ |
|---------------------------------|------------------------------------|------------------------------|
| Magnetic Field                  | <b>Non-uniformity</b>              | <b>21</b>                    |
|                                 | Offset and reproducibility         | 4                            |
|                                 | NMR measurement                    | 2                            |
| Detection Efficiency estimation | <b>Method</b>                      | <b>18</b>                    |
|                                 | <b>Statistics of MC simulation</b> | <b>17</b>                    |
| RF System                       | $Q_L$ value of RF cavity           | 6                            |
|                                 | RF power                           | 5                            |
|                                 | RF frequency                       | 5                            |
| Material Effect                 | <b>Thermalization of Ps</b>        | <b>&lt;20</b>                |
|                                 | Gas density dependence             | 7                            |
|                                 | <b>Quadrature sum</b>              | <b>40</b>                    |

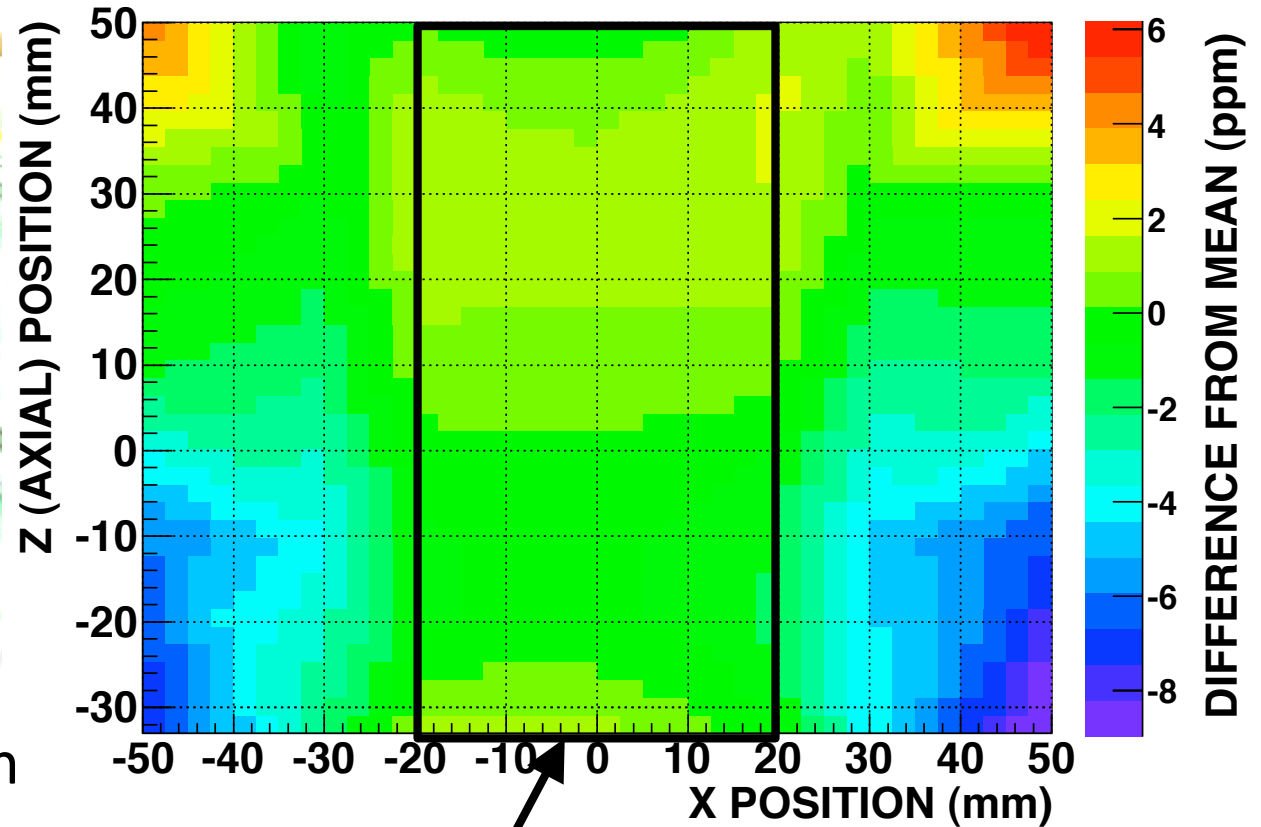
# Prospects & Current status

- Magnetic Field: Compensation magnets  
→ O(ppm) magnetic field uniformity (Done → )
- Material Effect: Measurements at various pressures of gas → Estimate the Stark Effect (Final measurement)  
Precisely measure the Ps thermalization  
(Now taking data → )
- RF System: The experimental environment (temperature) control → Almost cleared.
- Statistics: 85-day prototype run achieved 11 ppm. A measurement with a precision of O(ppm) is expected within a few years.
- Detection efficiency: Will be carefully studied and will be estimated by real data.  
→ O(ppm) systematic error. (Not yet)

# Compensation Magnet



Magnetic Field distribution (Horizontal)  
(0 is the center of the cavity)



- 2 ring-coils are rolled on the cavity flange.
- They make the opposite field and reduce the gradient.

**0.9 ppm (RMS) uniformity** in the Ps formation volume (10.4 ppm w/o coils)  
→ It is installed in the final run setup.

# Material Effect on Ps-HFS

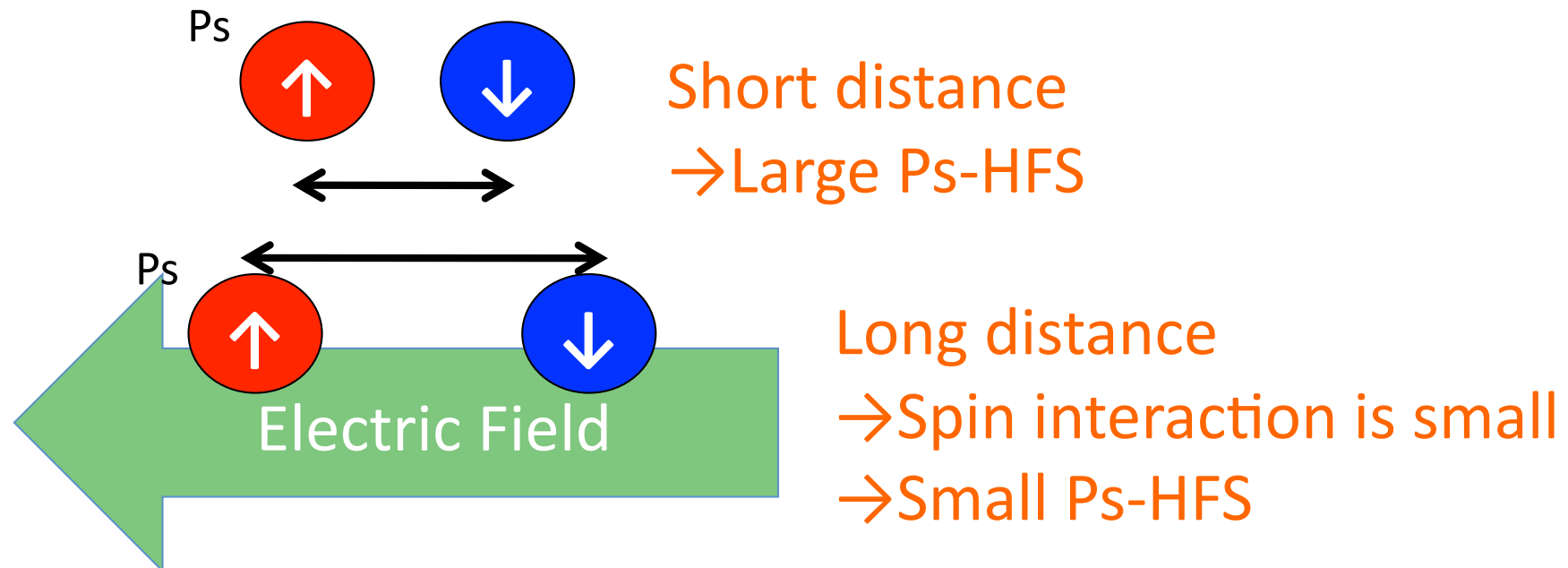
Spin-spin interaction between  $e^+$  and  $e^-$

→ Depends on their distance

Electric field of surrounding materials

→ Changes the distance of  $e^+$  and  $e^-$  of Ps

→ Shift of Ps-HFS (Stark Effect)



# Material Effect Estimation in Previous Experiments

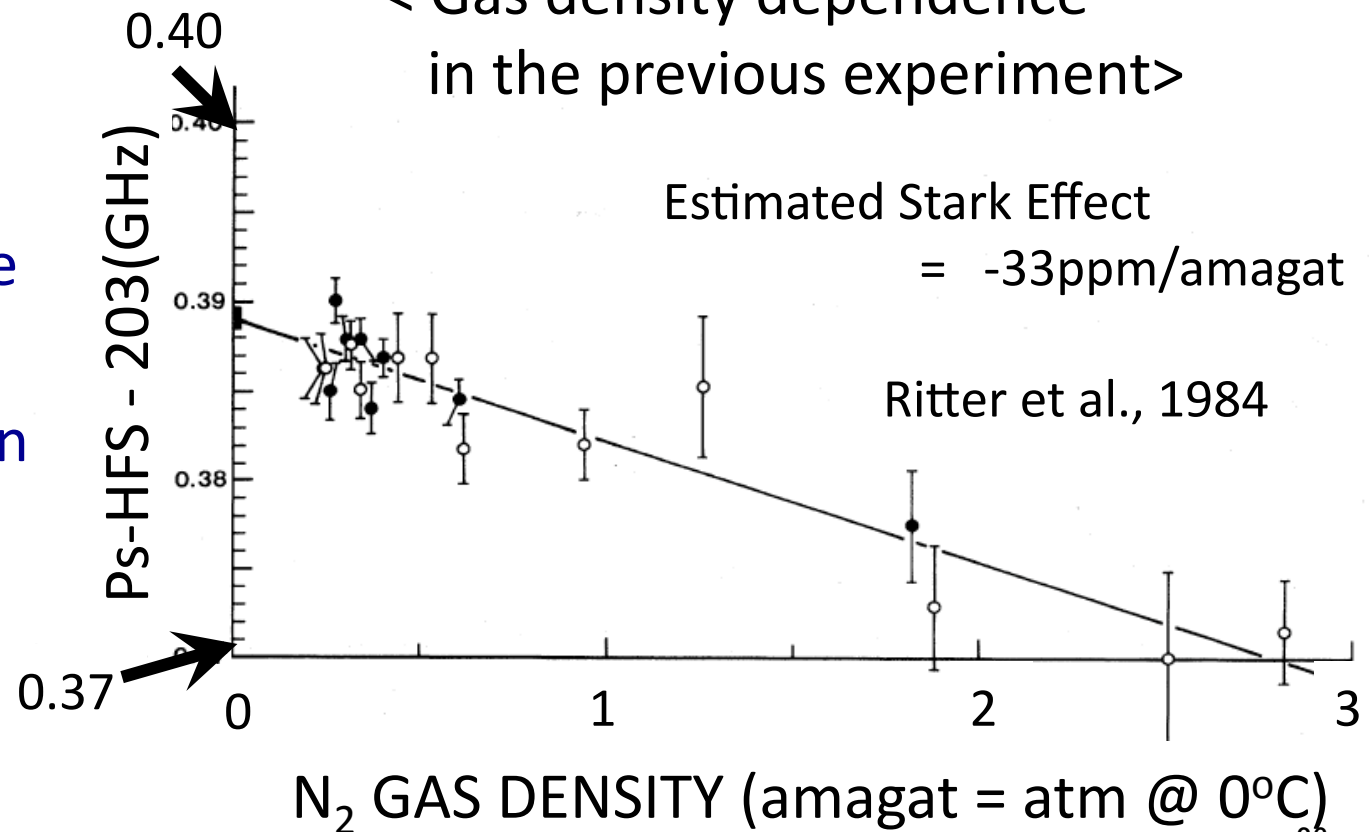
Stark Effect on Ps-HFS

$\propto$  Collision rate with materials

$$= \text{(Material Density)} \times \text{(Cross Section)} \times \text{(Ps velocity)}$$

- If the velocity of Ps is constant, the effect is just proportional to the material density.
- Linear extrapolation method is used in all the previous experiments with this assumption.

< Gas density dependence in the previous experiment >





# Ps Thermalization Problem

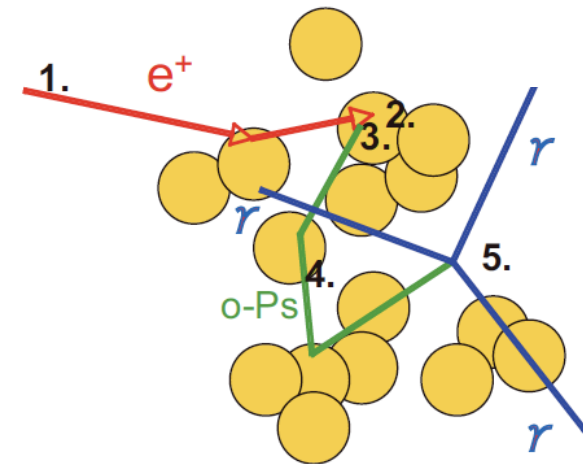
Formed o-Ps has a kinetic energy of about 1 eV.

o-Ps deposits its energy to the room temperature (1/30 eV) by collision with surrounding materials (the thermalization process).

If it takes much time to thermalize, the material effect ( $\propto$  collision rate) **is not proportional to material density**.

In fact, **it affects seriously** (“o-Ps lifetime puzzle” (1990’s)).

→ Ps thermalization effect can be a serious systematic error in Ps-HFS measurement.



# Material Effect Estimation including Ps Thermalization Effect

$(\sigma_m, E_0) =$

DBS:  $(13.0 \times 10^{-16} \text{cm}^2, 2.07 \text{eV})$

ACAR:  $(37 \times 10^{-16} \text{cm}^2, 2.07 \text{eV})$

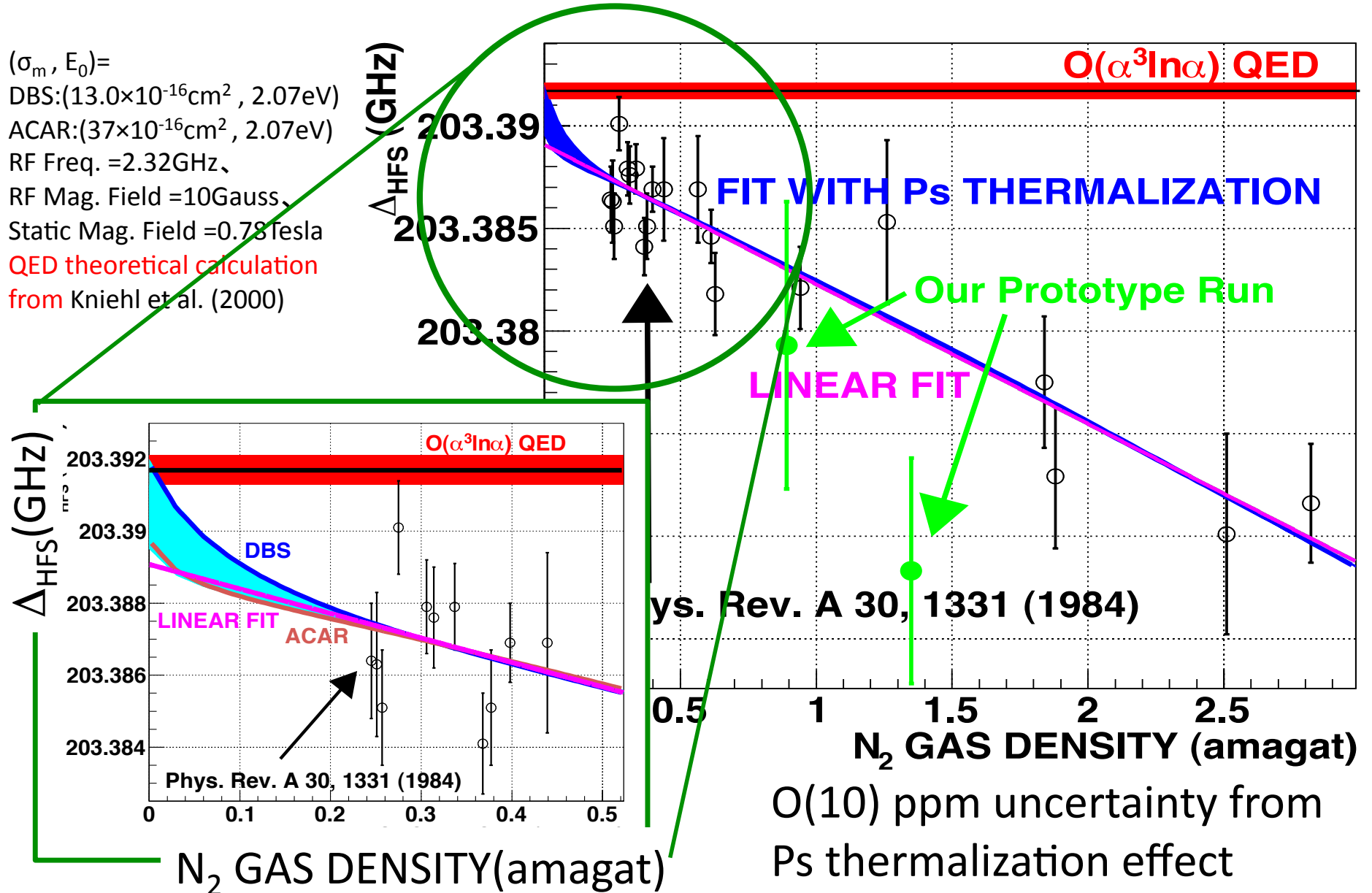
RF Freq. = 2.32 GHz,

RF Mag. Field = 10 Gauss,

Static Mag. Field = 0.78 Tesla

QED theoretical calculation

from Kniehl et al. (2000)

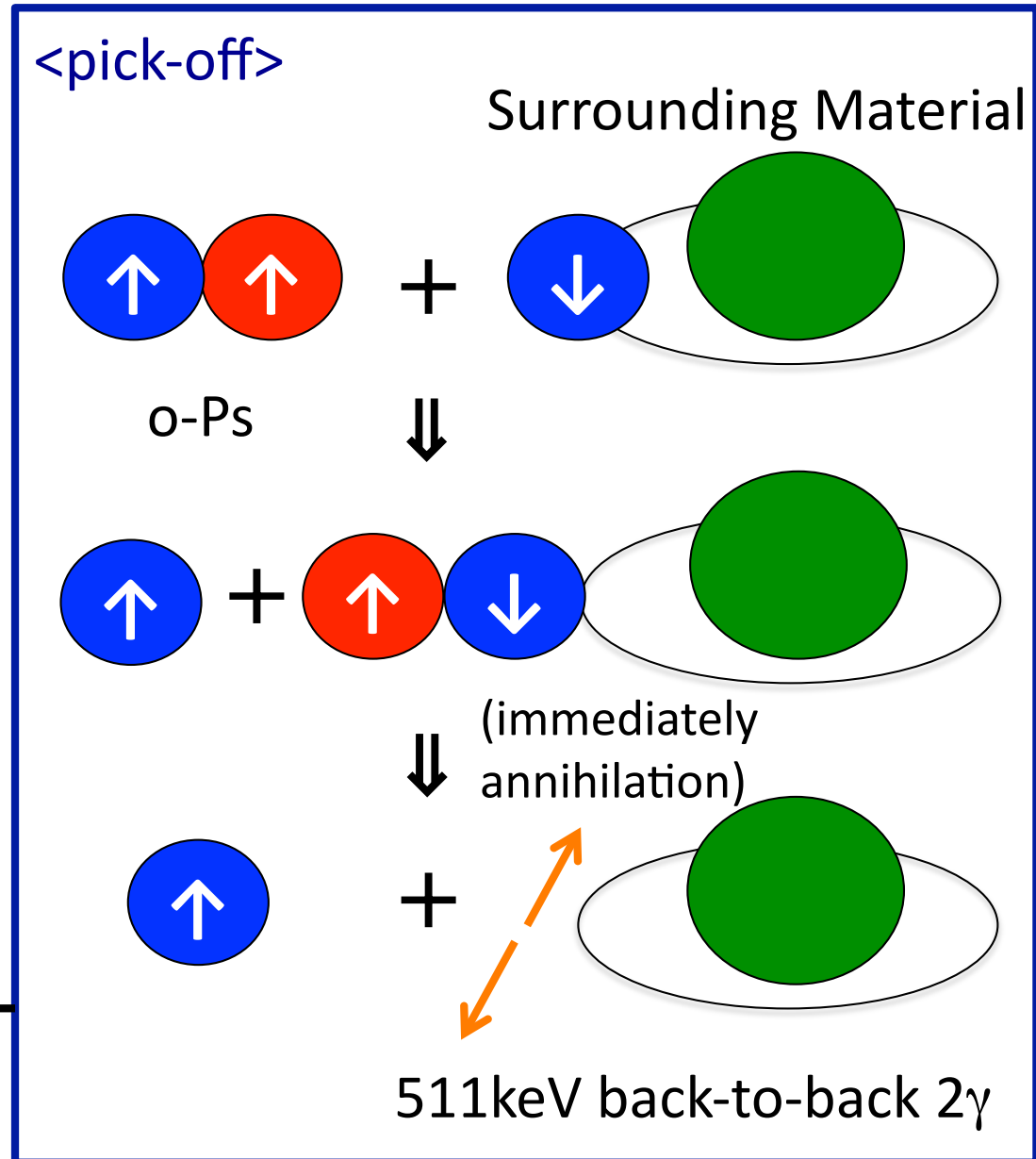


# How to Measure Ps thermalization?

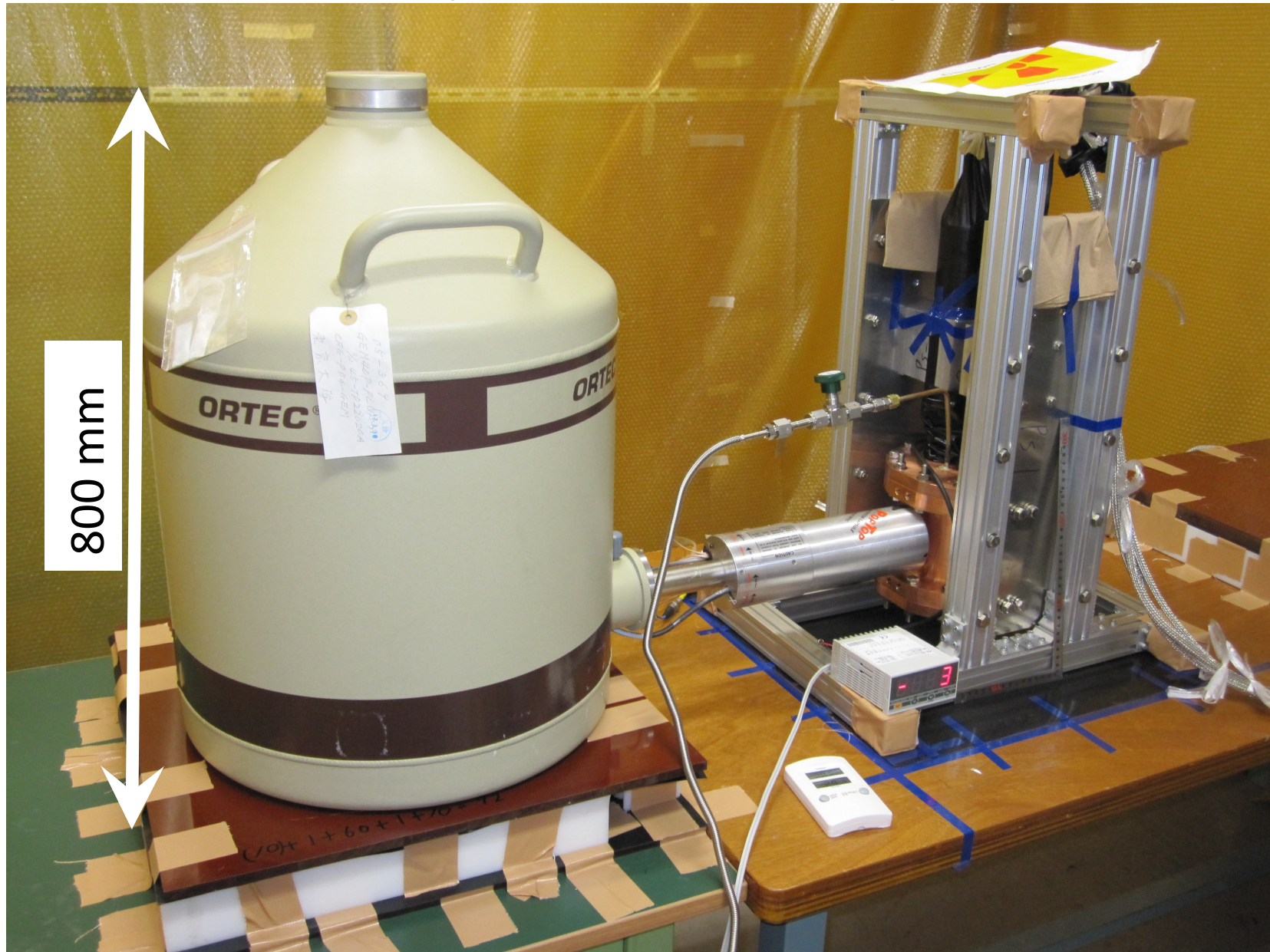
- Use o-Ps' pick-off  $2\gamma$  annihilation

- pick-off (t)
  - $\propto$  cross section of collision ( $\sigma$ )
  - $\times$  material density
  - $\times$  o-Ps amount (t)
  - $\times$  v(t)

$$\frac{\sigma \cdot v(t)}{\propto} \frac{\text{pick-off (2}\gamma \text{ decay)}}{\text{o-Ps (3}\gamma \text{ decay)}}$$



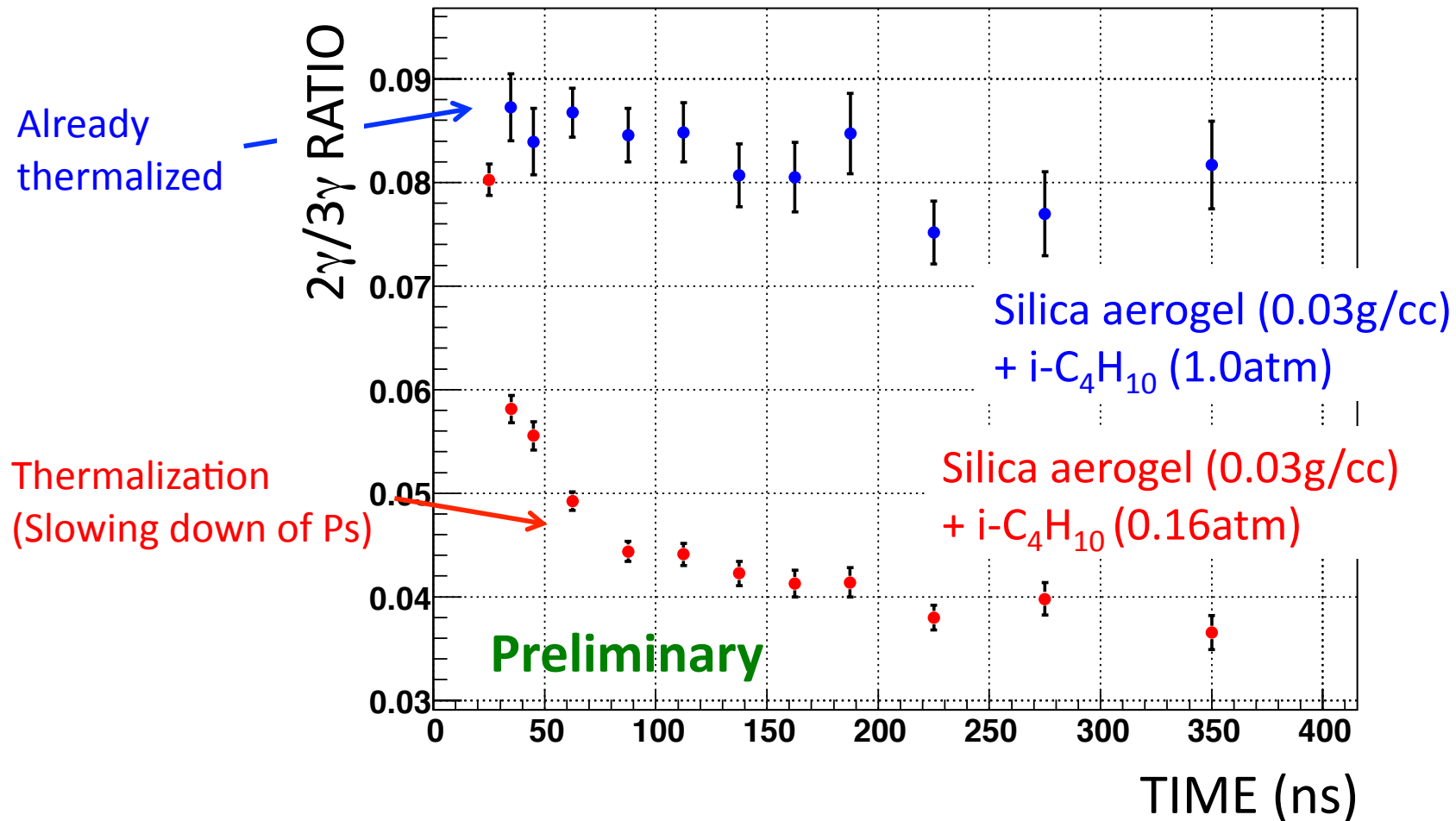
# Measurement of Ps Thermalization Experimental Setup





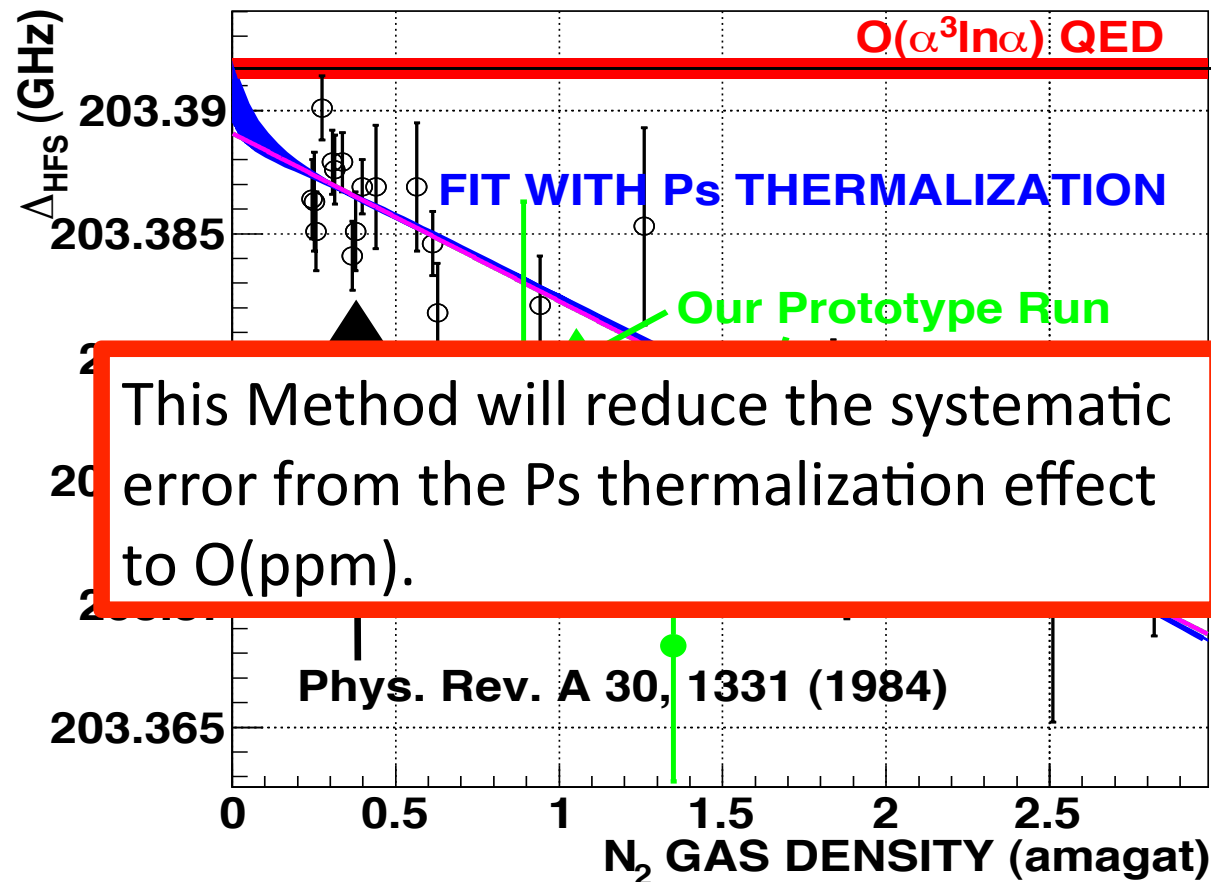
# $2\gamma/3\gamma$ Ratio

- $2\gamma/3\gamma$  ratio is obtained by 1-month run
- The more  $i\text{-C}_4\text{H}_{10}$  pressure, the faster the Ps thermalization



# Method of Material Effect Correction to Our Data

1. Measure the Ps thermalization parameters precisely.
2. Fit the obtained HFS data with nonlinear function including Ps thermalization effect (in the final run).



# Conclusion of my part

- There is a  $3.9 \sigma$  discrepancy in the ground state Ps-HFS between the experimental results and the QED prediction.
- The prototype run has been performed.
- Our new experimental setup uses 3 new methods.
  1. Superconducting magnet ( $\rightarrow$  Good uniformity of magnetic field in large volume)
  2.  $\beta$ -tagging system and Timing information ( $\rightarrow$  Correct treatment of Ps thermalization effect)
  3. High performance  $\gamma$ -ray detectors ( $\rightarrow$  High statistics)
- The preliminary value of Ps-HFS with an accuracy of 41 ppm has been obtained from the prototype run.
- A new result with an accuracy of O(ppm) will be obtained within a few years which will be an independent check of the discrepancy.

# Backup



# Members (Indirect Measurement)

Department of Physics, Graduate School of Science and  
International Center for Elementary Particle Physics (ICEPP),  
the University of Tokyo

A. Ishida, Y. Sasaki, G. Akimoto, T. Suehara,  
T. Namba, S. Asai, T. Kobayashi

Department of General Systems Studies, the University of Tokyo

H. Saito

High Energy Accelerator Research Organization (KEK)

M. Yoshida, K. Tanaka, A. Yamamoto

# Members (Direct Measurement)

Department of Physics, Graduate School of Science and  
International Center for Elementary Particle Physics (ICEPP),  
the University of Tokyo

T. Yamazaki, A. Miyazaki, T. Suehara, T. Namba, S. Asai,  
T. Kobayashi

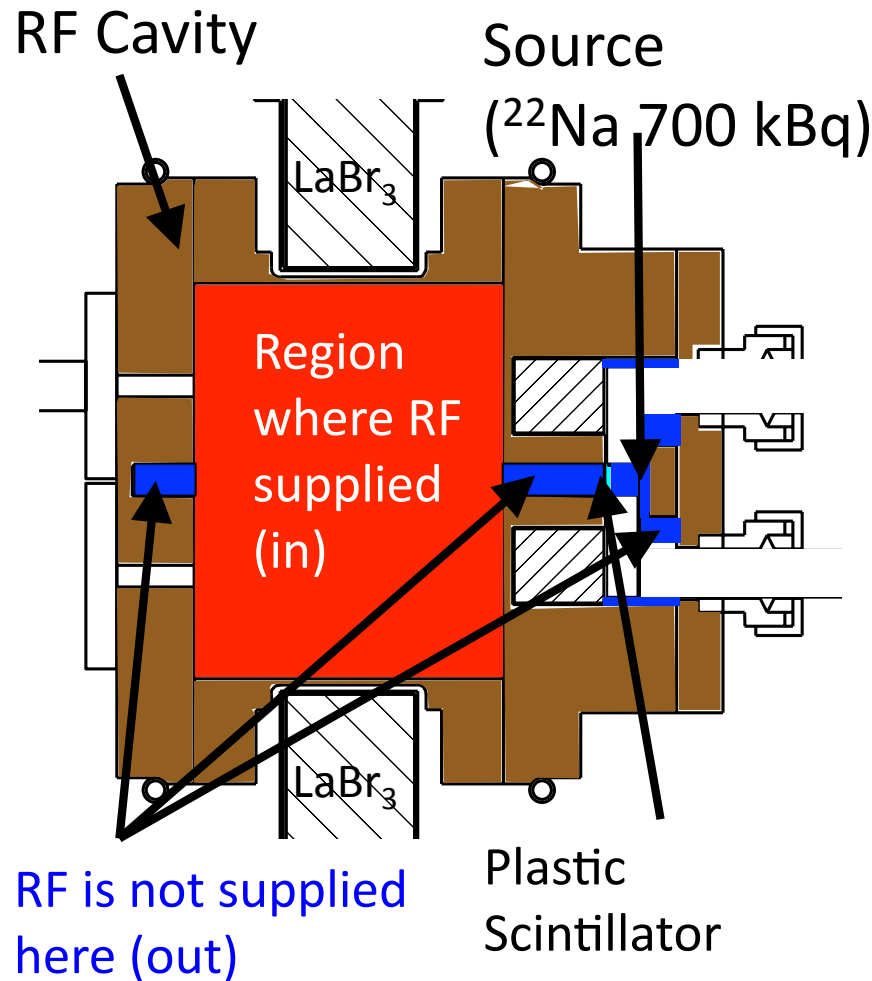
Department of General Systems Studies, the University of Tokyo  
H. Saito

Research Center for Development of Far-Infrared Region,  
University of Fukui (FIR-FU)

T. Idehara, I. Ogawa, Y. Urushizaki

Institute of Electronics of Bulgarian Academy of Science  
S. Sabchevski

# Fitting the Energy Spectra



- There is a region where RF is supplied and a region where RF is not supplied.
- Ps can be formed and decay in both region.
- When RF is OFF,  $2\gamma/3\gamma$  decay ratio does not depend on the region.

OFF Spectrum

$$S_{OFF} = \frac{A_{OFF} (S_{3\gamma MC, out} + \beta S_{2\gamma MC, out})}{A_{OFF} (S_{3\gamma MC, in} + \beta S_{2\gamma MC, in})}$$

Normalized by livetime.

Region without RF (top denominator)  
Region with RF (bottom denominator)

- When RF is ON,  $2\gamma/3\gamma$  decay ratio changes only in the “in” region.

ON Spectrum

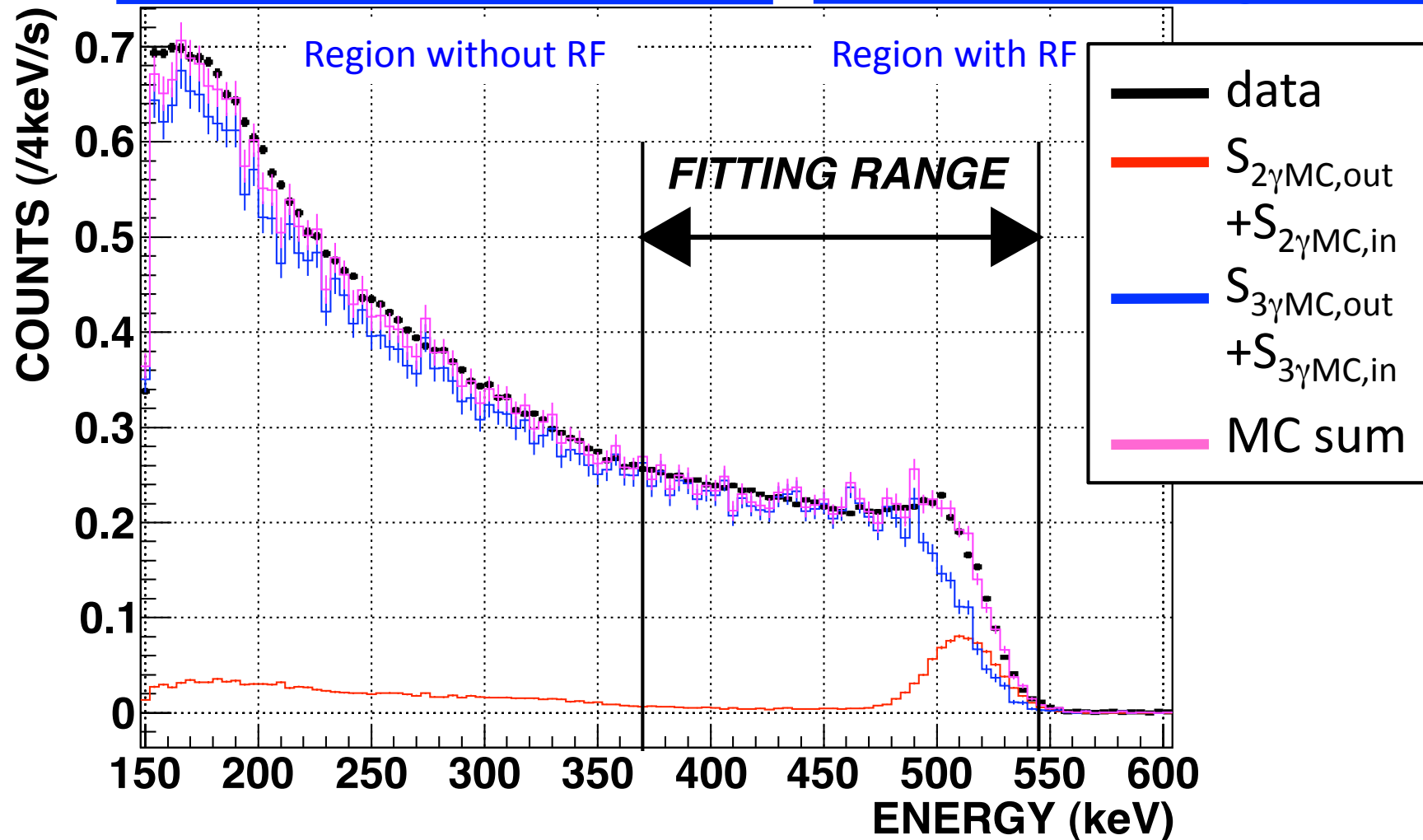
$$S_{ON} = \frac{A_{OFF} (S_{3\gamma MC, out} + \beta S_{2\gamma MC, out})}{A_{ON} (S_{3\gamma MC, in} + \Gamma S_{2\gamma MC, in})}$$

Region without RF (top denominator)  
Region with RF (bottom denominator)

$A_{OFF}$  ,  $A_{ON}$      $3\gamma$  decay prob.  
 $\beta$     ,  $\Gamma$          $2\gamma/3\gamma$  decay ratio  
 $S_{3\gamma MC}$  ,  $S_{2\gamma MC}$     MC spectra

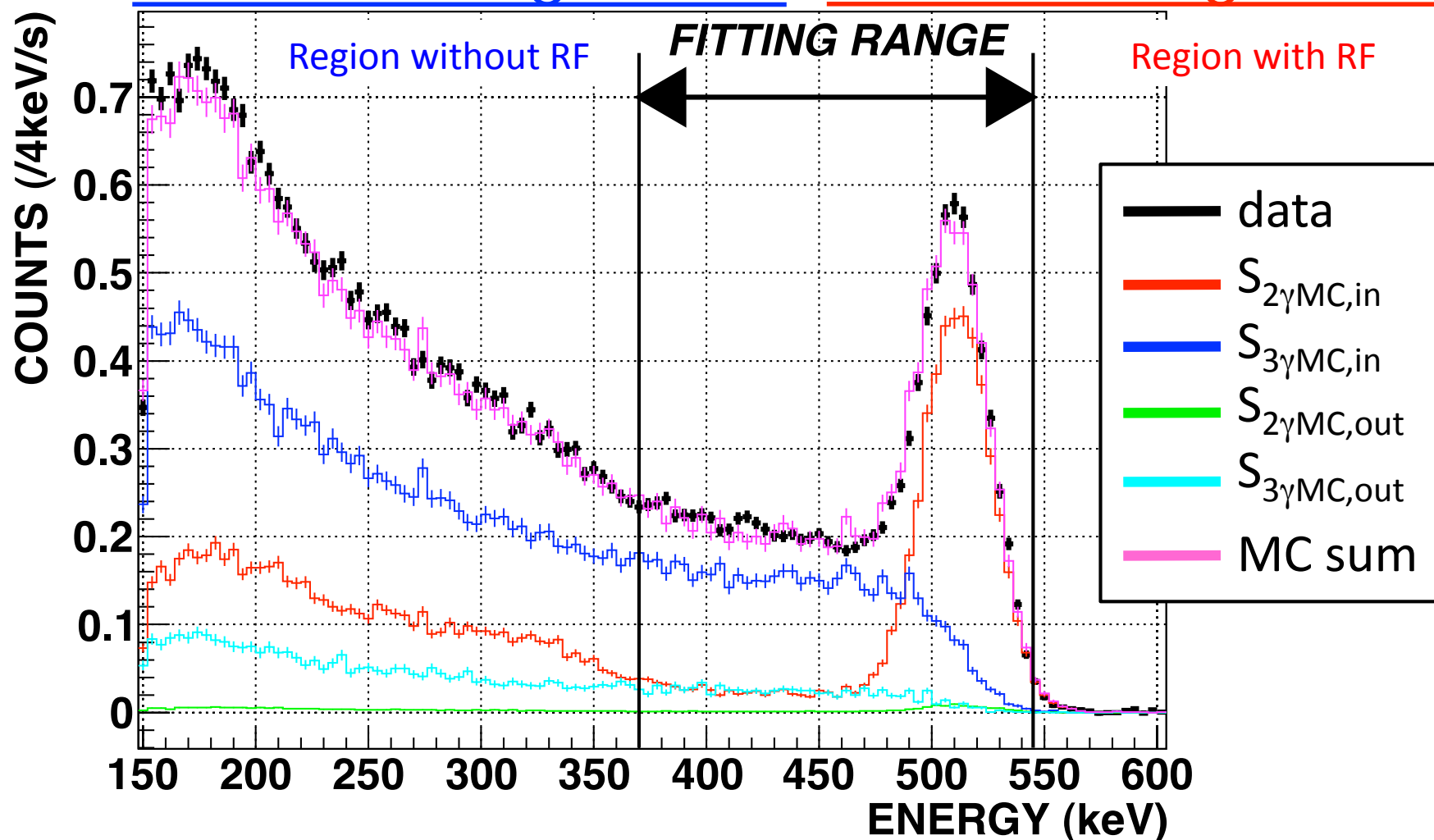
# Fitting the Energy Spectrum by Monte Carlo Simulation (RF-OFF)

$$S_{OFF} = A_{OFF} \left( S_{3\gamma MC, out} + \beta S_{2\gamma MC, out} \right) + A_{OFF} \left( S_{3\gamma MC, in} + \beta S_{2\gamma MC, in} \right)$$



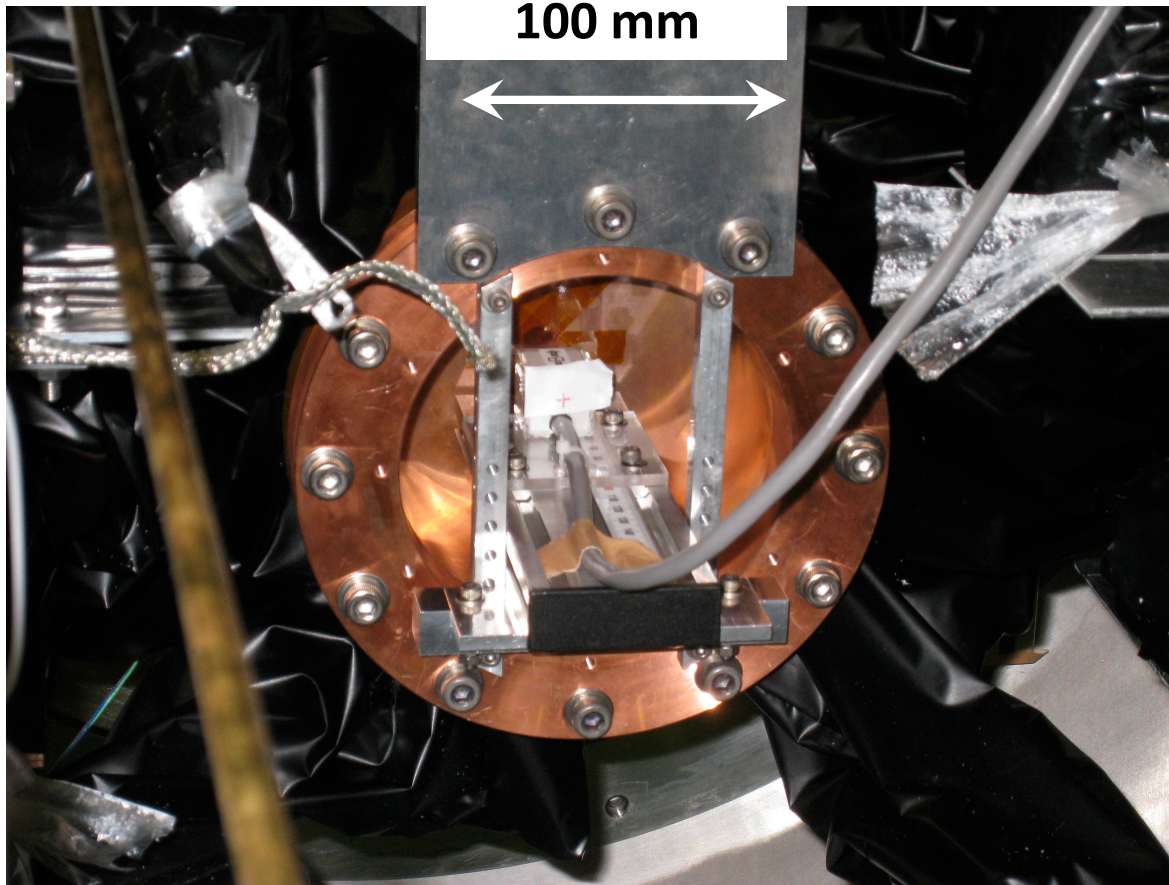
# Fitting the Energy Spectrum by Monte Carlo Simulation (RF-ON)

$$S_{ON} = A_{OFF} \left( S_{3\gamma MC, out} + \beta S_{2\gamma MC, out} \right) + A_{ON} \left( S_{3\gamma MC, in} + \Gamma S_{2\gamma MC, in} \right)$$



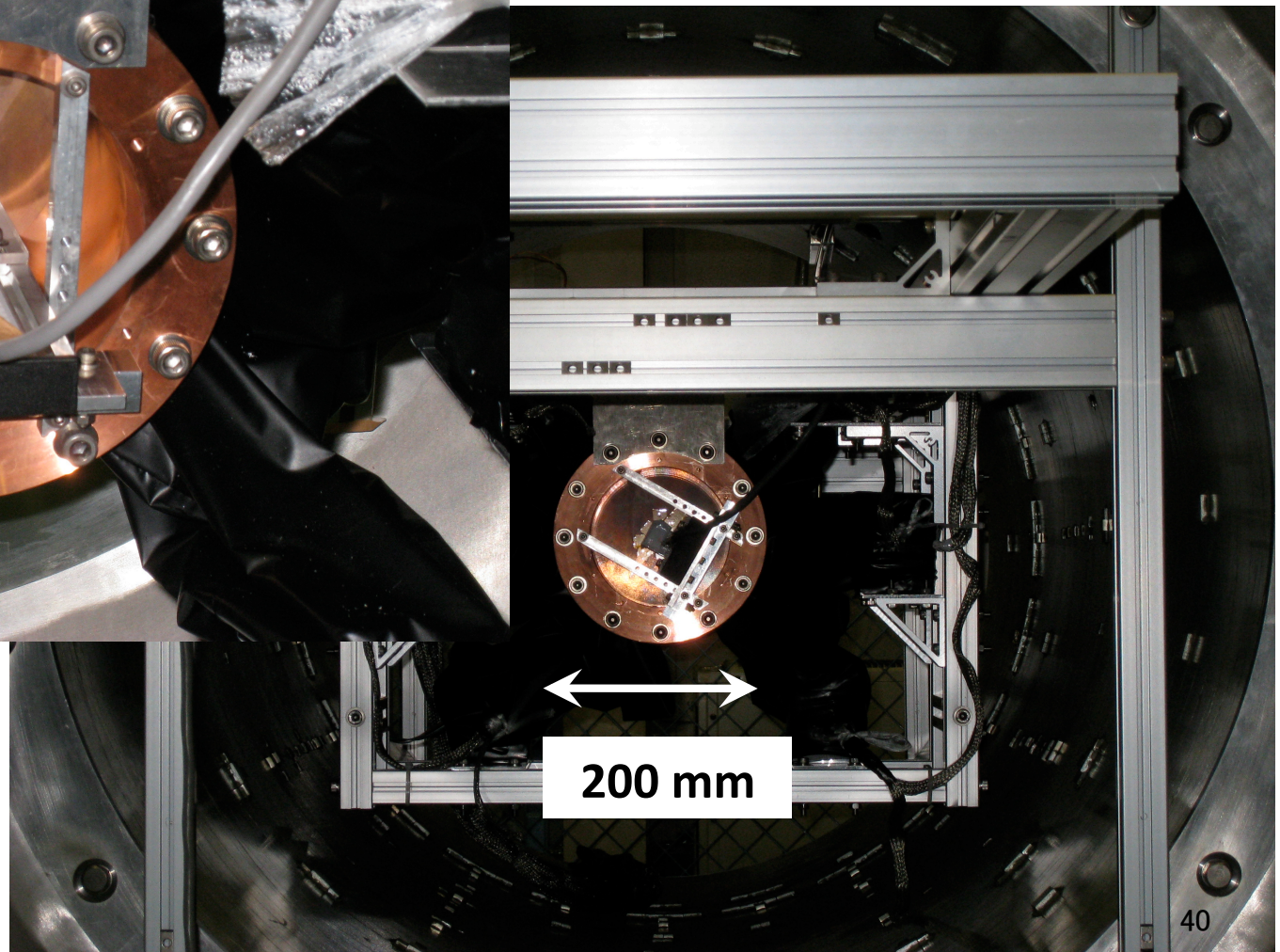


# Magnetic Field Measurement

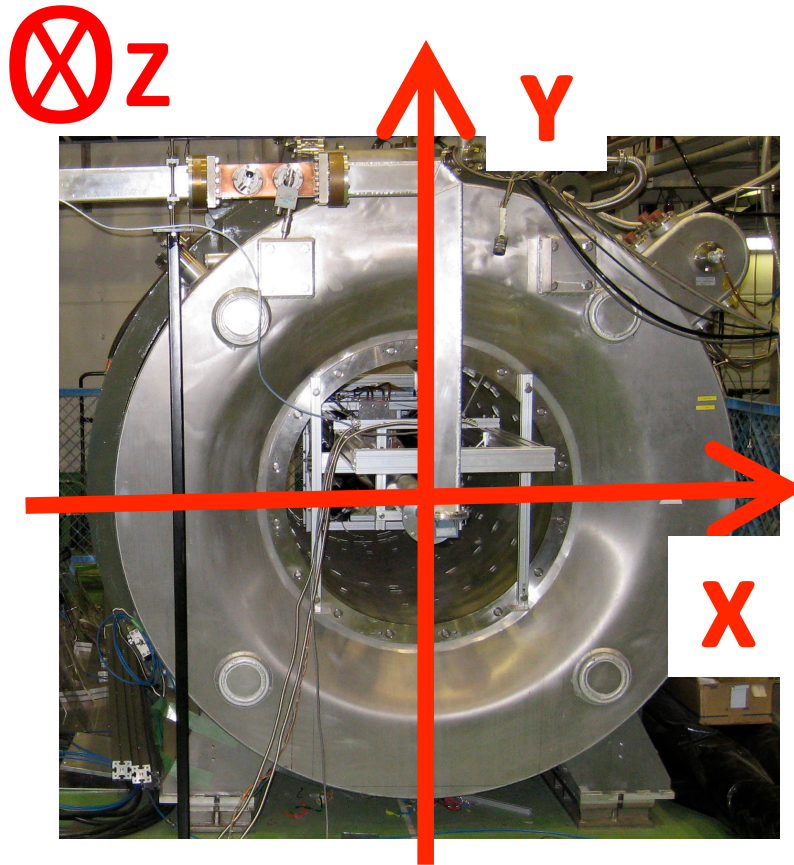


Measured the magnetic field at 310 points in the RF cavity using NMR probe.

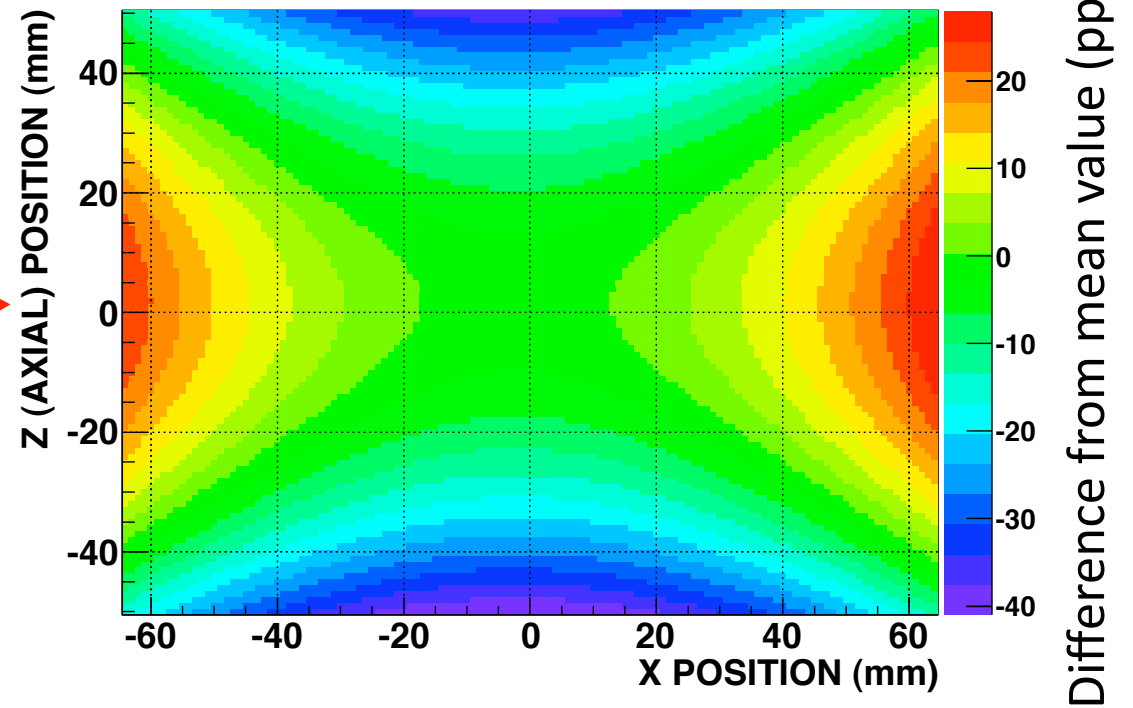
Made the map of the magnetic field.



# Non-Uniformity of the Magnetic Field



Magnetic field distribution on Y=0 plane. (0 is the center of the cavity)



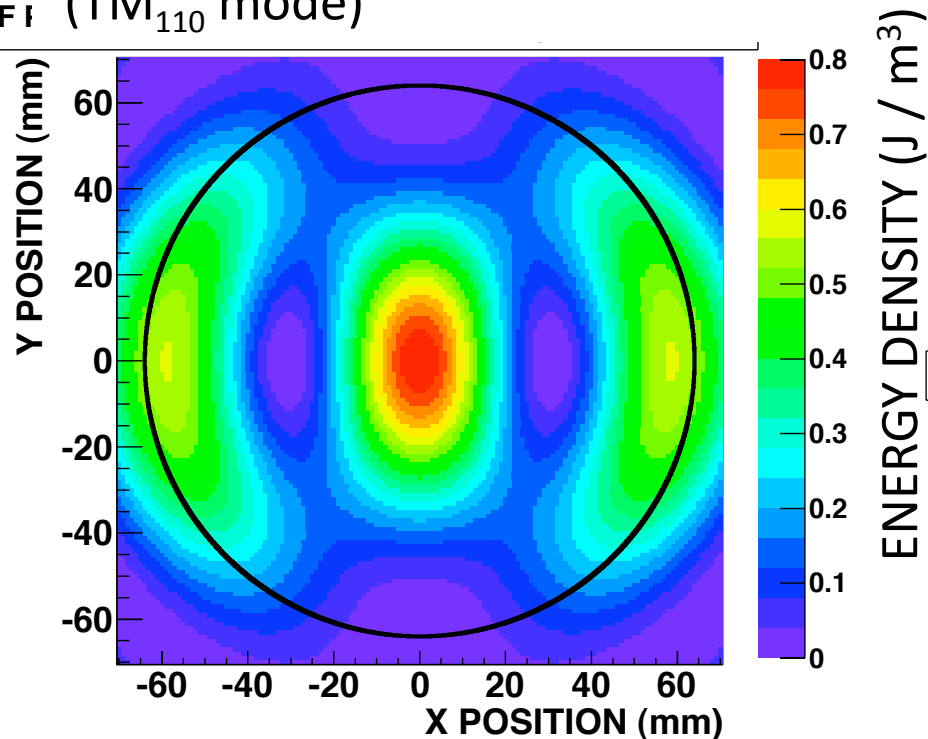
- Non-uniformity of the magnetic field is serious systematic uncertainty.
- Non-uniformity in the RF cavity is 23.1 ppm (RMS).



# Weight 1. RF Power distribution

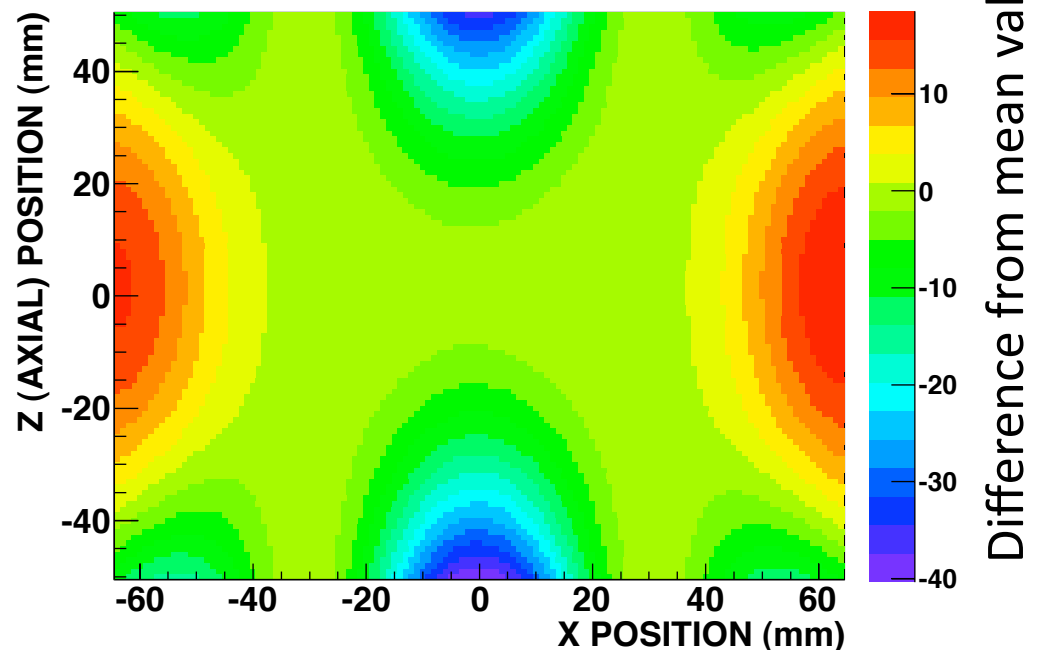
Energy distribution of RF magnetic field

RF I (TM<sub>110</sub> mode)



After weighting the RF magnetic field power

Magnetic field distribution on Y=0 plane  
(O is the center of the cavity)

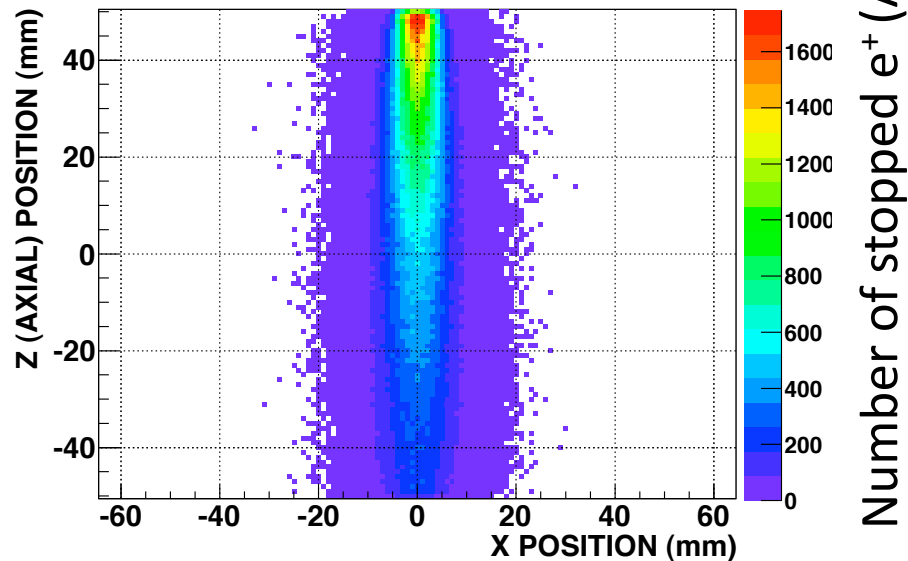


Uniformity gets better to  
14.2 ppm (RMS)



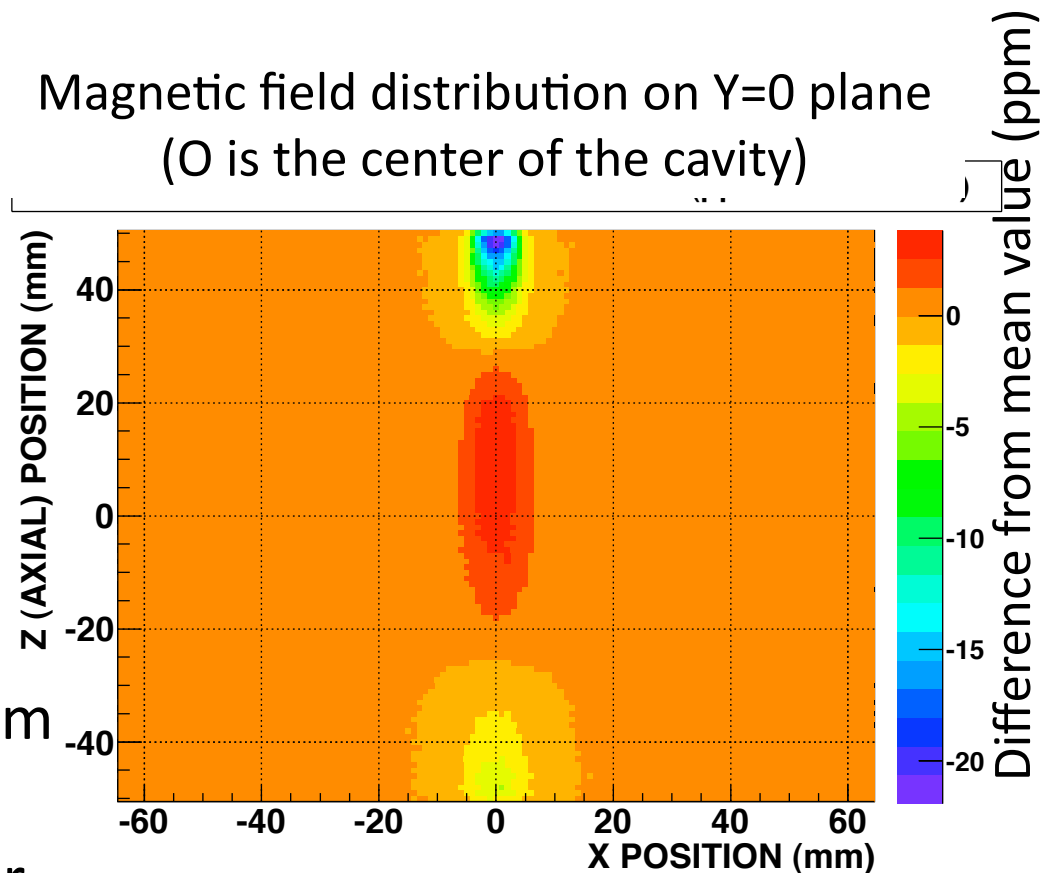
# Weight 2. Positron Stop Position

$e^+$  stop position distribution  
(Geant4 MC simulation)



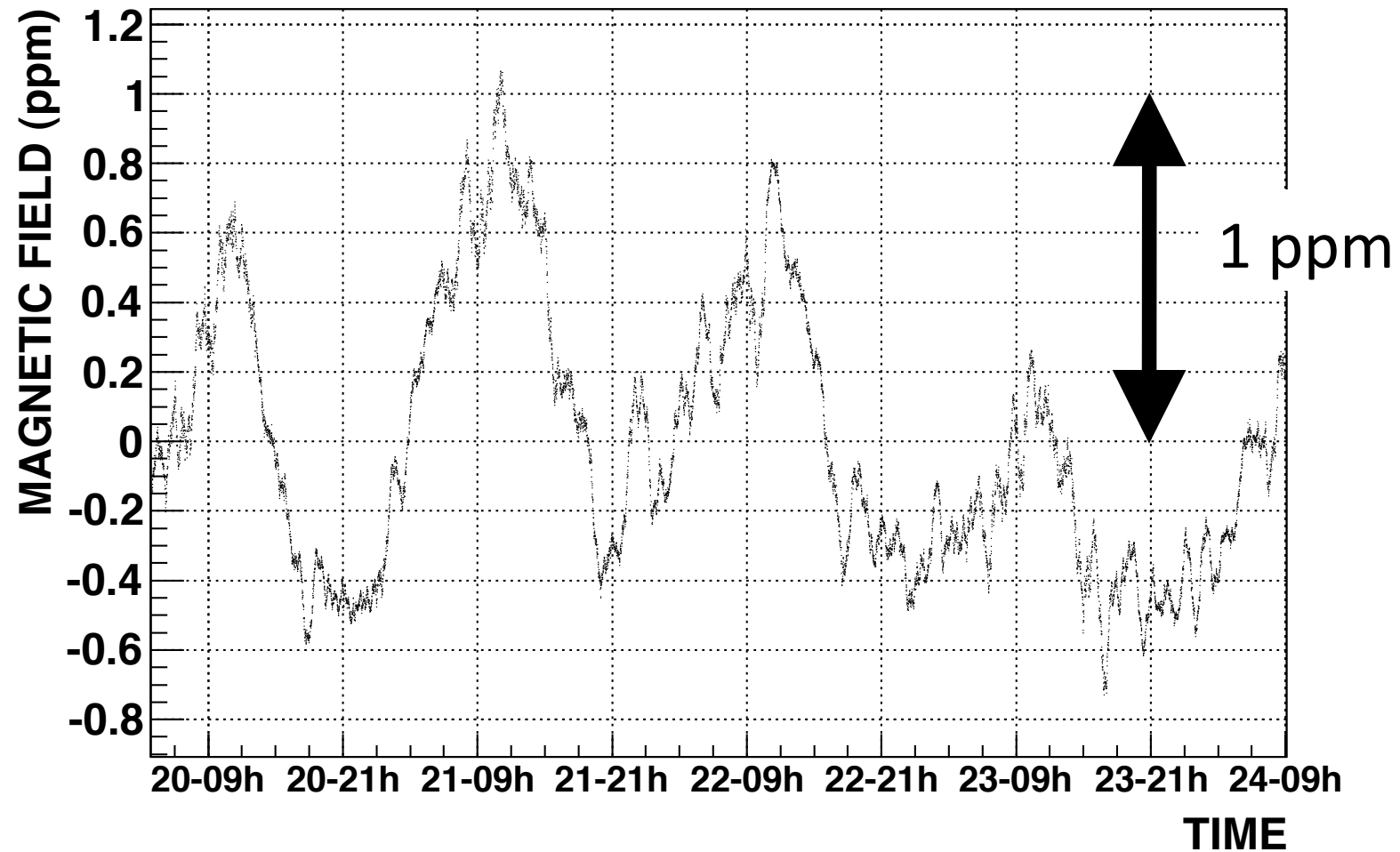
After applying the RF power  
and  $e^+$  stop position weight

Magnetic field distribution on Y=0 plane  
(0 is the center of the cavity)

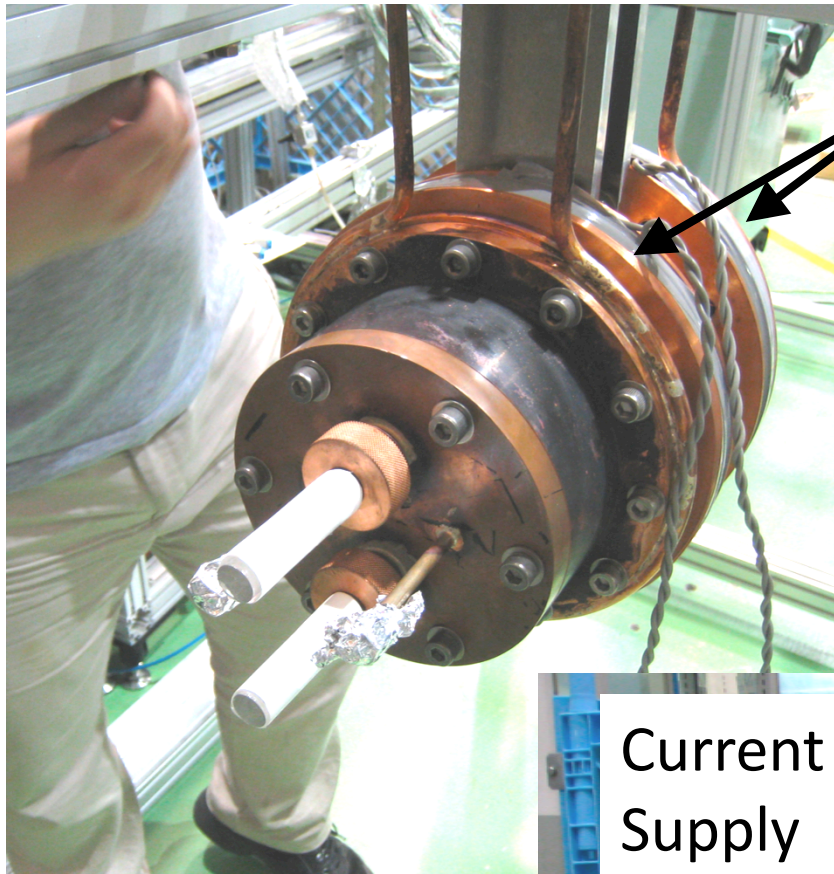


Uniformity gets better to 10.4 ppm  
(RMS) (21 ppm in HFS)  
→ This is the final systematic error.

# Stability of the magnetic field



# Compensation Magnet



2 ring coils

Clock  
Generator &  
NMR  
Magnetometer

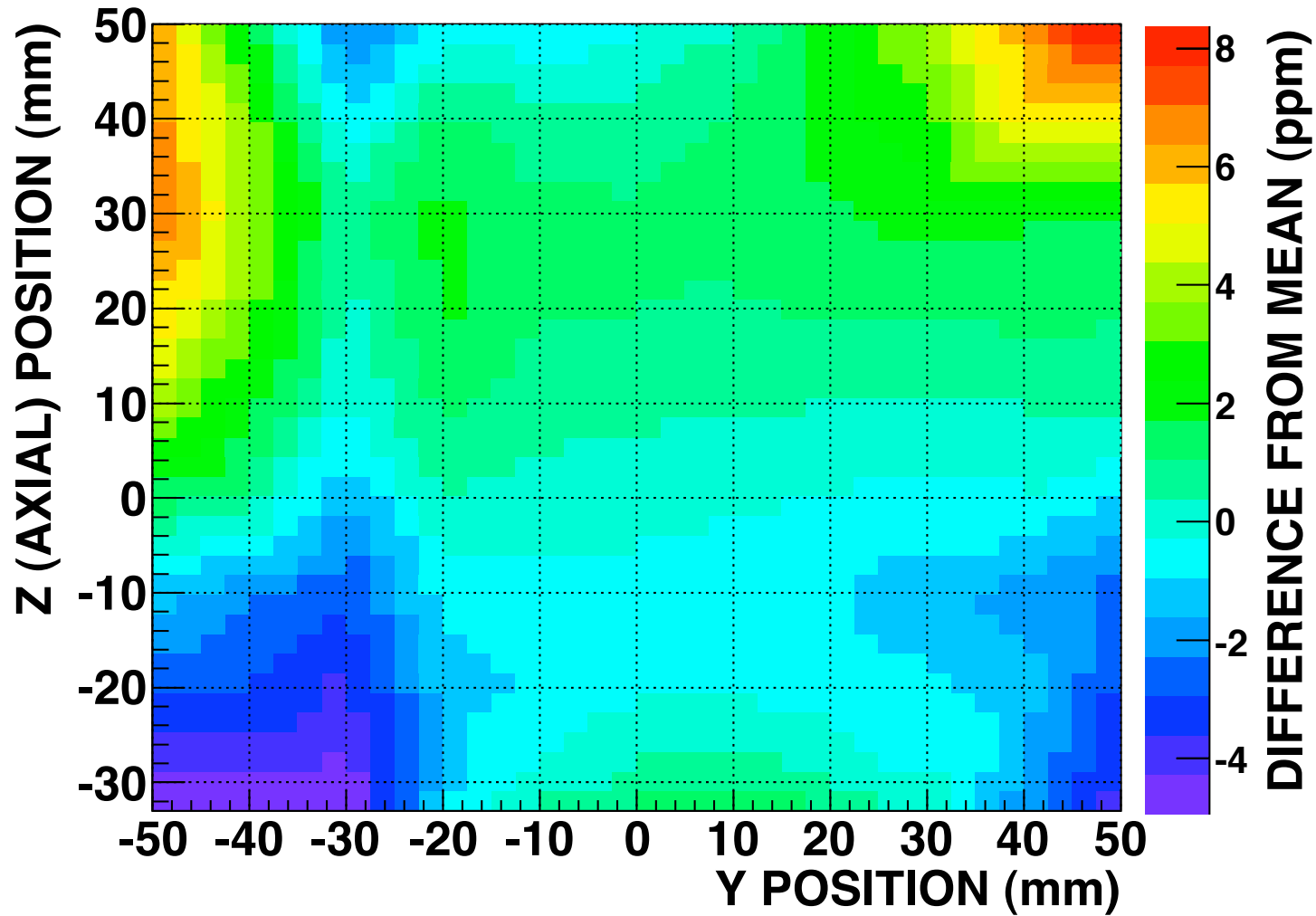
Oscilloscope



Current  
Supply

# Compensation Magnet

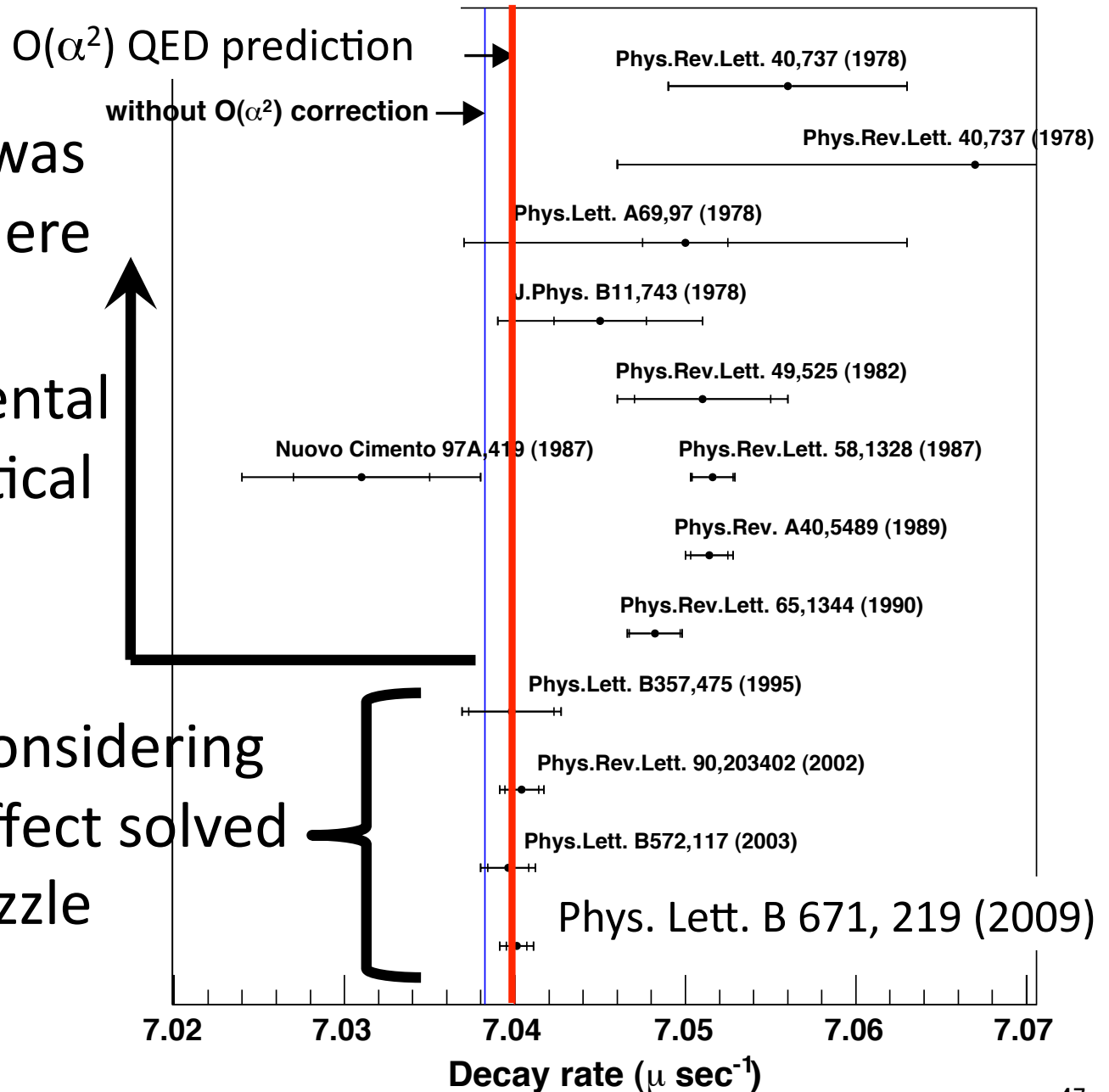
## MAGNETIC FIELD DISTRIBUTION



# Solution to o-Ps lifetime puzzle

Ps thermalization was not considered. There was a discrepancy between experimental values and theoretical calculation.

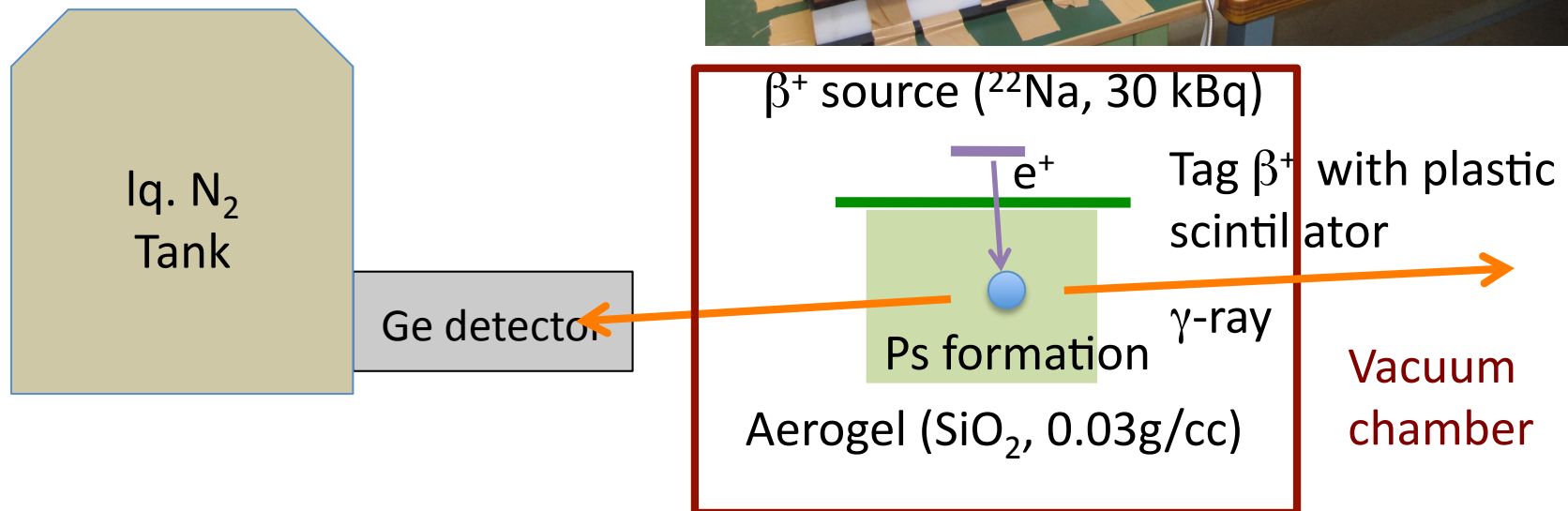
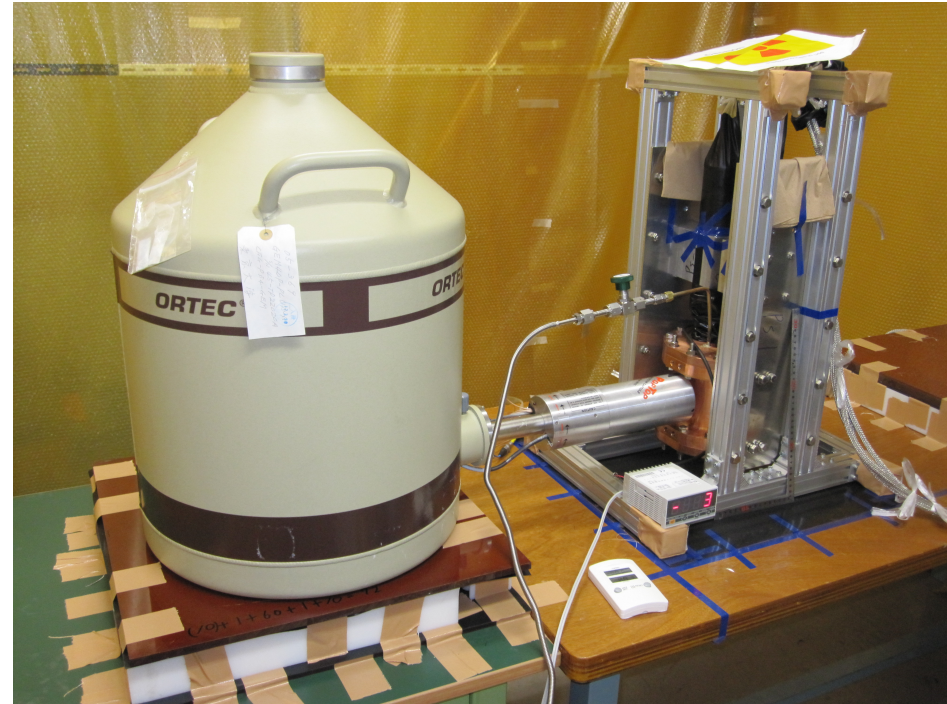
New experiments considering Ps thermalization effect solved the o-Ps lifetime puzzle





# Measurement of Ps Thermalization Experimental Setup (Overall)

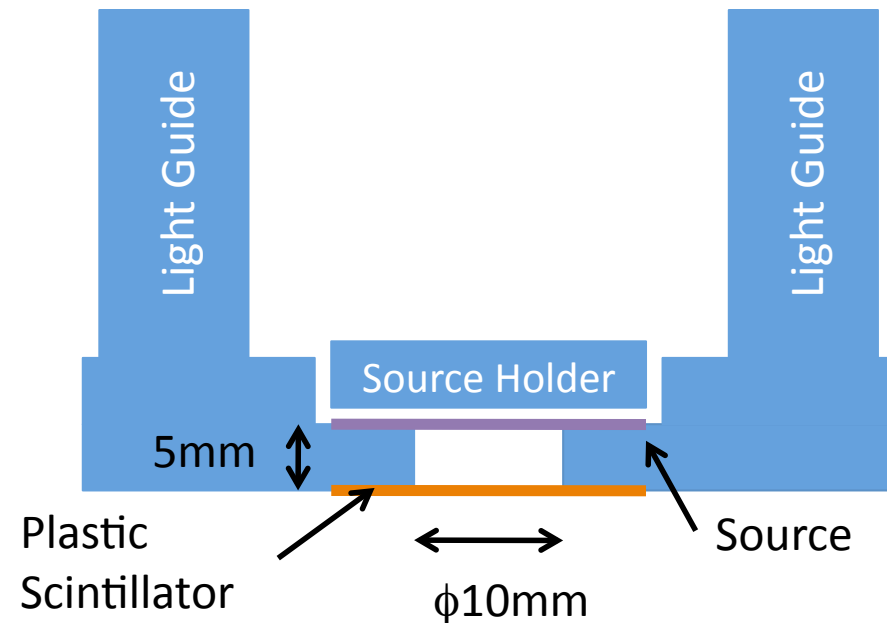
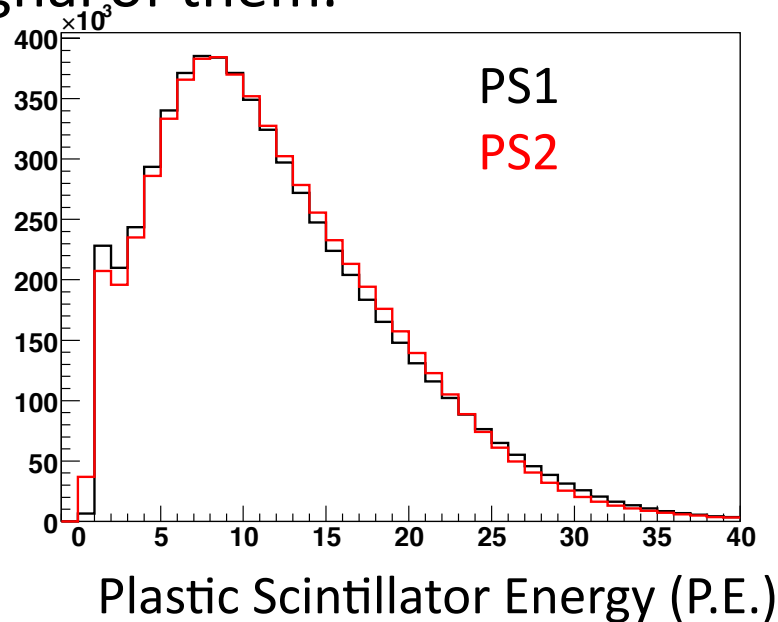
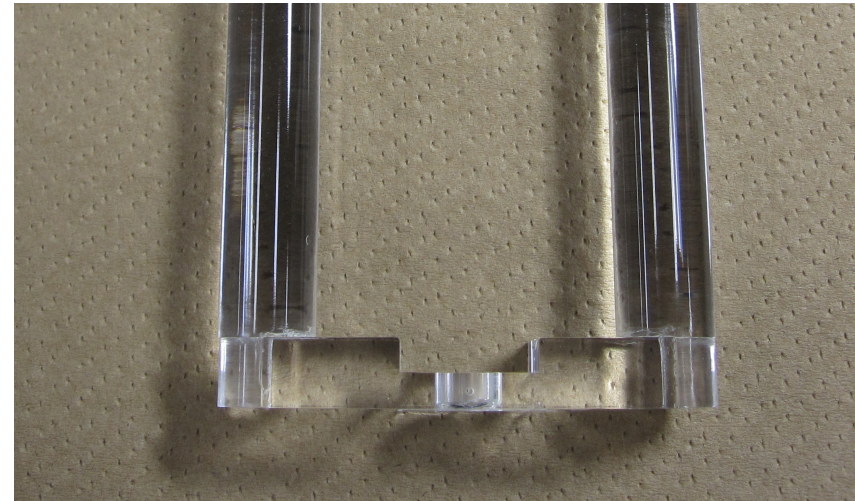
- Timing; START by Plastic Scintillator & STOP by Ge detector
- Stop  $e^+$  in Silica aerogel and form Ps
- Source is inside the vacuum chamber.
- Change thermalization condition by changing the gas and its pressures.



# Ps Thermalization Experimental Setup ( $\beta^+$ -System)

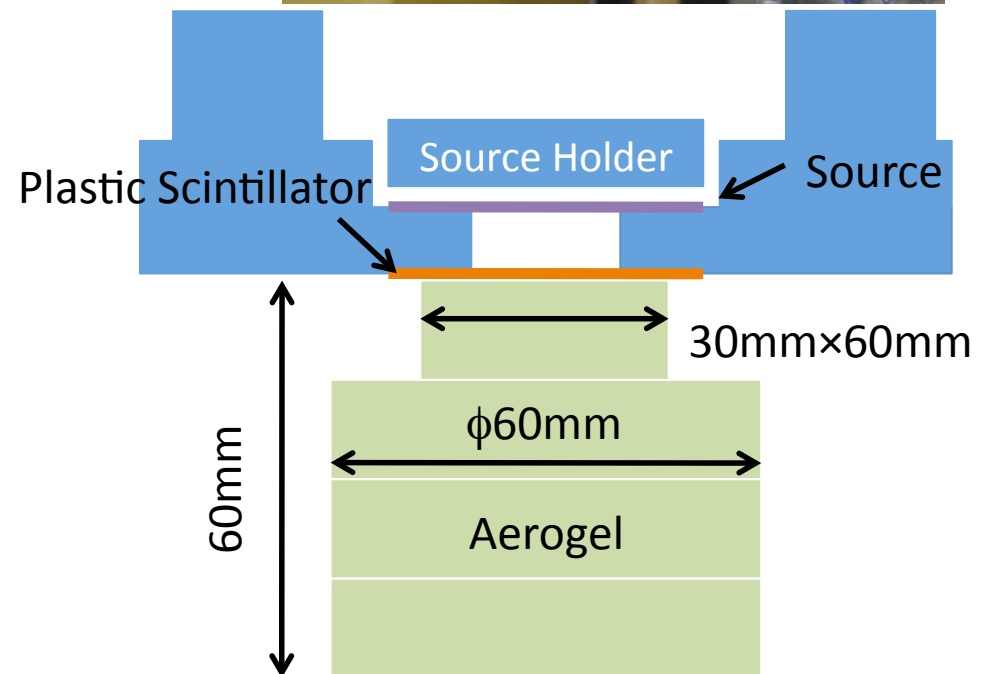
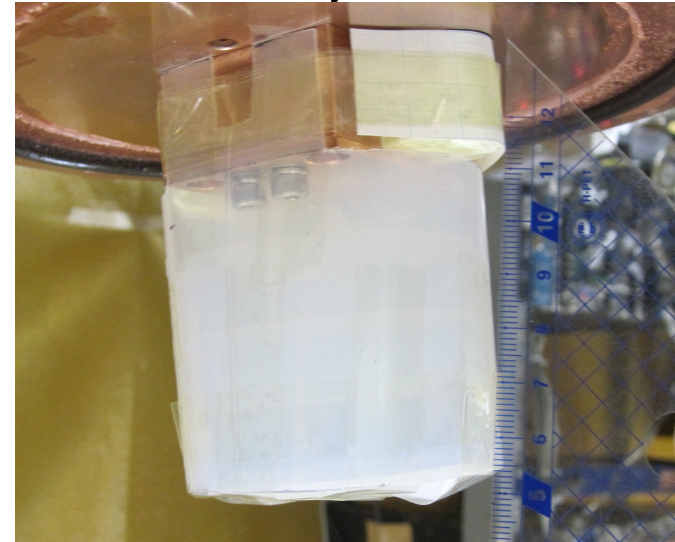
- Source:  $^{22}\text{Na}$  (30kBq, Ti foiled)
- $\beta^+$ : Detect by Plastic Scintillator (200 $\mu\text{m}$  thick)
- The scintillation lights are guided through light guides into two R329s.

→START is made by coincidence signal of them.



# Ps Thermalization Experimental Setup (Aerogel, Vacuum Chamber)

- Silica Aerogel: 0.03g/cc  
(High Ps formation fraction.  
Effect from aerogel is measured independently.)
- Vacuum Chamber: Oxygen-free Copper  
 $\phi 130\text{mm} \times 100\text{mm} \times t 1.5\text{mm}$



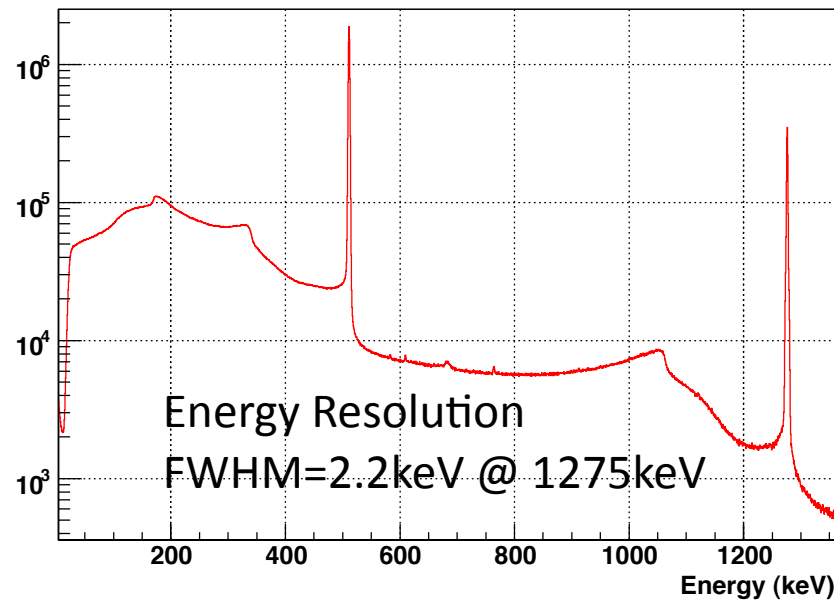


# Ps Thermalization Experimental Setup ( $\gamma$ -ray Detector)

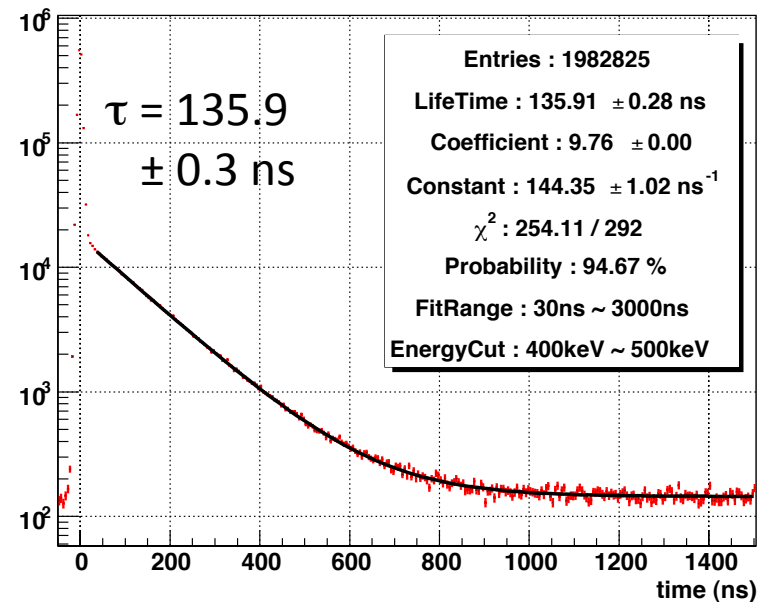
- Ge detectors (Ortec GEM 38195-P-plus series)
- Timing Correction is performed by cutting the slow components using triple threshold.

< Measurement with Silica aerogel (0.03 g/cc) + i-C<sub>4</sub>H<sub>10</sub> (0.16 atm) >

Energy Histogram

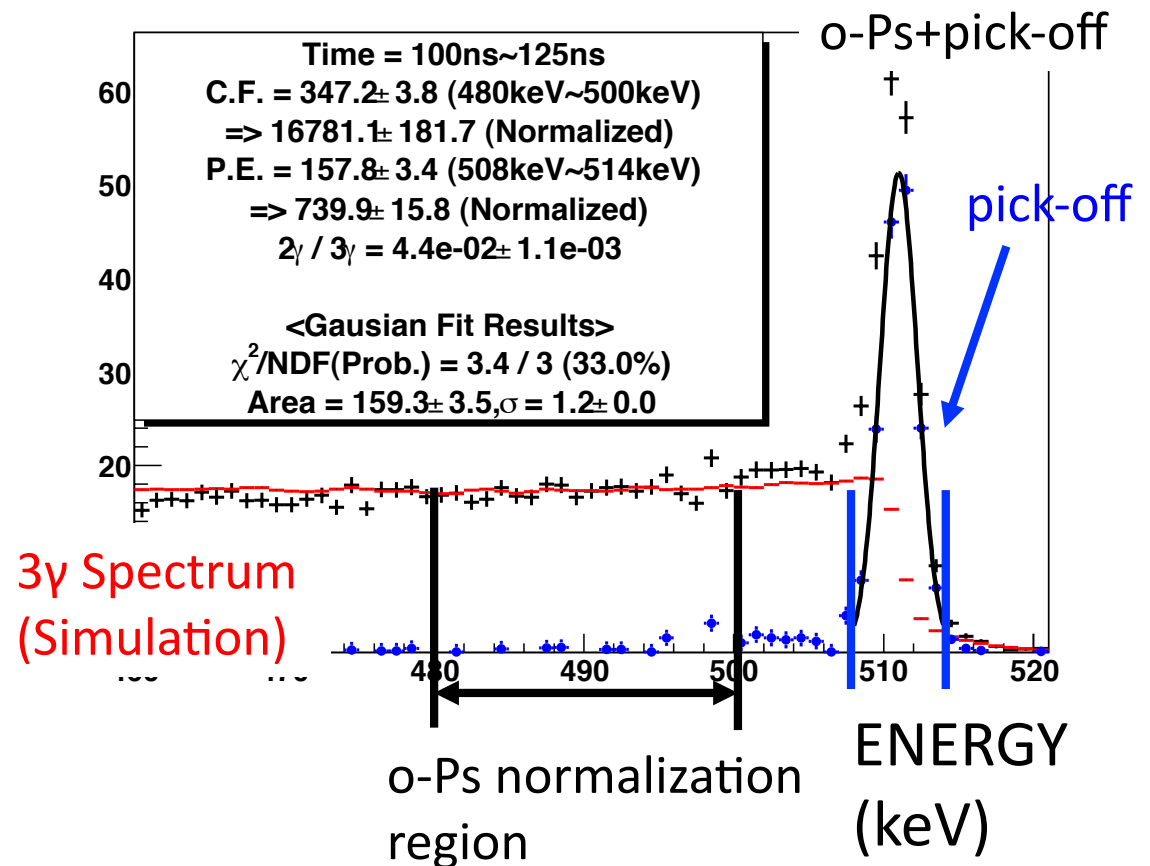
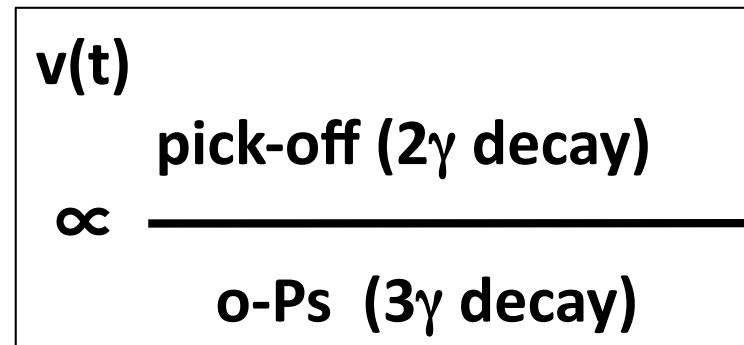


Timing Histogram  
(after correction)



# Estimation of o-Ps and pick-off annihilation

- 1, Make energy spectra at each time.
- 2, o-Ps ( $3\gamma$ ) is normalized at continuous Compton-free region (480—500 keV)
- 3, pick-off spectrum  
= data  
– o-Ps spectrum  
(count pickoff events in 508—514 keV)
- 4, Correction of o-Ps, Pick-off by MC simulation



# ACAR

## Angular Correlation of Annihilation Radiation

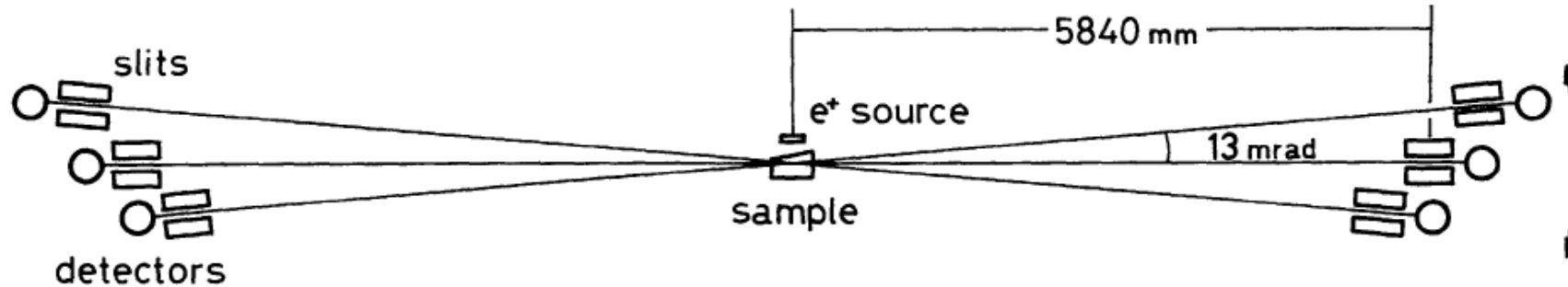


Fig. 1. One dimensional angular correlation apparatus having three pairs of long (800 mm) NaI(Tl) scintillation detectors. Adjacent pairs are separated by 13 milliradians.

Phys. Rev. A 52, 258 (1995)

J. Phys. B 31, 329 (1998)

J. Phys. B 36, 4191 (2003)

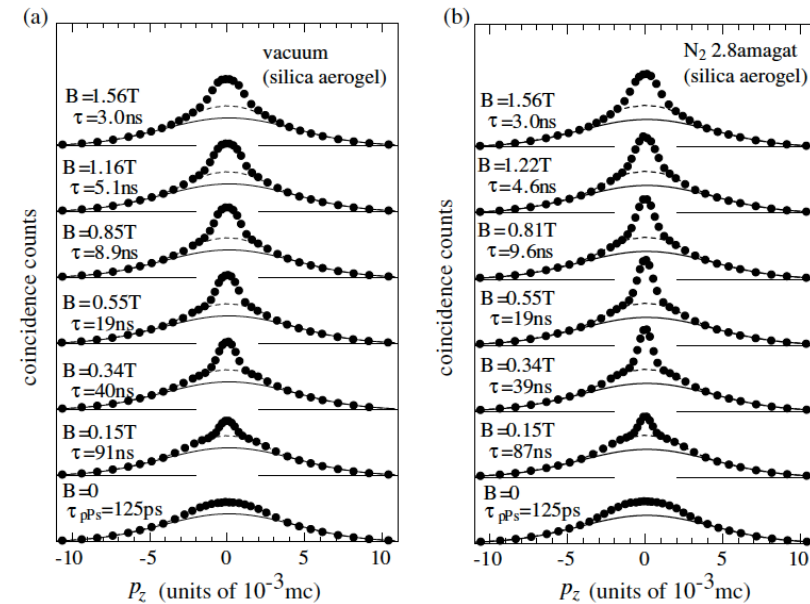


Figure 1. ACAR data for silica aerogel (a) in vacuum and (b) in 2.8 amagat of  $N_2$ . The full and broken curves indicate the broad component and the  $p$ -Ps component, respectively. The data are normalized to the broad component intensity. The magnetic flux density and the mean lifetime of  $\sigma^+$ -Ps,  $\tau$ , are indicated in the figure. The mean lifetime of  $p$ -Ps,  $\tau_{pPs}$ , is also indicated for the case of no magnetic field.

# DBS

## Doppler-Broadening Spectroscopy

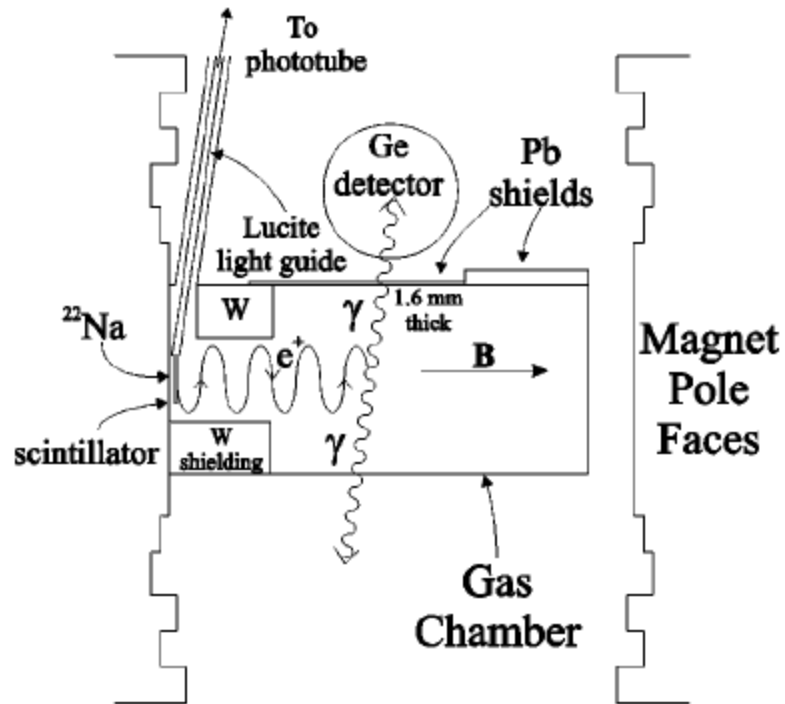


FIG. 2. Experimental apparatus. Positrons from  $^{22}\text{Na}$  decay pass through a thin scintillator and enter a gas chamber. A magnetic field confines the trajectories near the axis. Positrons that stop in the gas can form Ps. Annihilation  $\gamma$  rays are detected in a Ge crystal.

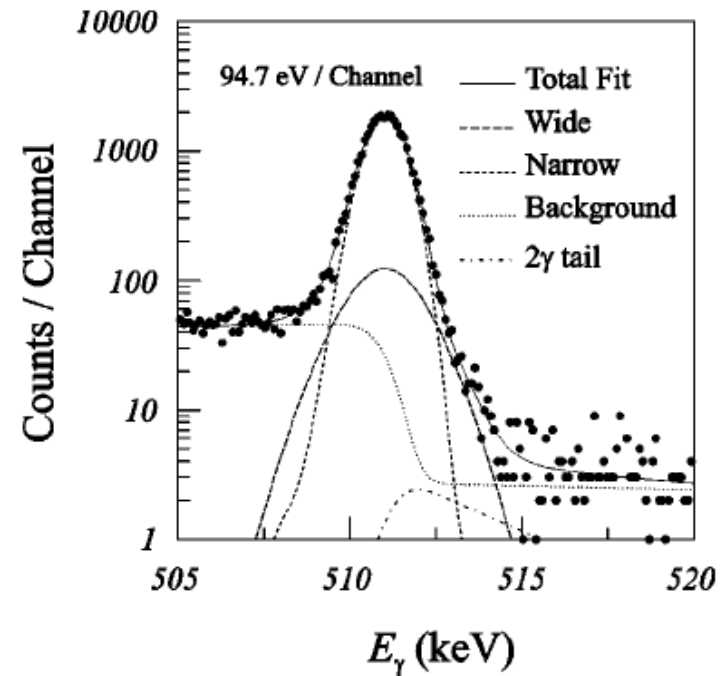


FIG. 3. Typical thermalization data. The Doppler-broadened 511-keV photopeak is resolved into two Gaussians, a step background, and a  $2\gamma$  tail. The first three components are shown convoluted with the intrinsic detector resolution; the  $2\gamma$  tail is also convoluted with the narrow Gaussian.

Phys. Rev. Lett. 80, 3727 (1998)

Phys. Rev. A 67, 022504 (2003)

# Ps thermalization function

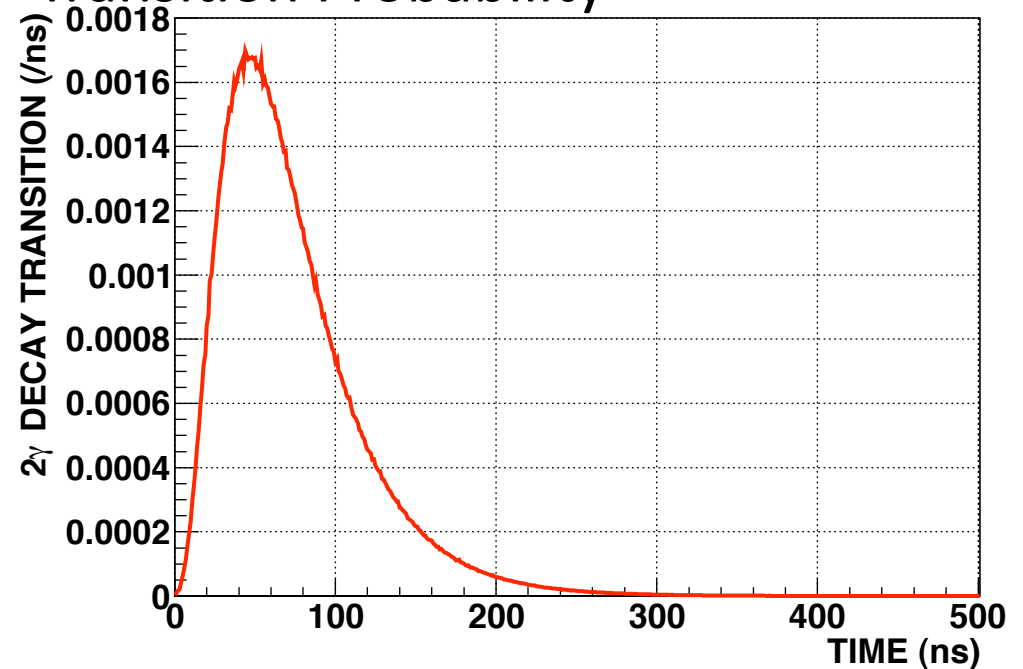
$$\frac{dE_{av}(t)}{dt} = -\sqrt{2m_{Ps}E_{av}(t)} \left( E_{av}(t) - \frac{3}{2}k_B T \right) \left( \frac{8}{3} \sqrt{\frac{2}{3\pi}} \frac{2\sigma_m n}{M} + \alpha \left( \frac{E_{av}(t)}{k_B T} \right)^\beta \right)$$

$$E_{av}(t) = \left( \frac{1 + Ae^{-bt}}{1 - Ae^{-bt}} \right)^2 \frac{3}{2} k_B T . \quad b = \frac{8}{3} \sqrt{\frac{2}{3\pi}} \frac{2\sigma_m n}{M} \sqrt{3m_{Ps}k_B T}$$

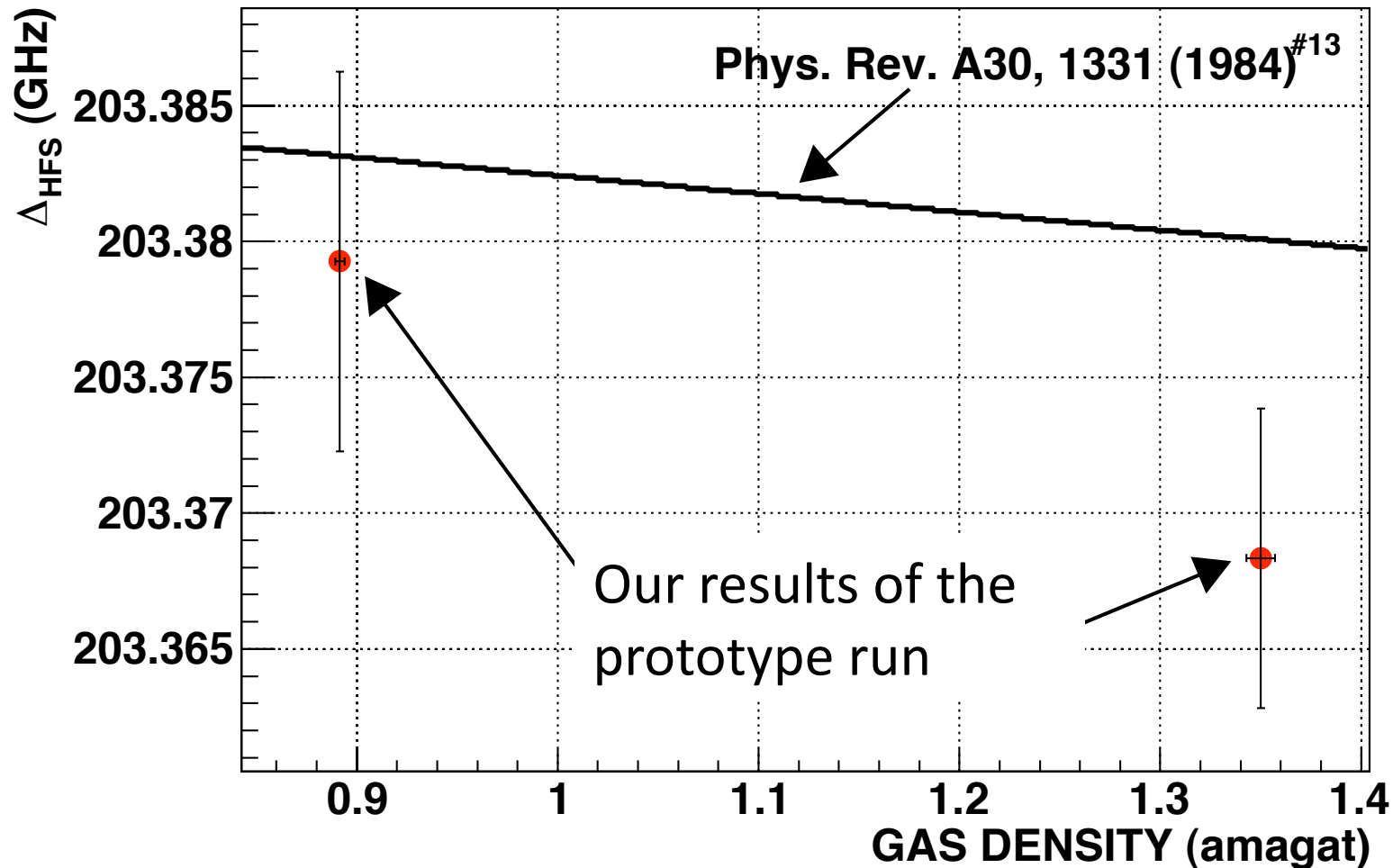
$$A = \frac{\sqrt{E_0} - \sqrt{\frac{3}{2}k_B T}}{\sqrt{E_0} + \sqrt{\frac{3}{2}k_B T}}$$

| Gas                                | $E_0$ (eV)                             | $\sigma_m$ (Å <sup>2</sup> ) |
|------------------------------------|--|------------------------------|
| N <sub>2</sub>                     | 2.07 <sup>+0.04</sup> <sub>-0.03</sub> | 13.0 ± 0.5                   |
| iso-C <sub>4</sub> H <sub>10</sub> | 3.1 <sup>+1.0</sup> <sub>-0.7</sub>    | 146 ± 11                     |

Weight Function:  
Transition Probability



# Gas Pressure Dependence

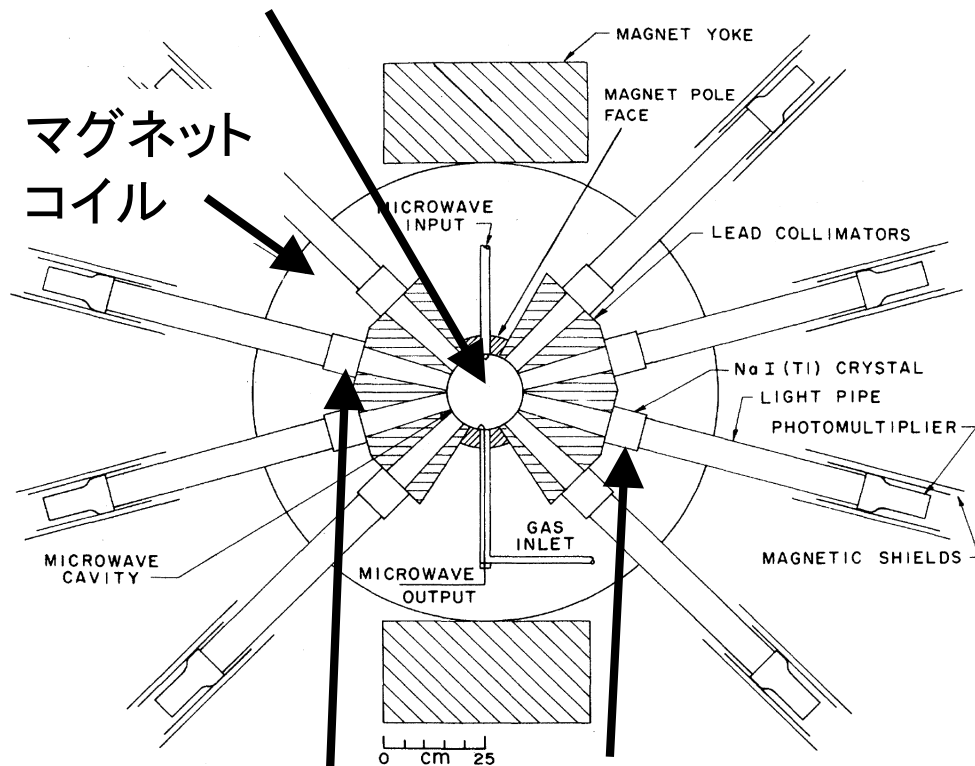


The pressure dependence is not clarified by our results of the prototype run, but it is consistent with the previous experiment.

→ Apply a correction of -33 ppm/atm (Ritter et al., 1984)

# 過去の実験と、考えられる系統誤差

RFキャビティにガスを入れて  
 $\beta^+$ 線からポジトロニウムを生成



NaI(Tl)シンチレータで  
Back-to-backに測定

「磁石の神様」V. ヒューズらの  
実験セットアップ(80年代)

## 系統誤差1. 磁場の非一様性

磁場の不定性がそのまま  
測定結果の主な系統誤差に。

一方、ポジトロニウムの  
生成領域は数cmに及ぶ。

→ 大きなサイズでppm精度での  
磁場制御は非常に困難。

## 系統誤差2. 物質の効果

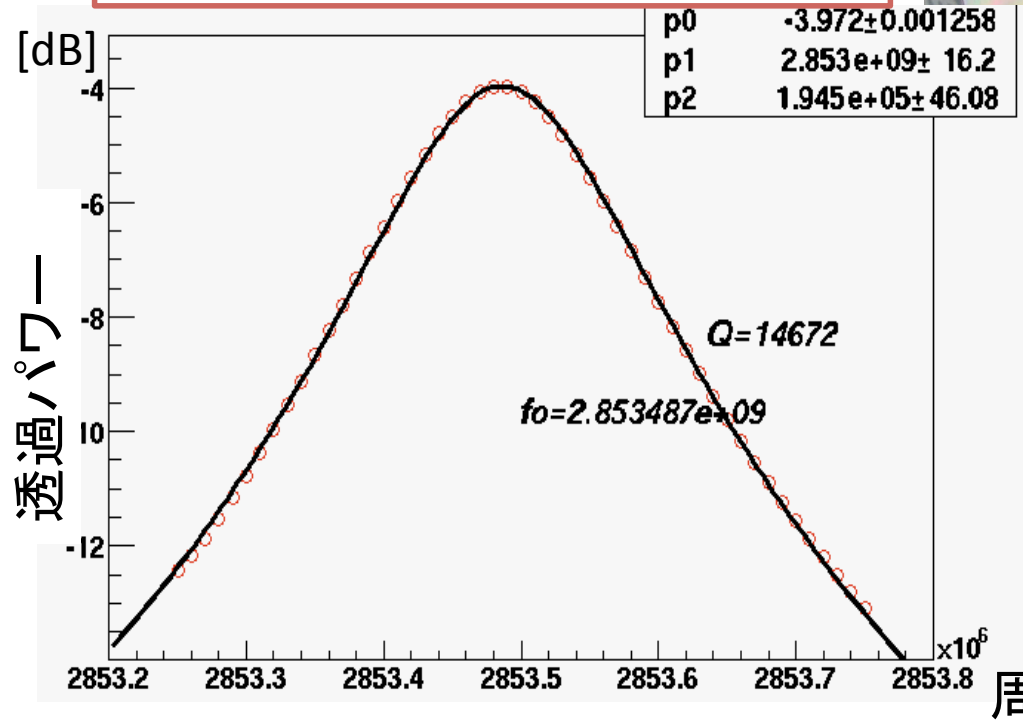
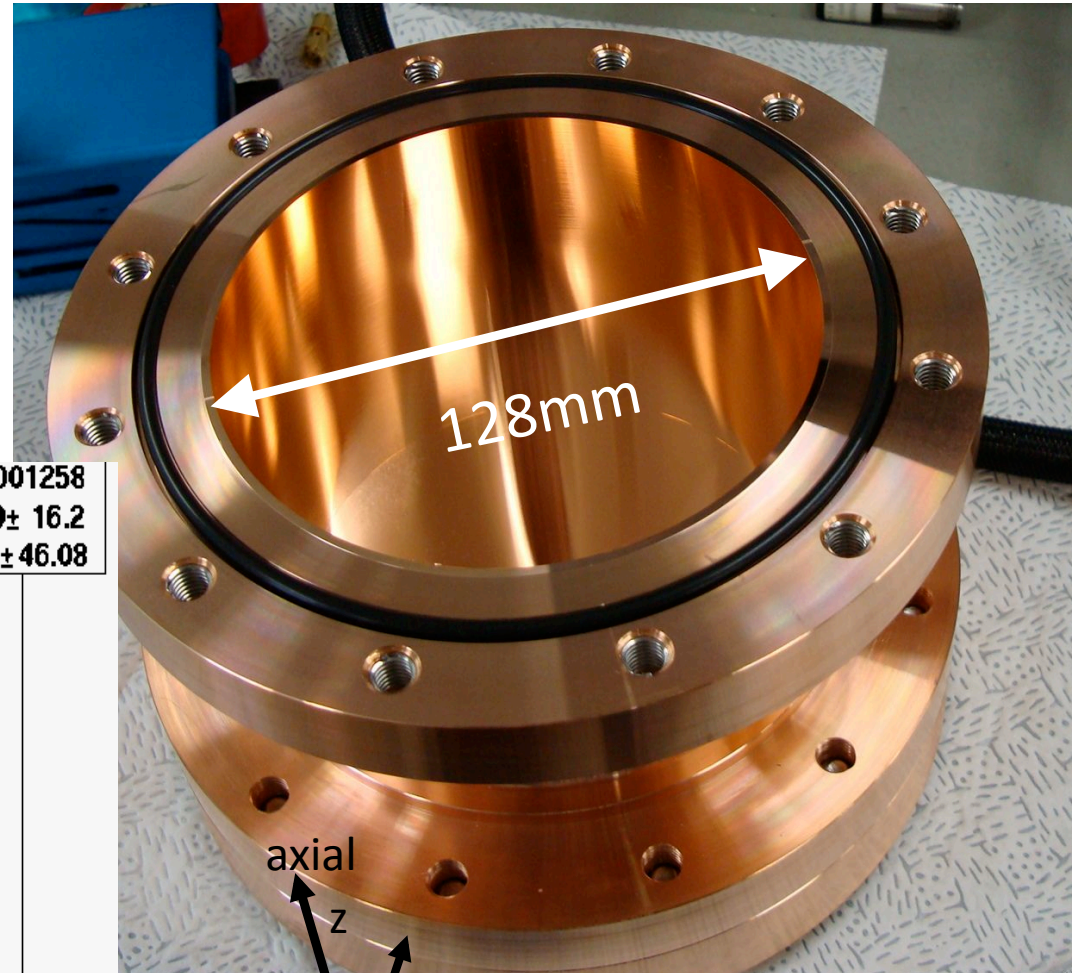
ポジトロニウム生成には、物質  
(ここではガス)が必要不可欠だが、  
物質は、HFSの値をずらしてしまう。

過去の実験では、物質の効果  
の評価が、十分でなかった可能性  
がある。



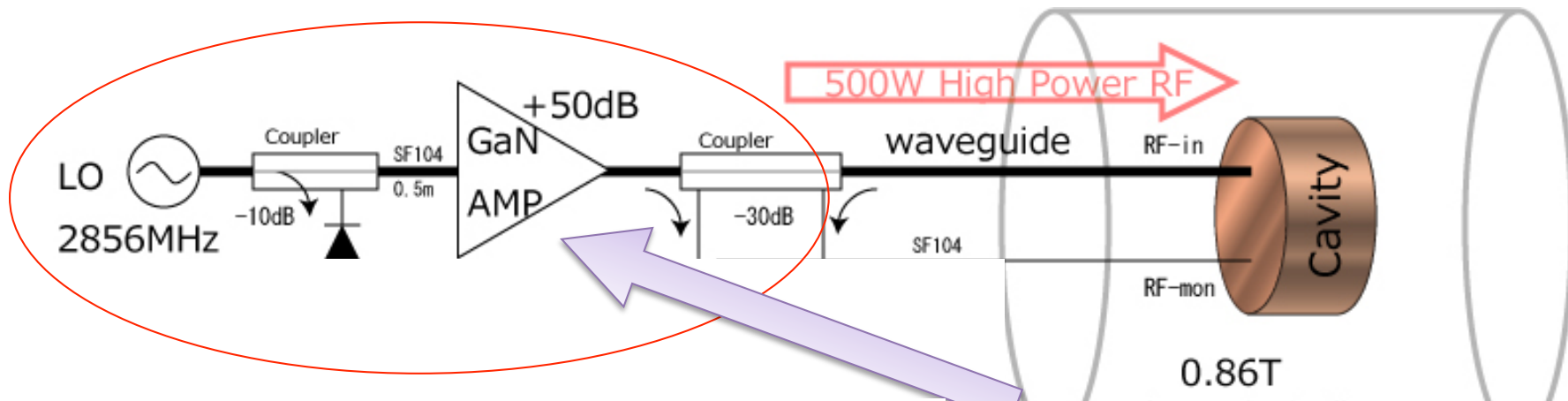
# RF キャビティ

1. 共振周波数:  
2856MHz
2. 共振モード:  $TM_{110}$
3. RF耐圧: 500W [CW]
4. 側面厚(Cu): 2.0 mm
5.  $Q=14700$

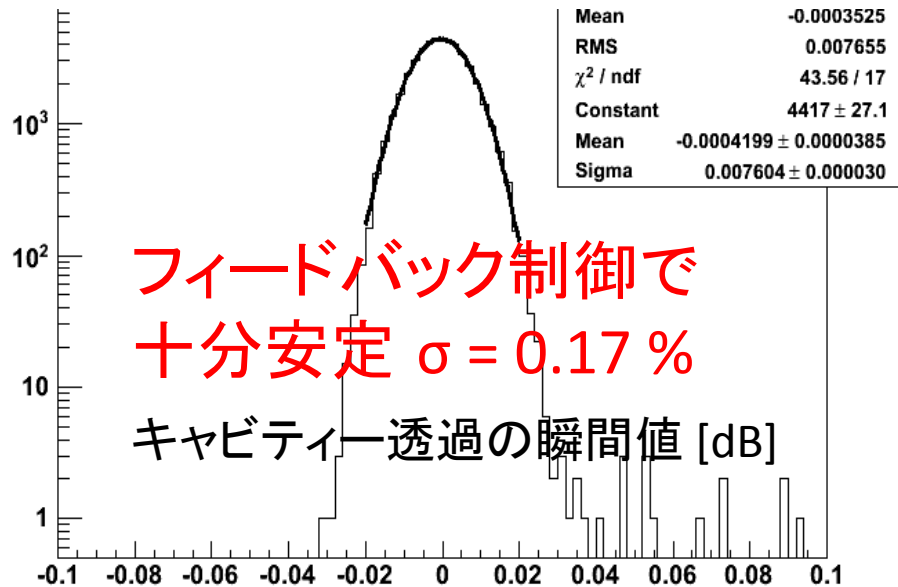




# RF AMP

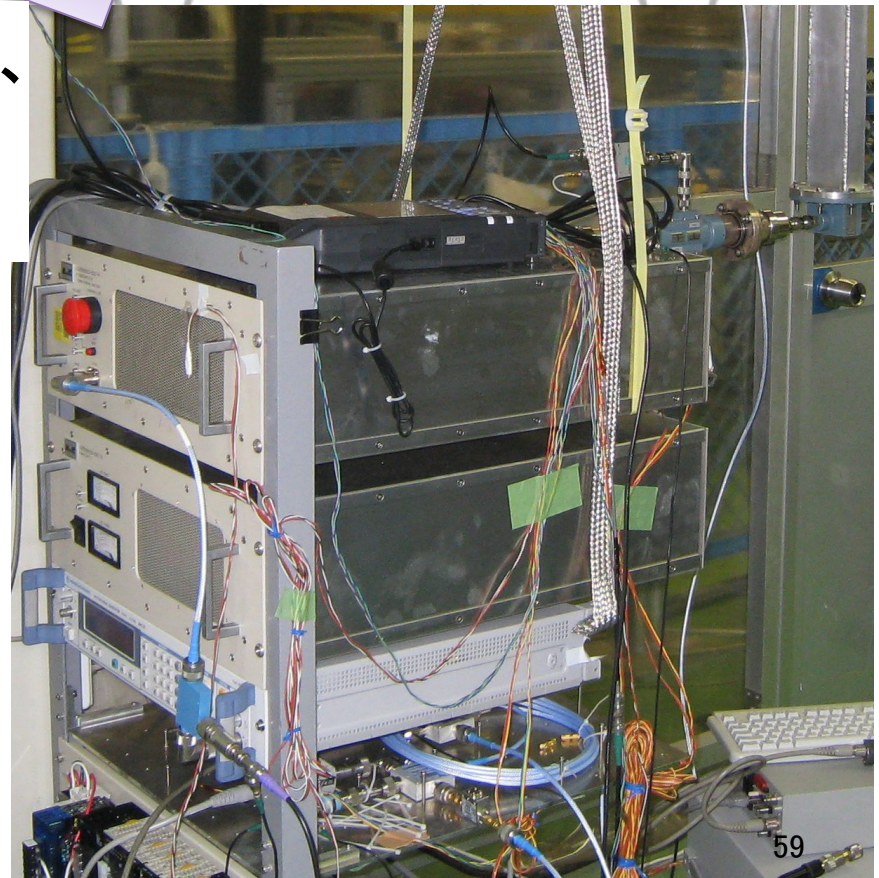


Signal Generatorで2856MHzのRFを出力、  
GaN AMPで+50dBの増幅をする。  
キャビティー内には、**409 W** 入る。

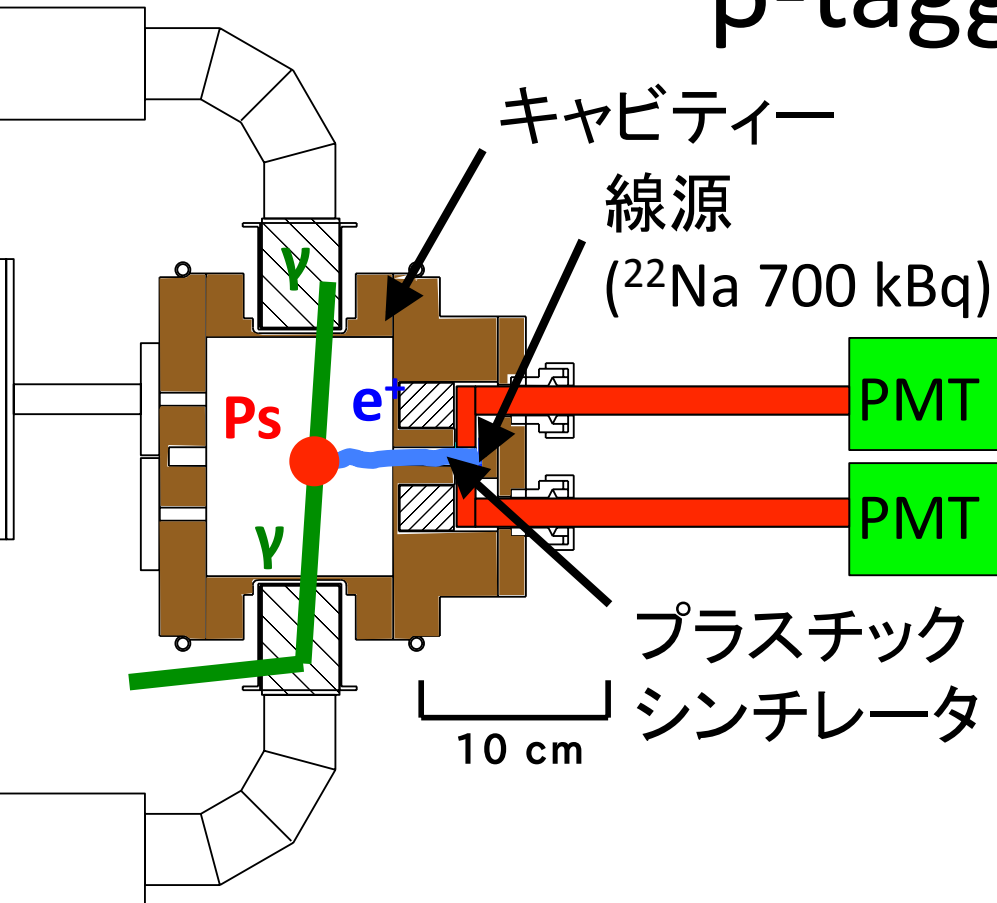


**フィードバック制御で  
十分安定  $\sigma = 0.17\%$**

キャビティー透過の瞬間値 [dB]



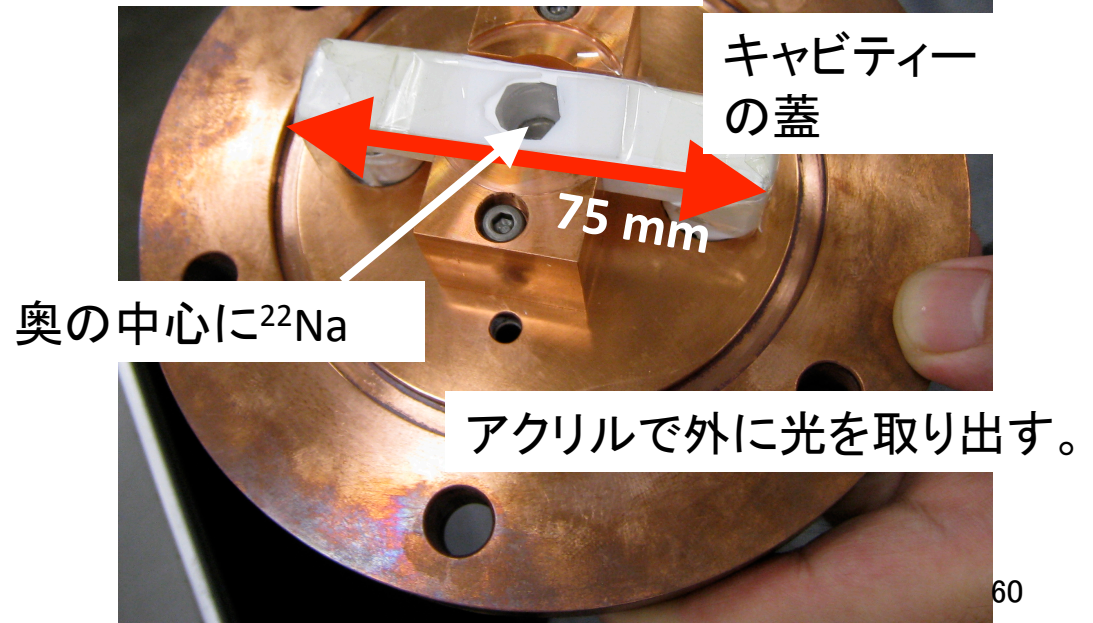
# $\beta$ -tagging system



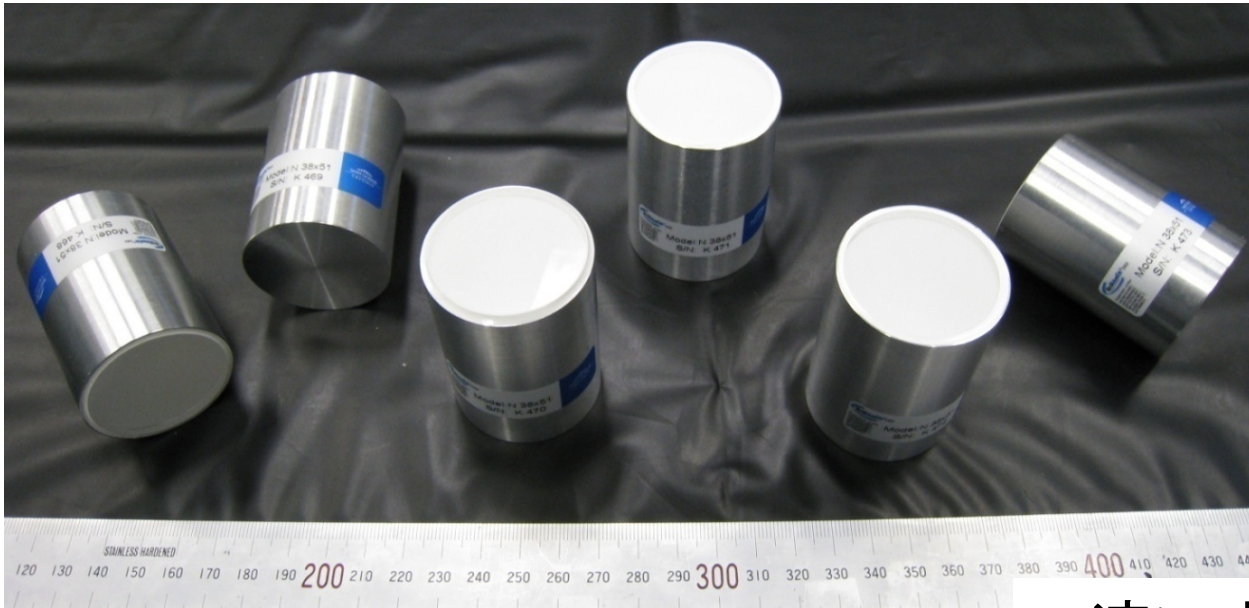
- ・プラスチックシンチレータを使って、線源から放出された $e^+$ をタグ。
- ・シグナルは、ファインメッシュPMTで両側読み出し。
- ・この時刻をポジトロニウム生成時刻( $t=0$ )とする。

- ・2つのPMTのシグナルをコインシデンスする。
- ・十分な光量( $\sim 10\text{p.e.}$ )が得られることを確認。

15 mm四方、厚さ0.2 mmのプラスチックシンチレータ



# ガンマ線検出器 (1) $\sim \text{LaBr}_3 \sim$

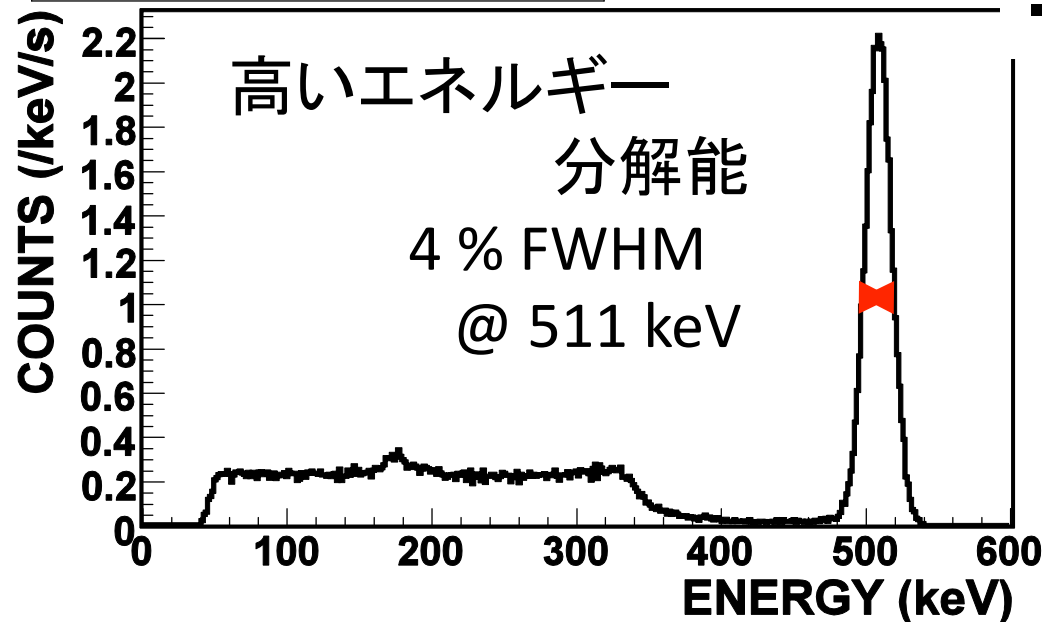


LaBr<sub>3</sub>(Ce)シンチレータ  
(直径1.5インチ、長さ2インチ)  
を6個使用

UVTライトガイドで光を導き、  
ファインメッシュPMTで、  
磁場中での読み出しを行う。

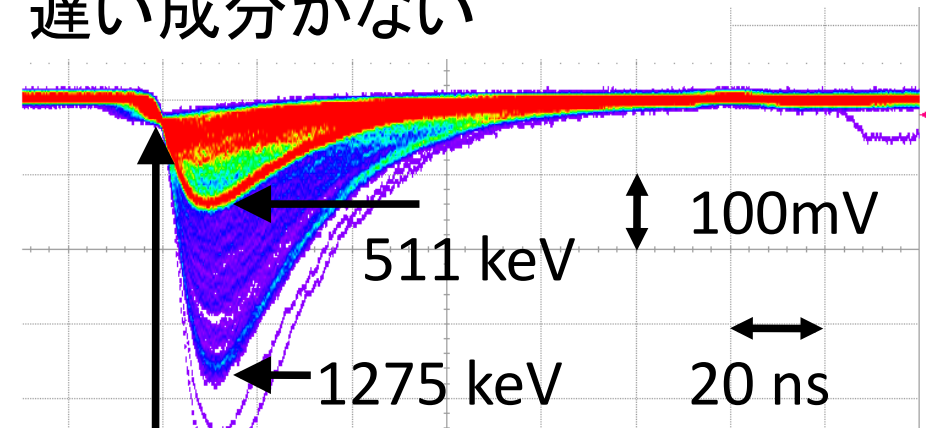
## ENERGY SPECTRUM

$^{22}\text{Na}$



- 速い立ち上がり
- 遅い成分がない

$^{22}\text{Na}$

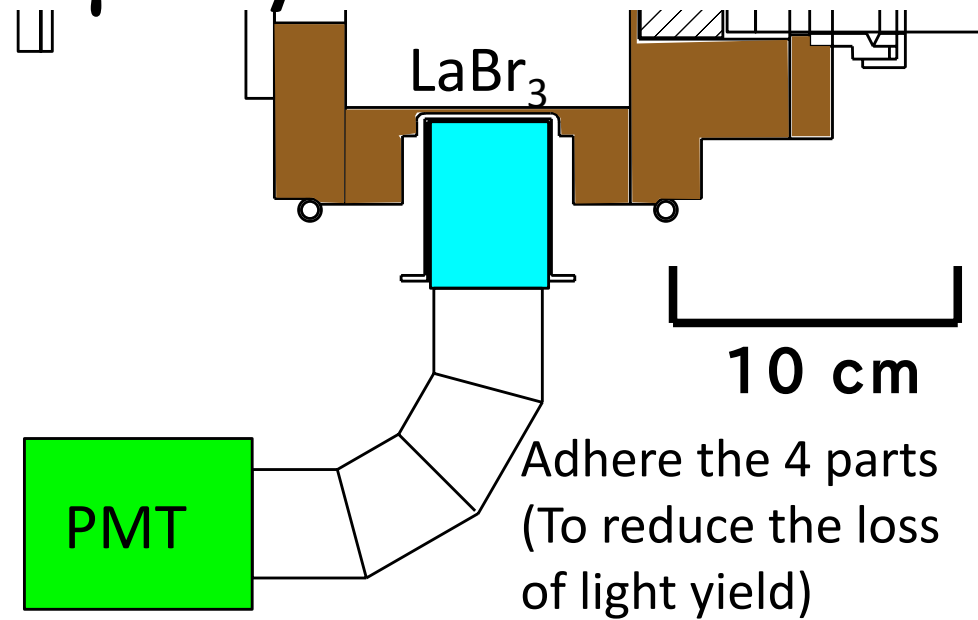


高い時間分解能

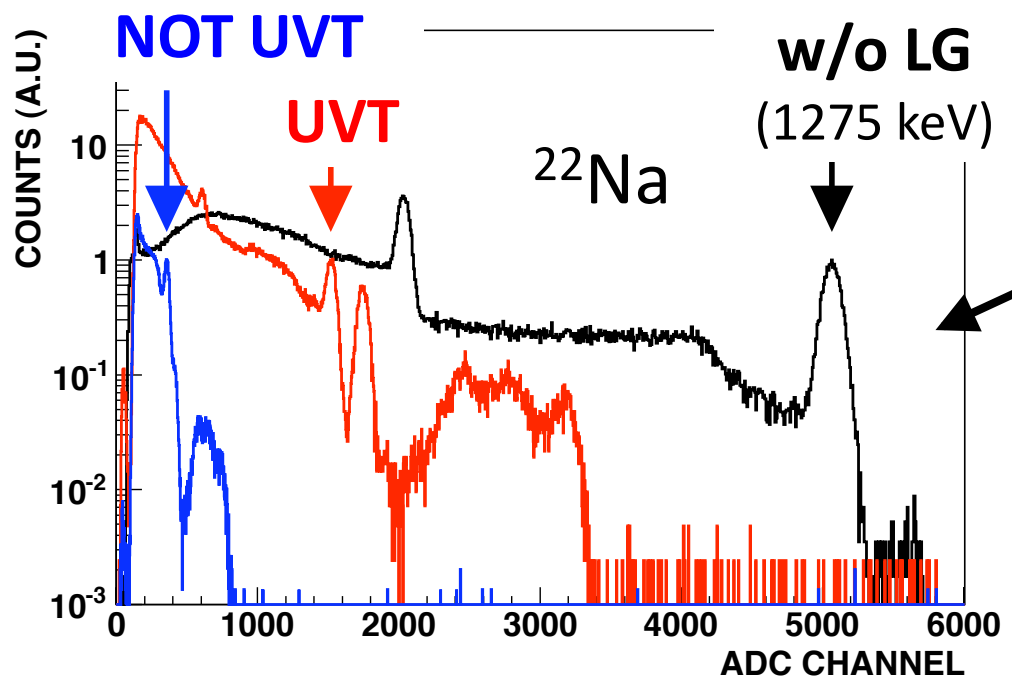
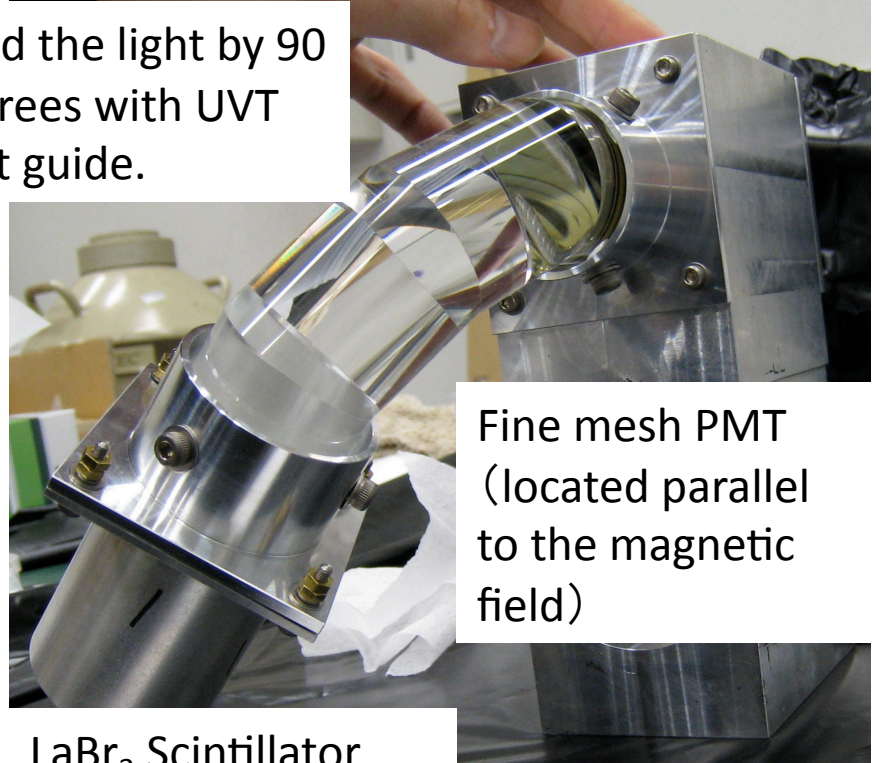
200 ps FWHM @ 511 keV



# $\gamma$ -ray Detectors $\sim$ UVT Light Guides $\sim$

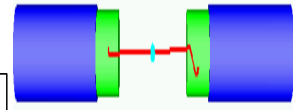
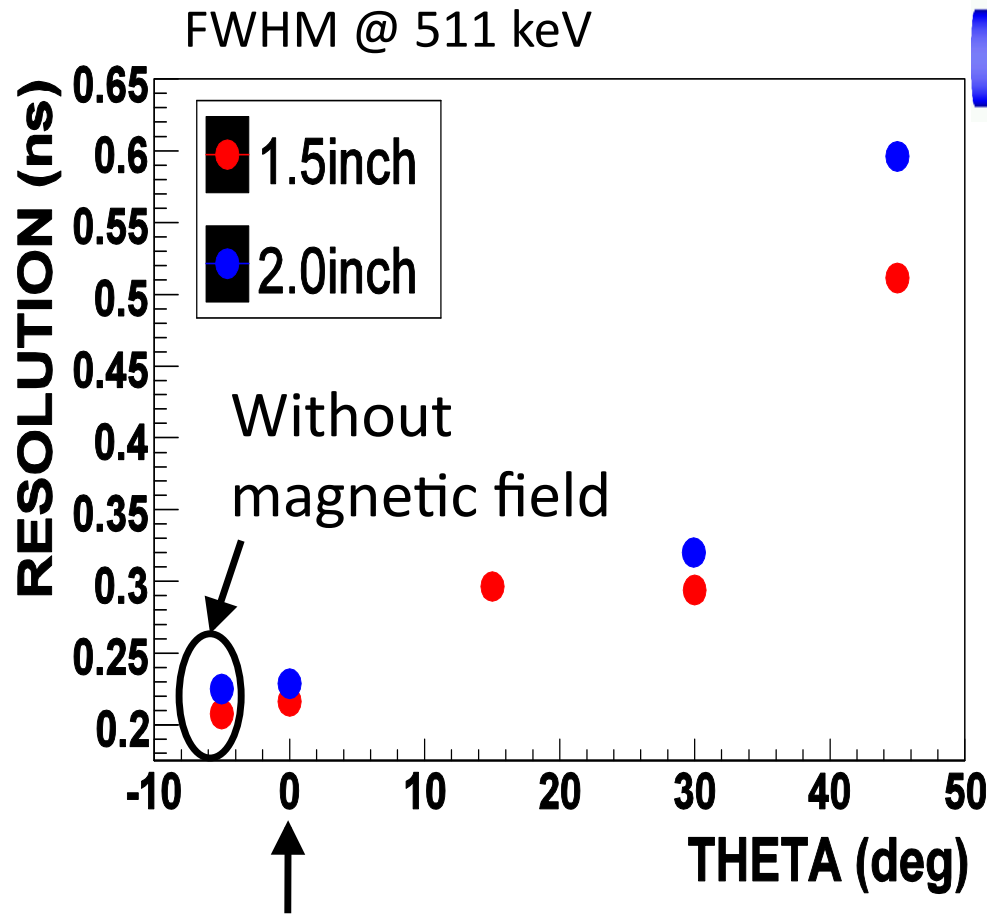


Bend the light by 90 degrees with UVT light guide.



Change of light yield with light guides  
 Light yield with **UVT** light guide is 30 % of that without light guide.  
 (only 7 % with **NOT UVT** light guide)

# Angle ( $\theta$ ) dependence of Timing Resolution

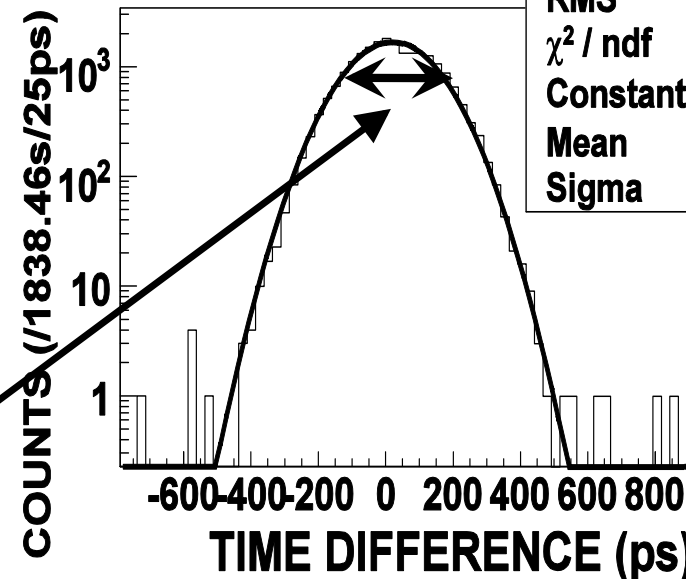


511 keV back-to-back

↓ Timing Difference without magnetic field (1.5 inch + 2.0 inch coincidence)

## TIMING SPECTRUM

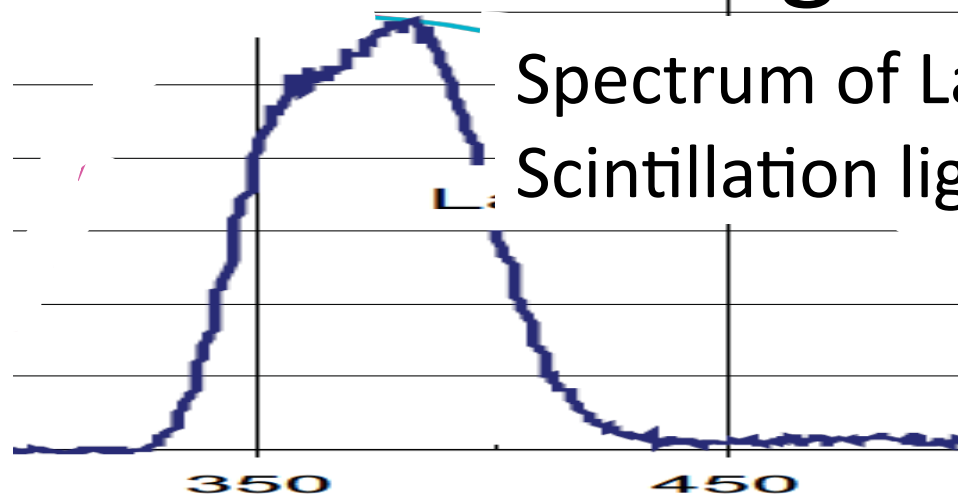
| pmt1_511keV_pmt2_511keV |                  |
|-------------------------|------------------|
| Entries                 | 21312            |
| Mean                    | 20.86            |
| RMS                     | 125.2            |
| $\chi^2 / \text{ndf}$   | 203.1 / 43       |
| Constant                | $1692 \pm 13.9$  |
| Mean                    | $20.67 \pm 0.86$ |
| Sigma                   | $124.4 \pm 0.6$  |



No change in  $0^\circ$ .

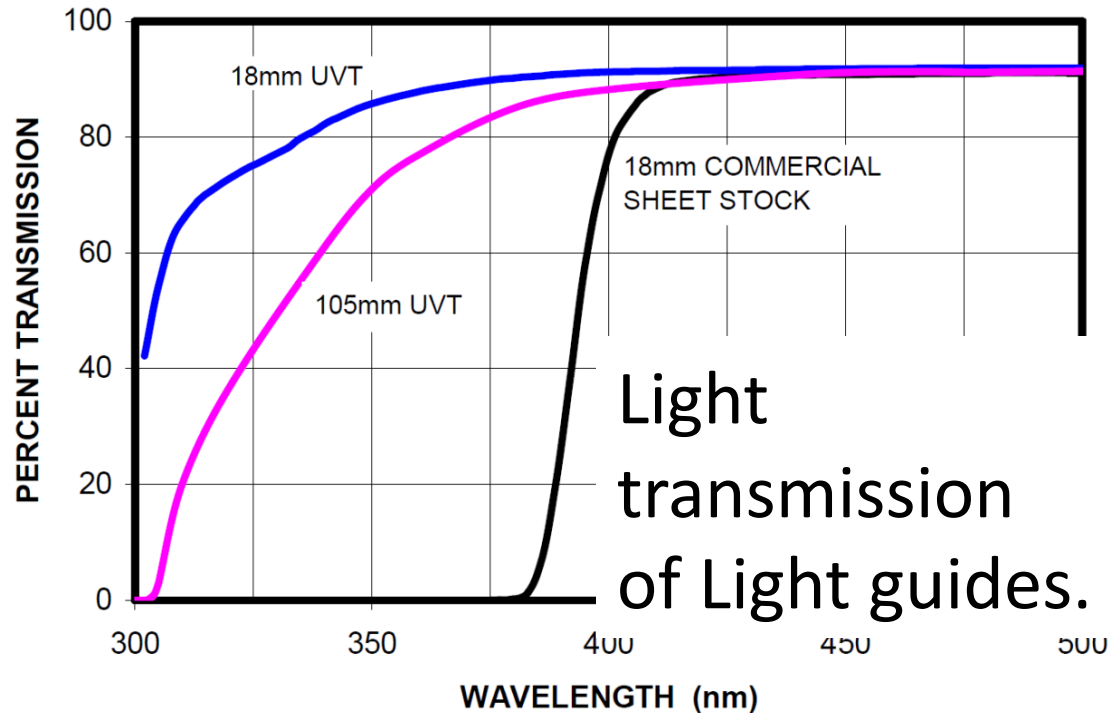
FWHM 293 ps @ 511 keV

# UVT Light guides



Spectrum of LaBr<sub>3</sub>  
Scintillation light

Wavelength of the LaBr<sub>3</sub> scintillation light is  $\lambda=380$  nm.

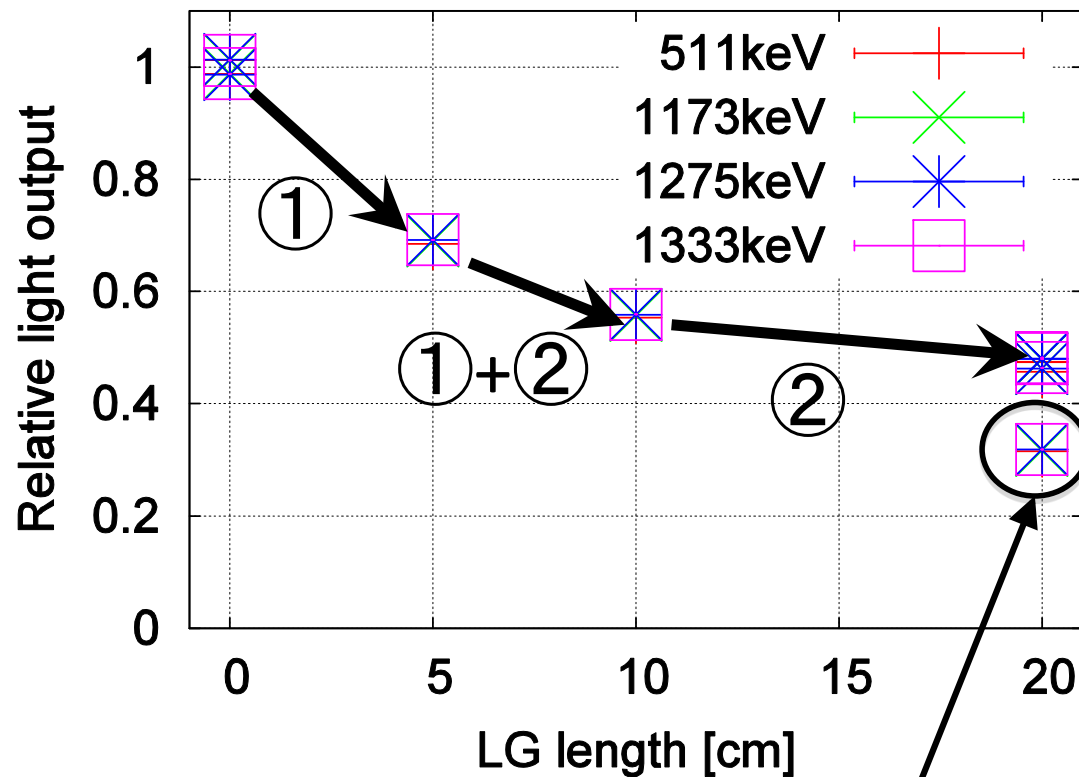


Light transmission of Light guides.

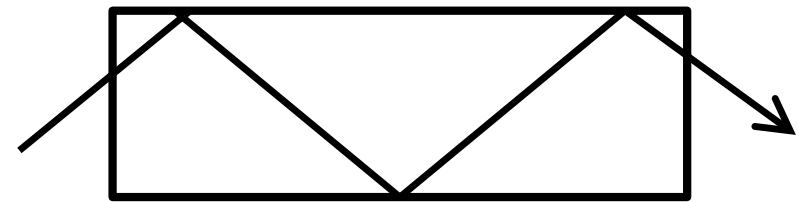
We use UVT (Ultra-Violet Transmitting) light guide.



# Light guide length dependence of light attenuation



① Loss by total Reflection condition.

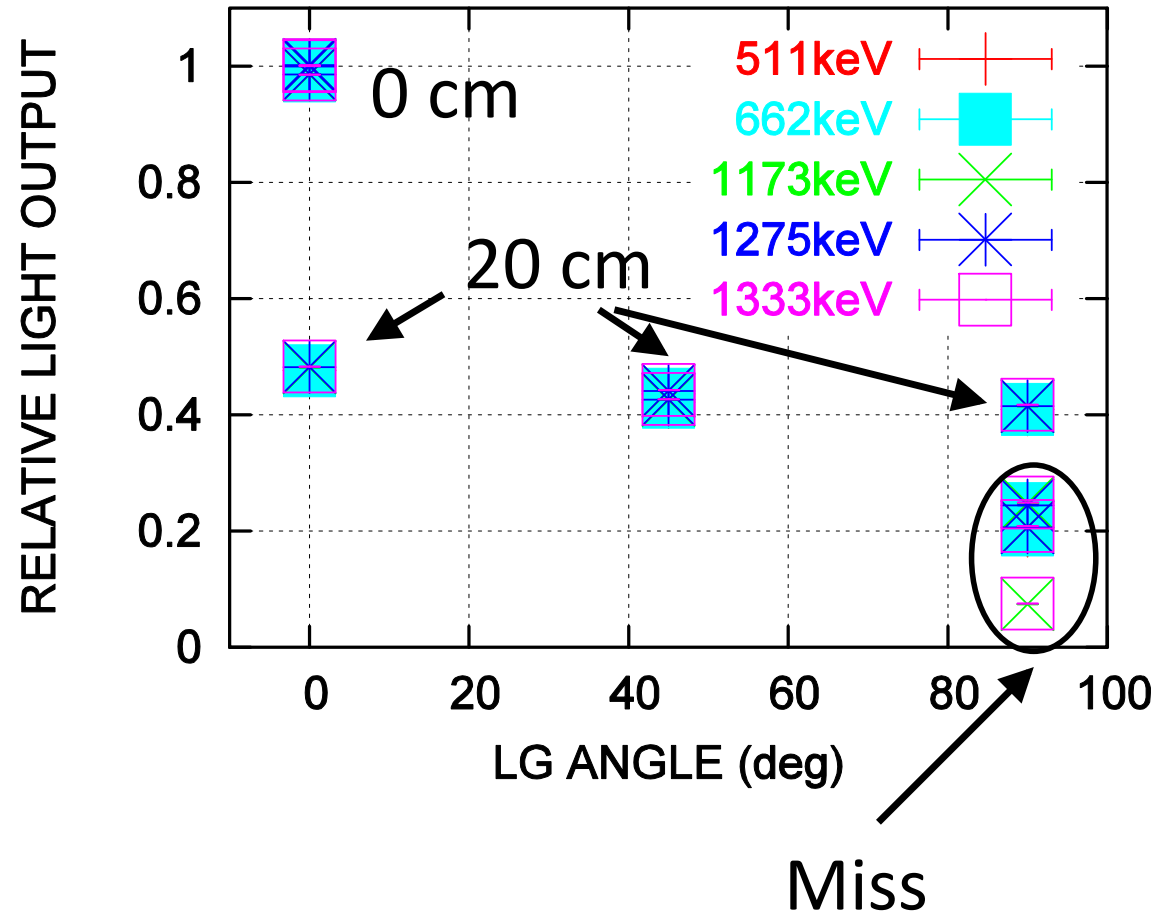


② Loss by absorption (small contribution).

LG was not glued perfectly.

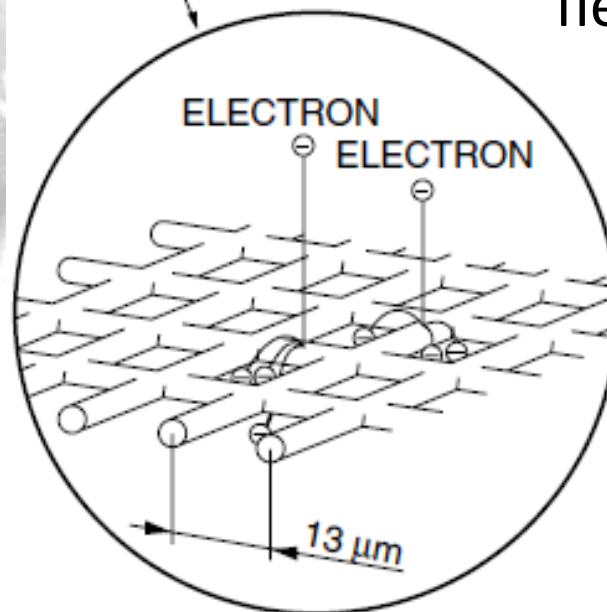
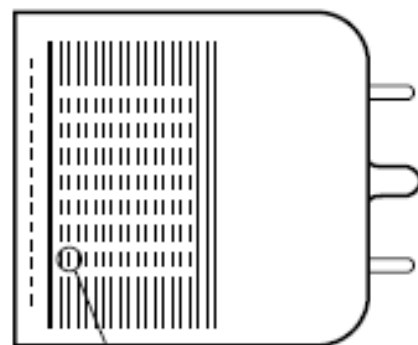
Half at 20 cm, but it seems to be almost constant at this length.

# LG Binding Angle dependence



- At 20 cm, there is no clear dependence on the binding angle.
- Small effect by binding LG.

# Fine Mesh PMT



FINE-MESH TYPE

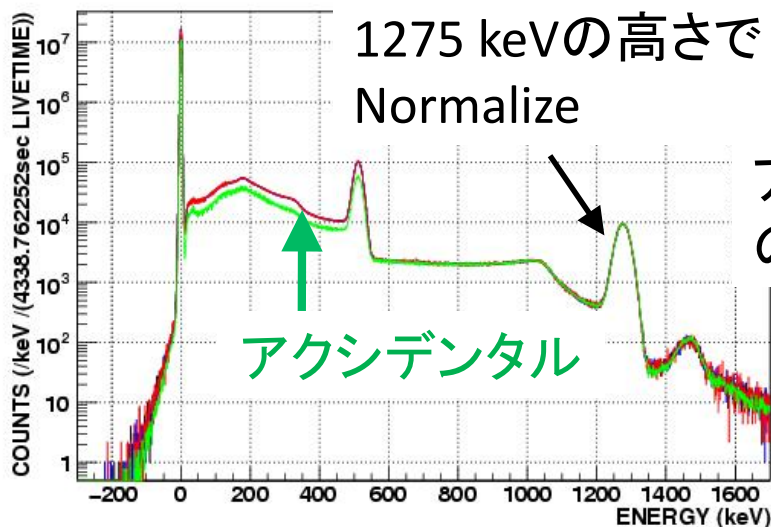
The Fine Mesh PMT contains Kovar (Alloy mainly of Fe, Ni, and Co. Ferromagnetic) and affects the magnetic field.

From the measurement at KEK,  
A few cm from the center  
→ 100 ppm  
10 cm  
→ 10 ppm

# 低速陽電子 (Slow Positron)

- ・ ガス中で、陽電子は、ガス分子との衝突を繰り返し、エネルギーを失う。
- ・ エネルギーを失ってほぼ止まった後、陽電子の多くは、遅くなったまま生き続け、Psを生成したり、対消滅したりせず、 $\sim 180$  ns の寿命を持つ  $\rightarrow$  低速陽電子
- ・ タイミングカットをかけて、アクシデンタルを引いても、低速陽電子が対消滅するときの $2\gamma$ が、大きなバックグラウンドとなる。
- ・ 2008年末のテスト測定では、これが大きな問題となった (30–400 ns タイミングウィンドウのなかで、アクシデンタルを引いた後のイベントの、60%を、低速陽電子が占めていた)。
- ・ イソブタンなどのガスは、低速陽電子の寿命を短くする、クエンチャーの能力がある。  $\rightarrow$  今回の測定では、イソブタンを混ぜ、バックグラウンド除去に成功した。

低速陽電子があると……



アクシデンタルを引いても、  
511 keV が残ってしまう。  
(RF ONもOFFも同じに見える)

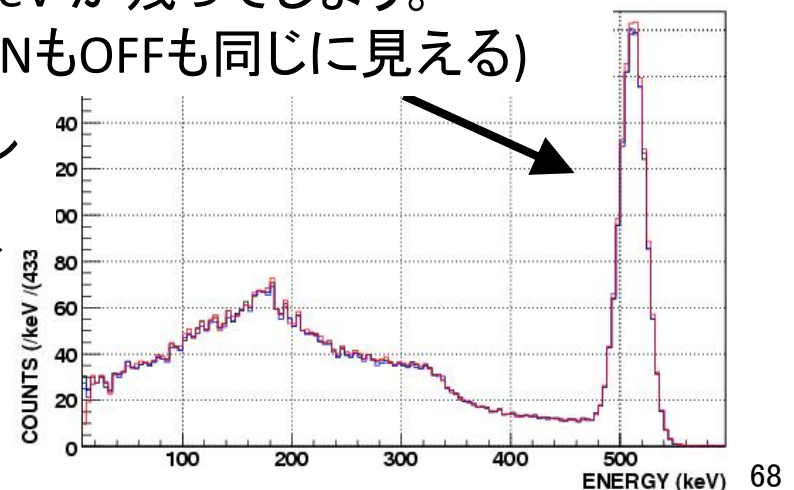
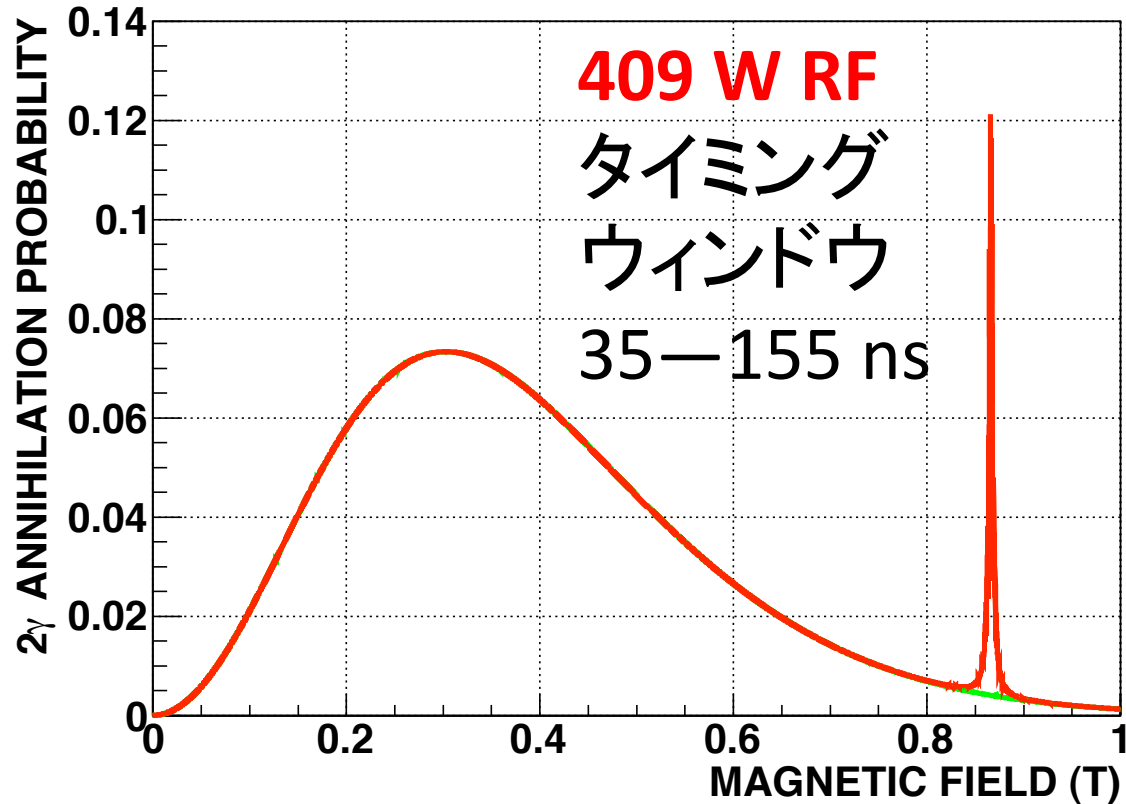


# Table of Scintillator Properties

| Scintillator           | Density             | Refractive index | Photons per MeV | Emission Maximum | Decay Constant | Radiation Length |
|------------------------|---------------------|------------------|-----------------|------------------|----------------|------------------|
|                        | g / cm <sup>3</sup> |                  |                 | nm               | ns             | cm               |
| NaI (TI)               | 3.67                | 1.85             | 38000           | 415              | 230            | 2.59             |
| CsI (TI)               | 4.51                | 1.79             | 59000           | 565              | 1000           | 1.86             |
| LYSO                   | 7.25                | 1.81             | 32000           | 420              | 40             | 1.15             |
| YAP (Ce)               | 5.55                | 1.93             | 19700           | 347              | 28             | 2.7              |
| LaBr <sub>3</sub> (Ce) | 5.08                | 1.9              | 63000           | 380              | 16             | 1.88             |

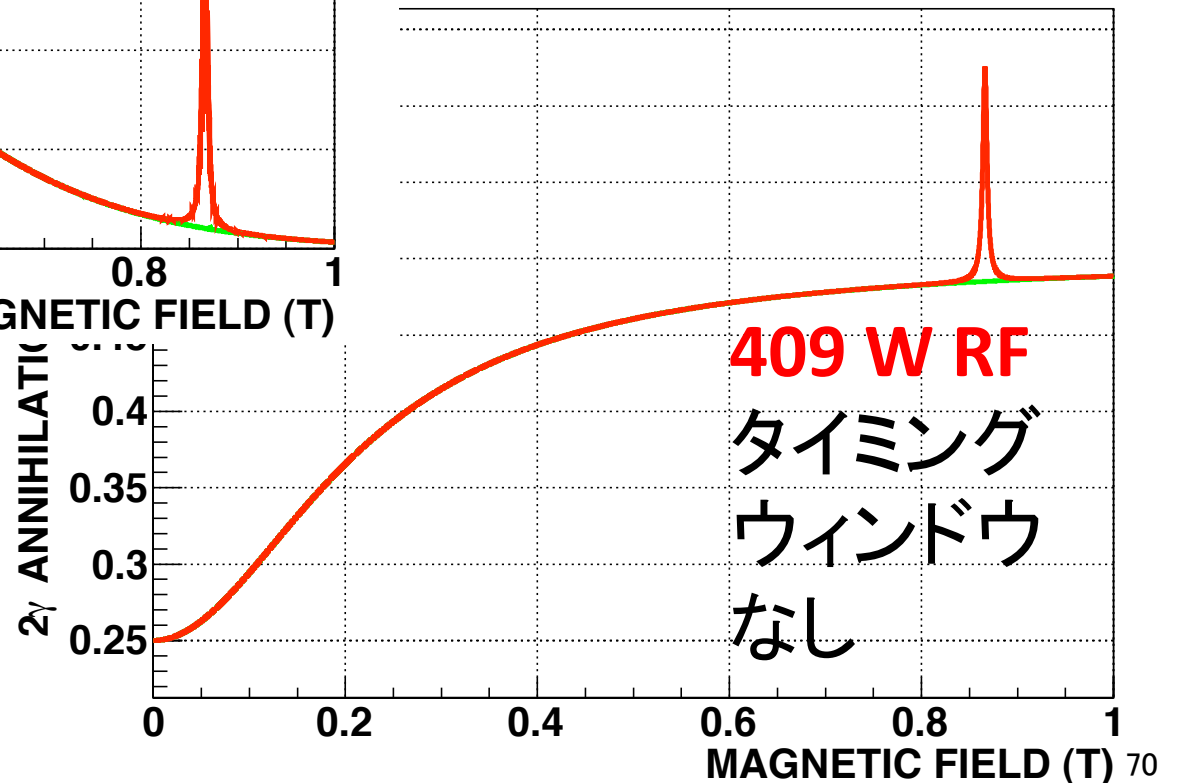
# 2 $\gamma$ 崩壊確率

WITH TIMING CUT 35--155 ns



タイミングウィンドウ による  
2 $\gamma$ 崩壊確率の違い。  
タイミングウィンドウによっ  
て  
BGを減らすことができる。  
(図は $Q_L=14700$ の理論値)

INDOW





# タイミングウィンドウの選び方

